Master Thesis

Predicting Ecological Diversity of Floodplains Using a Hydromorphic Model (CAESAR)

A Reduced Complexity Approach on Reach Scale for the Tagliamento River

Nico Bätz
August 2010

Technische Universität Berlin
Department of Soil Science

WAGENINGEN UNIVERSITY
WAGENINGEN UR
Land Dynamics group

Thesis for the Soils Science Master specialisation
Land Science of Wageningen University.
Realised in cooperation with the TU Berlin,
Institut für Ökologie, Fachgebiet Bodenkunde

LAND DYNAMICS Group
P.O. box 47
6700 AA Wageningen
The Netherlands

Supervisors
Dr. Arnaud Temme (Wageningen University)
Dr. Friederike Lang (TU Berlin)

Examiners
Dr. Arnaud Temme
Dr. Jeroen Schoorl

Summary

Eco-hydromorphic interactions between ecological and hydromorphic processes are especially relevant for braided rivers, in which feedbacks keep the system in a dynamic equilibrium. This equilibrium is delicate and susceptible to human impact so that most braided rivers disappeared from the European pre-alpine landscape. Especially changes in hydromorphic behaviour, due to intensive human river regulation, are key factors for the disappearing. Changes in river hydromorphology can be predicted by models but results were rarely linked to ecology.

The aim of the study is to evaluate the possibility of linking hydromorphic variables to the spatial distribution of ecological conditions and to check the suitability of the proposed method for human impact assessment. Prediction of the spatial distribution of ecological units is based on the hydromorphic model CAESAR which includes basic interactions with vegetation.

As study site the Tagliamento River between Cornino and Flagogna is chosen, which is assumed to be a model ecosystem of European importance.

After the input data were pre-processed and the preliminary settings of CAESAR were defined spin-up was run to create a heterogeneous sediment distribution. Next, using process description taken from literature, a multi scale calibration was done to find the proper erosion settings of CAESAR. The validation is done by comparing model output with aerial pictures and by field data.

In addition, a field survey was done to characterise and map the ecological diversity of the floodplain. Four landscape types were defined and statistically characterised: bare sediments, large scale patchy (LS patchy), small scale patchy (SS patchy) and wood. Thickness of fine substrate, grain size, elevation above main channel and distance from bare sediments were found to distinguish the landscape types but only the last two could be used for prediction because they are computable through CAESAR.

A Multinomial regression analysis was done to define the probabilities for vegetated landscape types based on the spatial explicit variables predicted by CAESAR. The landscape type with the highest probability was assigned to each raster cell. The non vegetated landscape type bare sediment was classified out of the vegetation index computed by CAESAR.

To assess the prediction, landscape type pattern is compared to the mapped units.

The application of CAESAR based mainly on literature showed to be possible. Nevertheless, errors during the spin-up run because of flushing-out of the study site fine sediments, did not allow the use of the grain size information for the ecological prediction.

The overall prediction has an R^2 of 0.69 for a resolution of 10m. Decreasing the resolution until 210m led to an R^2 of 0.80.

The results show the potential of the CAESAR vegetation growth model, which in future could be ameliorated by the integration of further succession steps than just grass growth. This would give additional information where vegetation has the opportunity to reach the stage of wood. Nevertheless, adding more independent variables, such as grain size, which can be predicted correctly by CAESAR is expected to further improve the statistical model.

Overall, the integrated basic eco-hydromorphic feedbacks of CAESAR, the matching of landscape types with FFH habitats and the acceptable overall accuracy of prediction, which has the potential to improve, make this approach a good tool for the general assessment of human impact.

Zusammenfassung

Öko-hydromorphologische Wechselbeziehungen zwischen Ökologie und Hydromorphologie sind vor allem für die Furkationszone von Flüssen von essentieller Bedeutung. Das dynamische Gleichgewicht ist gegenüber menschlichen Eingriffen sehr anfällig, so dass heutzutage die meisten verflochtenen Flüsse aus den Vor-Alpen verschwunden sind. Die hydromorphologischen Veränderungen durch Flussregulierungsmaßnahmen sind Hauptursache für das Verschwinden der Furkationszone und davon abhängiger Ökosysteme. Hydromorphologische Veränderungen können mit Hilfe von Modellen vorhergesagt werden, dennoch wurden diese selten mit ökologischen Eigenschaften verknüpft.

Das Ziel dieser Studie ist es Möglichkeiten zur Verknüpfung hydromorphologischer Variablen mit der räumlichen Verteilung ökologischer Standortfaktoren aufzuzeigen und abschließend die Evaluierung dieser Methode zur Prüfung menschlicher Eingriffe durch zu führen. Die Prognose ökologischer Einheiten basiert auf dem hydromorphologischen Modell CAESAR.

Der Flussabschnitt des Tagliamento zwischen Cornino und Flagogna ist als Untersuchungsgebiet gewählt worden. Der Tagliamento gilt als Referenzökosystem von europäischer Bedeutung.

Nachdem die Eingangsdaten vorbereitet und vorläufige CAESAR Einstellungen vorgenommen wurden, wurde ein Spin-up-lauf simuliert, um eine heterogene Verteilung der Eingangssedimentgrößenverteilung zu gewährleisten. Prozessbeschreibungen aus der Literatur wurden für eine mehrskalige Kalibrierung verwendet um CAESARs Erosionsparameter einzustellen. Die Validierung wurde durch den Vergleich von Modellergebnissen mit Luftbildern und Felddaten erreicht.

Die ökologische Diversität des Überschwemmungsgebietes wurde auf der Basis von Felduntersuchungen beschrieben. Vier Landschaftstypen wurden definiert: unbewachsenes Sediment, großräumig lückenhaft, kleinräumig lückenhaft und waldartig. Mächtigkeit des Feinsubstrates, Korngröße, Höhe über dem Hauptarm und Entfernung von unbewachsenem Sediment unterscheiden die Landschaftstypen. Dennoch konnten nur die letzten zwei Variablen für die Prognose verwendet werden, da nur diese durch CAESAR berechnet werden konnten.

Eine multinominale Regressionsanalyse wurde verwendet um Wahrscheinlichkeiten jedes vegetationsbedeckten Landschaftstypen auf Grundalge der von CAESAR berechneten räumlich Variablen zu definieren. Für eine flächige Darstellung der Ergebnisse wurde der Landschaftstyp mit der höchsten Wahrscheinlichkeit der jeweiligen Rasterzelle zugewiesen. Der Landschaftstyp unbewachsenes Sediment wurde auf der Basis des von CAESAR berechneten Vegetationsindex von den anderen drei Landschaftstypen unterschieden.

Die klassifizierten Landschaftstypen wurden mit den kartierten Landschaftstypen verglichen. Die Genauigkeit der Prognose liegt bei R^2=0.69 für eine Auflösung von 10m. Die Verringerung der Auflösung auf 210m erhöht die Genauigkeit auf R^2=0.80. Die Ergebnisse zeigen das Potential des von CAESAR integrierten Vegetationsmodels, dass in Zukunft verbessert werden könnte, indem weiter Sukzessionsphasen, die über die des Grases hinausgehen, berücksichtigt werden. Dies würde eine weitere Informationsgrundlage schaffen, zur Prognose von Flächen in denen höhere Sukzessionsphasen erreicht werden können. Gleichwohl erwarten wir durch das Einbringen weiterer unabhängiger Variablen, wie z.B. Korngröße die durch CAESAR berechnet werden kann, dass das statistische Model verbessert werden kann.

Zusammenfassend lässt sich sagen, dass durch die Berücksichtigung öko-hydromorphologischer Wechselbeziehungen in CAESAR, die Zuordnungsmöglichkeit gefährdeter Biotope zu den Landschafstypen und durch die akzeptable Prognosengenauigkeit, die sogar noch weiteres Verbesserungspotential aufzeigt, die hier vorgestellte Methode ein nützliches Instrument zur generellen menschliche Eingriffsbewertung darstellt.

Table of contents

1 Introduction

Hydromorphology concentrates on physical variables such as flow velocity, sediment regimes, channel and floodplain dimension, topography and substratum. Interaction between morphology and hydrology are studied in a spatio-temporal arrangement. Ecology addresses distribution and dynamics of individuals, populations or communities and interactions between biotic and abiotic ecosystem compounds (VAUGHAN et al. 2009).

Despite strong interactions between both, hydromorphic and ecological processes, they were rarely linked. Only few scientists recognised this in past, naming this approach "biogeomorphology (VILES, 1988), ecogeomorphology (PARSONS et al., 2003), ecohydrology or hydroecology (WASSEN and GROOTJANS, 1996), eco-hydromorphology (CLARKE et al., 2003) and geobiology" (NOFFKE, 2005), however meaning the same interdisciplinary approach (cited in (VAUGHAN *et al.* 2009)).

In this research we will call interactions between hydromorphic and ecological processes eco-hydromorphology, since we deal with interactions between ecology and hydromorphology.

Comprehensive approaches never had great attention because of research focusing more on water quality than on relation between biotic and hydromorphic compounds (VAUGHAN et al. 2009). In addition, interactions between aquatic and terrestrial/riverine ecosystems were hardly investigated. Only recently this approach gained more and more interest, because of the need to understand and quantify human impact on rivers and develop new river management practices taking in consideration climate change (FRANCIS, CORENBLIT and EDWARDS 2009; MÜLLER 2005; TOCKNER et al. 2006; VAUGHAN et al. 2009).

Legally, European Environmental and Strategic Impact Assessment and Habitats Directive Assessment, demands an evaluation for all private and public projects, plans and programs with significant effects on environment (EC 1985, 1992, 2001). To understand which impact for instance a dam has on riparian vegetation, a compressive approach is needed to be able to assemble a sound evaluation.

Moreover, also European Water Framework (EC 2000), focusing more on river environment, asks for development of European streams into a "good ecological status" by 2015. Because water quality improvement through reducing pollutants input reached its limit, it is necessary to consider a comprehensive approach which recognises relationships between ecology and physical processes. In this way it is possible to reach the stated goal (VAUGHAN et al. 2009).

Further, science is concerned in assessing consequences for river ecosystems and river morphology due to climate change and exploitation of resources, to identify key issues for a sustainable development (VAUGHAN et al. 2009).

The need to understand the system from an interdisciplinary view, encourage recently development of eco-hydromorphological approaches.

Recent studies are starting to understand first eco-hydromorphological feedbacks; still knowledge is not enough to develop predictive numerical models. Especially quantification of processes and feedbacks is a key concern for future model development (MÜLLER 2005; VAUGHAN et al. 2009)..

Eco-hydromorphological interactions are especially relevant for braided rivers and riparian habitats, because vegetation growth is controlled by sedimentation and island aggradation. On the other hand, vegetation influences sedimentation as well by enhancing roughness of the surface. This is an example of feedback linking hydromorphic and ecological processes, but more, possibly unknown, exist at different scales (FRANCIS et al. 2009).

Overall goal of this study is to present and test a methodology to link hydromorphology to habitat distribution of braided rivers.

A cellular automata model, integrating simple eco-hydromorphic feedbacks, is used to calculate spatially explicit morphological variables. Habitats were characterised based on statistical analysis of field survey data. Later, both results, hydromorphic simulation and habitat characterisation, were integrated to predict spatial distribution of habitats.

As study site the Tagliamento River is chosen, which is assumed to be a model ecosystem of European importance (TOCKNER *et al.* 2003).

1.1 Hydromorphic modelling with CAESAR

COULTHARD (COULTHARD and VAN DE WIEL n.d.) designed a model to simulate hydromorphic changes of alluvial landscapes called CAESAR (Cellular Automaton Evolutionary Slope And River model).

CAESAR is a reduced complexity model, meaning that physical equations controlling river dynamics, such as flow equation, are simplified using straightforward rules (COULTHARD, HICKS and VAN DE WIEL 2007). These simplifications are based on the idea, that not the complex processes are simulated but the easier to model general behaviour. In addition, only

processes having a major impact on river hydromorphology are integrated in the simulation (COULTHARD *et al.* 2007).

Further, landscape and its properties (e.g. digital elevation model, sediments, water depth,..) are represented through a grid (COULTHARD n.d.; VAN DE WIEL *et al.* 2007). Local interactions, based on previous explained simplified processes, between these grid cells allow simulation of riverine landscapes development (COULTHARD *et al.* 2007).

Simplification of reality permit a decrease in computational time (VAN DE WIEL *et al.* 2007) , enabling so CAESAR operating from temporal ranges of 10`s to 10˙000 years and covering spatial scales of reach and catchment (COULTHARD and VAN DE WIEL n.d.).

For both modes, reach and catchment, initial conditions, such as topography (DEM = Digital Elevation Model) and sediment distribution, have to be defined through an input grid (VAN DE WIEL *et al.* 2007). These files differ in the two modes only in resolution, ranging from 1-20 m for reach mode and >50 m for catchment mode. This is necessary to reduce computational time of CAESAR, being recommend to run best up to 500˙000 number of cells (COULTHARD and VAN DE WIEL n.d.).

Second, forcing conditions have to be defined. These are amount of rainfall for catchment mode and hydrograph and sediment inflow for reach mode. In both cases they have be specified for entire simulation period (VAN DE WIEL *et al.* 2007).

Iteration cycle starts with the topography, through which fluvial hillslope processes are driven (Figure 1). Forcing factors influence amount, while topography affects spatial distribution of erosion and sedimentation - ending in the adjusted topography. This is starting point for next iteration (VAN DE WIEL *et al.* 2007).

Flow direction and distribution is simulated by a four direction scan, which defines routing and sharing of multiple flow (VAN DE WIEL *et al.* 2007).

Moreover, CAESAR concentrates iterations on time periods in which geomorphic activity is highest, while increasing time span per iteration during low activity periods . Time simulated per iteration cycle depends on set maximum entrainment rates. By this, a more precise simulation can be done during floods (VAN DE WIEL *et al.* 2007).

Further, CAESAR allows simulation of entrainment of up to nine different sediment classes, which can be defined as bed load or suspended load. This allows selective erosion and deposition, so that spatially sediment heterogeneity results. Additionally, a layer file is used in which thickness of layer and proportion per sediment class is defined, allowing description of vertical distribution of sediments. These two properties change during simulation in relation to DEM and discharge (VAN DE WIEL *et al.* 2007).

Effect of vegetation is integrated by a simple linear growth model, which permits plants to grow on unflooded areas. When vegetation cover is greater than 50%, hydraulic roughness increases enhancing sedimentation and reducing erosion. Contrary, if a certain location stays under water, vegetation dies with a rate two times faster than growth (COULTHARD n.d.).
Moreover, vegetation can grow through sediments if buried, but if burying layer is too thick vegetation will die back and re-grow on surface (COULTHARD n.d.).
If shear stress increases above a set threshold vegetation is scoured away and growth reset to zero (COULTHARD *et al.* 2007) .

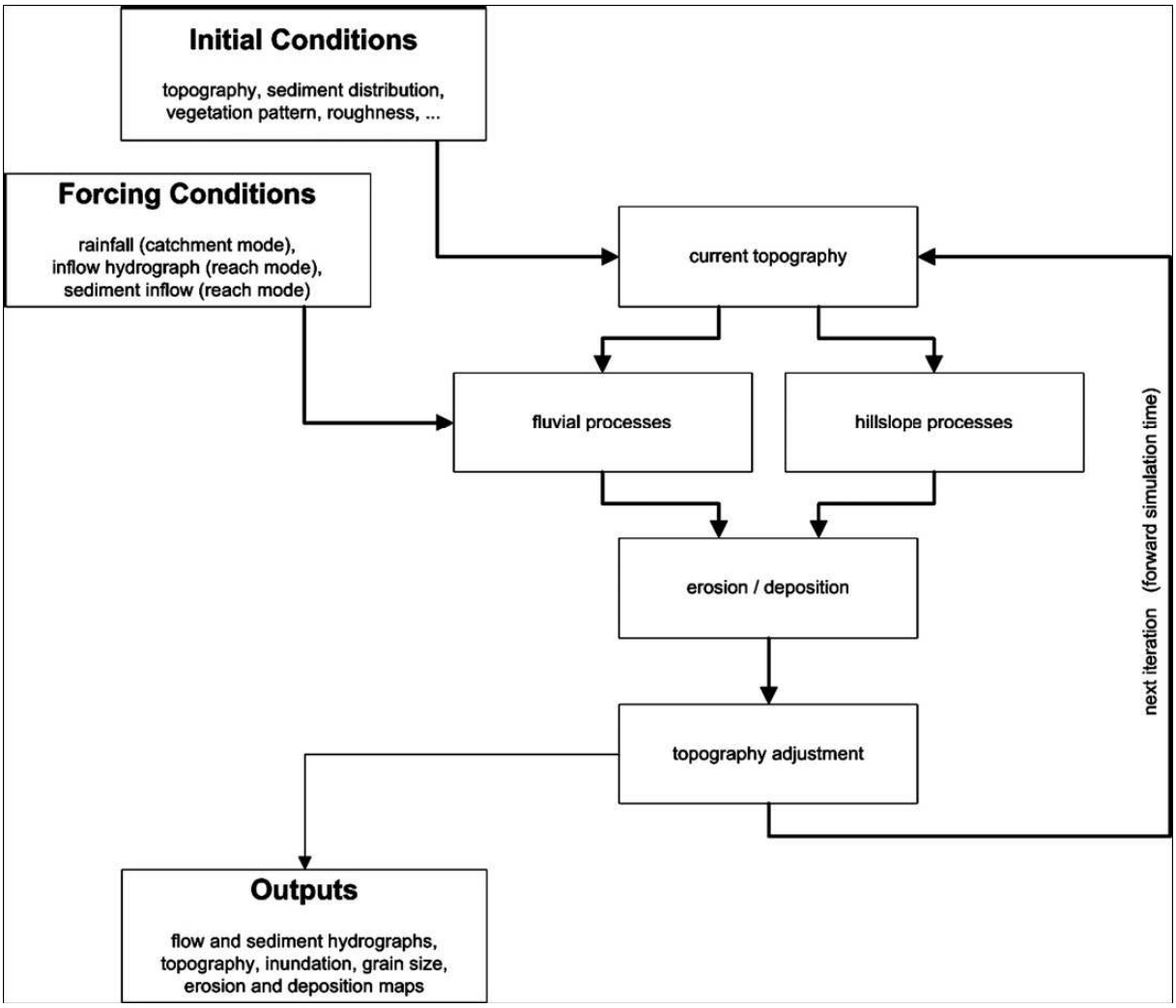

Figure 1: Structure of CAESAR (VAN DE WIEL *et al.* 2007)

The output of CAESAR is a flow and sediment hydrograph, new topography, and new distribution of sediment grain size over the inundation pattern (VAN DE WIEL *et al.* 2007).
Some limitations concerning CAESAR output should be considered. Due to simplified rules, quantitative data often do not correspond to reality, so that interpretation should be done in a

qualitative way. As an example, channel and island position should not be taken as an exact forecast of river hydromorphology but as indicator for river dynamics (COULTHARD *et al.* 2007).

Another limitation is the restricted possibilities of model validation. While flow depth and inundation areas can be validated through field data, erosion and sedimentation rates are hard to determine by field analyses. Some proposed validation methods include, comparison of aerial pictures, flume data or comparison with results of more sophisticated 2-D hydraulic models (COULTHARD *et al.* 2007).

Integration of different grain size and more complex multiple flow routing, gives CAESAR the opportunity to add several levels of complexity, being so one of the more elaborated cellular automata (VAN DE WIEL *et al.* 2007). Thus CAESAR fills the scale gap between physical based complex Computational Fluid Dynamic models (CFD), that are not applicable on large areas and events greater than a flood, and coarse resolution Landscape Evolution Models (LEM) that calculate landscape development over thousands of years averaging out single significant events (COULTHARD *et al.* 2007); (COULTHARD and VAN DE WIEL n.d.).

The filled gap corresponds to engineering time scale, a fundamental scale range in which human planning takes place (COULTHARD *et al.* 2007; FRISSELL *et al.* 1986).

Thus CAESAR allows comparison of "what if" scenarios and gives qualitative forecasts of human impact on river landscapes that could be integrated in the European Impact Assessment processes and the Water Framework goal attainment.

1.2 Eco-hydromorphic interactions and ecological processes of islands braided river

Feedbacks between hydromorphological and ecological processes take place at different time and space scale.

FRISSELL *et al* (1986) worked out a hierarchical framework for rivers in which a subdivision in six scale classes is designed: Watershed, Stream system, Segment, Reach, Pool/riffle and Microhabitats. In every class different eco-hydromorphology feedbacks occur and have an impact beyond scale-boundary. For instance, land-use changes within catchment modify overall setting of processes, such as discharge, at reach scale. Moreover, if considering interactions over large space and time spans, factors such as geology, climate or channel

slope, change (geologic time span >10^5) while over a few years these characteristics can be seen as constant (FRISSELL *et al.* 1986).

Here we will focus on interactions on reach scale over round 20-50 years (engineering time scale) which influences development of vegetated islands in braided river systems.

On this scale two main properties are found: first, sediment texture and structure, vegetation roots and roughness, control cohesiveness of landforms; second, water flow and dynamic, control remobilisation (FRANCIS *et al.* 2009). Different expression of those two factors regulate river pattern and so habitat template (FISHER *et al.* 2007). For instance, stream power, defined as maximum discharge times mean slope of the reach, is main controlling factor for vegetate island development. High stream power, variable discharge, erodible banks and wide shallow channels are characteristic for braided gravel-bed systems. Wandering gravel-bed systems ,which are frequently vegetated, in turn are characterised by lower stream power, leading to greater sediment aggradation and more stable channels (FRANCIS *et al.* 2009; GURNELL and PETTS 2006).

Lower stream power allows sedimentation of finer material, organic material and propagules. Further, lower stream power related to flooding frequency, allows vegetation to establish and fix into ground and is so harder removed by next floods (GURNELL and PETTS 2006). As soon as vegetation establishes, local positive feedback begins (FRANCIS *et al.* 2009).

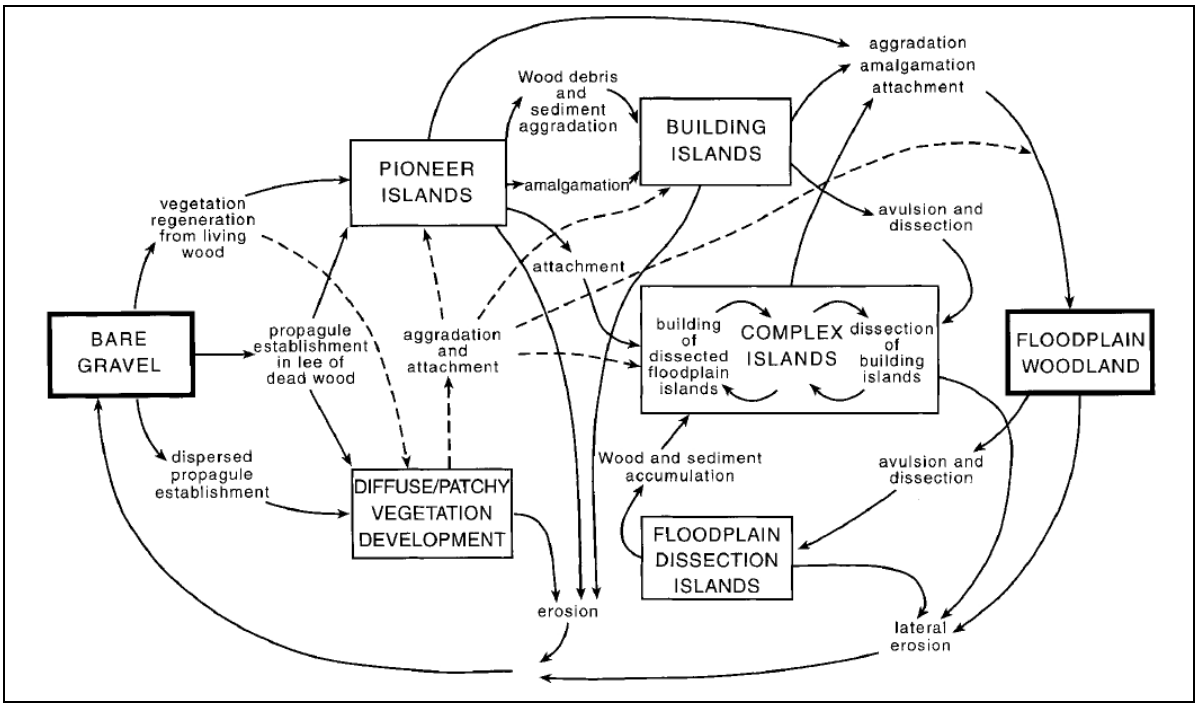

Figure 2: Conceptual model of island formation for the Tagliamento River (GURNELL *et al.* 2001).

GURNELL *et al.* (2001) proposes a conceptual model (Figure 2) for the Tagliamento River in which development of different island types is explained. Starting point, is a gravel bar on which, regenerating wood, death wood or propagules deposit in combination with fine sediments. Out if this setting, diffuse/patchy vegetation or pioneer island develop. The balance between aggradation and erosion influences further development time into building island or even complex island (GURNELL and PETTS 2006).

Different stages of succession correspond also to different risk of being reset by floods; the higher the succession stage the lower the risk (GURNELL and PETTS 2006; GURNELL *et al.* 2001).

Despite factors influencing previous explained island formation, species composition of vegetation depends on further variables such as timing of propagules dispersal, quality, flotation characteristics and type. Especially propagules transported by water are highly connected to flow dynamic of the river, whereby a maximum height of propagation in floodplain morphology corresponds to highest water level.

Establishment of vegetation is influenced by water and nutrient availability. After, erosion and burry resistance influences growth and survival (GURNELL and PETTS 2002).

Recently some reduced complexity models, such as CAESAR, integrate basic effect of vegetation on hydrogeomorphic processes (MURRAY *et al.* 2008).

CAESAR has been applied to assess morphological changes on the braided Waitaki River in New Zeeland. Dam building up-stream lowered flow pulses and floods, influencing disturbances on vegetation. High vegetation growth rate were expected to reduce sediment yield since stabilizing riverbed and banks. However, model output suggested the opposite: faster growing vegetation created a more effective single thread channel, eroding more material from river bed. Simplified interaction of vegetation with flow and sediment transport patterns led to an unexpected result, showing the potential of such a simple modelling approach (COULTHARD *et al.* 2007).

CAESAR does not integrate the complex interactions as proposed in the conceptual model of GURNELL (2001). MURRAY (2008) sees the reason in difficulty to parameterise impact of ecological process on flow, sedimentation and ecosystem succession as a function of morphology, flow and sediment transport.

However, studies concerned with eco-hydromorphic processes were looking at influence of vegetation on hydromorphic processes. Recently this is changing, focusing on effects of

hydromorphology on biological development and, moreover, cumulative effects of ecology on landscapes (MURRAY *et al.* 2008).

1.3 Research objectives

The main objective of this research is to link spatially variable hydromorphic characteristics with habitat diversity and assess the possible use of the overall method to study future scenario.
Following stepwise objectives are defined for this research:

1) **Application of the reduced complexity model CAESAR to the Tagliamento River.**

Is the application of CAESAR using general literature on braided rivers possible?
Is the simple vegetation growth model integrated in CAESAR sufficient to assess eco-hydromorphic interactions of the Tagliamento River?

2) **Identify properties which indicate habitat types.**

Which landscape properties can be used to statistically differentiate habitat types?

3) **Investigation of the link between the CAESAR calculated geomorphic variables and indices pattern and the actual habitats assortment.**

Is CAESAR able to predict the spatial distribution of variables which explain distribution of habitats?

4) **Assessing if the proposed method allows prediction of human impact on endangered NATURA 2000 habitats as a function of changes in morphological properties.**

Is the overall method suitable for human impact assessment on endangered habitats?

2 Material and methods

To link spatial explicit hydromorphic variables with habitat diversity, a methodology was developed. The approach is kept simple to get this methodology applicable on other study sites. This is considered important if such a model will be used for environmental impact assessment for Alpine braided rivers.

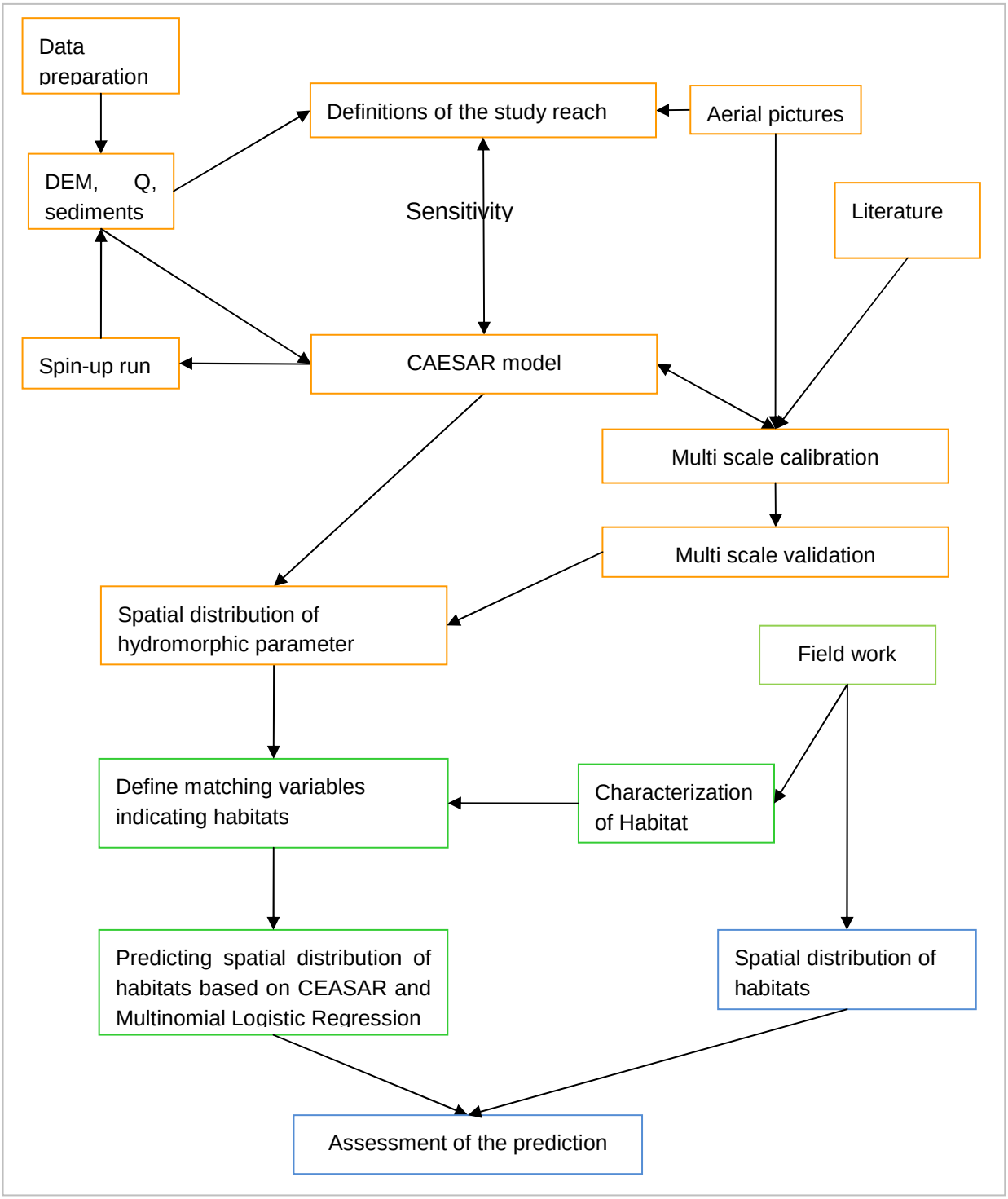

Figure 3: Methodological approach

The general methodology is shown in Figure 3. Three areas can be defined:

- Application of CAESAR (orange): first, input data are prepared. Afterward, the criteria resolution and calculation time are used to find a compromise in study area size and detailedness (sensitivity analysis). Next, a spin-up run is done to create a heterogeneous sediment distribution input file.

  As soon all input variables have been prepared a multi scale calibration is used to find proper settings of CAESAR. Finally, output is validated.
- Linking the hydromorphological model with habitat distribution (green): initially, a field survey is done to characterise the habitat. Additionally habitat distribution is mapped. A multinomial regression analysis is done to define probabilities for habitats based on spatial explicit variables predicted by CAESAR.
- Assessment of the prediction (blue): here the predicted pattern is compared to mapped habitat units. In this way performance of the overall method can be assessed. Moreover, evaluation of the overall method for impact assessment is done.

Before the method is described in detail a description of the study site is done.

2.1 The Tagliamento River and the ecology of braided rivers

The Tagliamento River is in the north-east of Italy, next to Venice. It is between the two regions Friuli-Venezia-Giulia and Veneto. The 172 km long river, is almost on entire length free from intensive human regulation (MÜLLER 2005). Catchment covers an area of 2580 km^2 of the limestone Dolomite Alps (Figure 3) (VAN DER NAT *et al.* 2002). Nevertheless, a clear boundary is difficult to draw due to ground water draining through limestone karst (TOCKNER *et al.* 2003).

The active floodplain reaches a width up to 1,5 km and is visible from satellite (VAN DER NAT *et al.* 2002). Figure 5 show the section of the river after it escape from the Alps at Venzone and flowing into the Adriatic Sea. The white stripe connecting the Alps with the sea shows the dimension of active zone of the river.

Three main landforms are found within the active zone: (vegetated) islands, bare islands and flowing water (VAN DER NAT *et al.* 2002). On 61 km^2 of the Tagliamento River these landforms are present (TOCKNER *et al.* 2003).

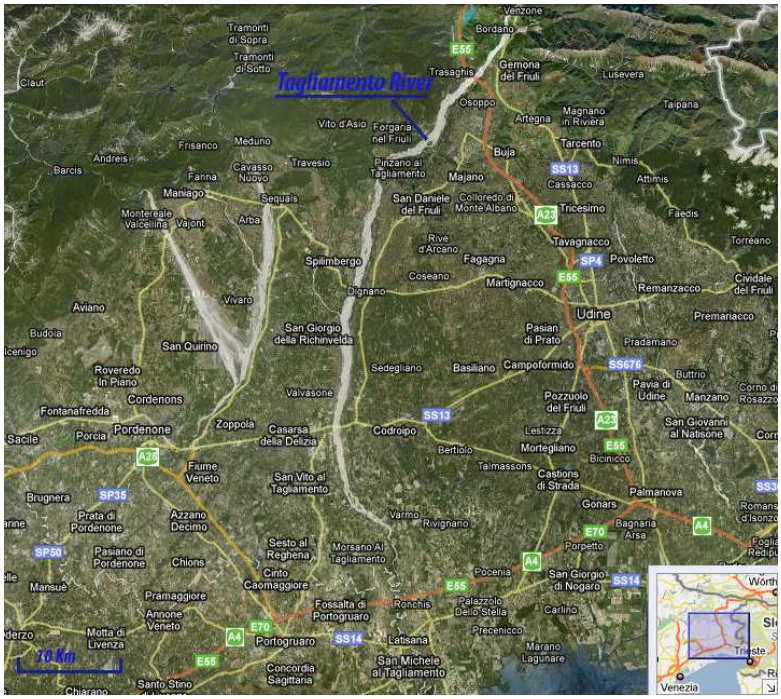

Figure 4: Aerial picture of the Tagliamento River and surrounding (GOOGLE MAPS 2009)

From hydrological point of view, the Tagliamento is characterised by a flashy pluvio-nival regime with bimodal flow pattern, having peaks in spring and autumn (Figure 6B) (TOCKNER *et al.* 2003; VAN DER NAT *et al.* 2002).

The term "flashy" refers to extreme and unpredictable rapid river discharge changes, (GURNELL *et al.* 2001; VAN DER NAT *et al.* 2002). On average discharge at Venzone is 90m^3s^{-1}, reaching two to ten times a year 2150m^3s^{-1} (GURNELL *et al.* 2001). The flood pulses and pulsing flow are the main actors in the active floodplain. The first are characterised by long duration and predictable discharge raise reaching bankfull level (Figure 6B). Flood pulse shapes previous explained land forms and keep the system in dynamic equilibrium (JUNK, BAYLEY and SPARKS 1989; VAN DER NAT *et al.* 2002). The pulsing flow (small water- level

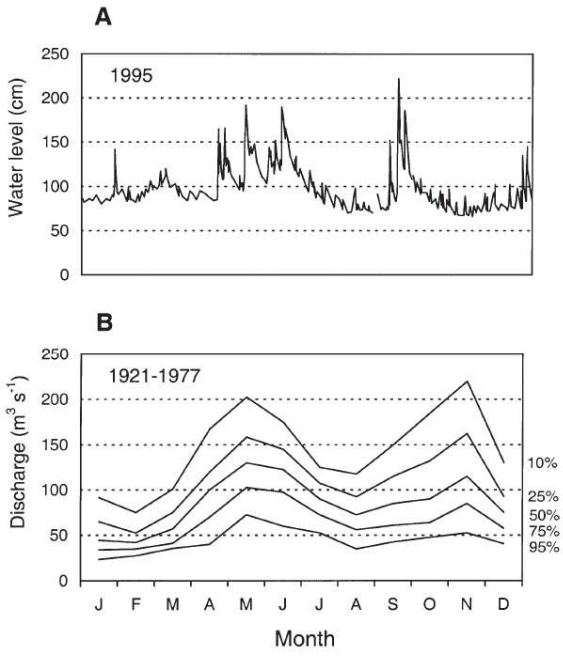

Figure 5: Hydrograph of the Tagliamento in 1995 (at Pinzano). B: Seasonal flow patterns (probability curves, in %, for 1921–1977; Electroconsult, 1979).

Cited in (TOCKNER *et al.* 2003)

fluctuation well below bankfull, see Figure 6A) creates an enormous expansion and contraction of water surface in the floodplain (TOCKNER *et al.* 2003), and so controlling connectivity of a mosaic of habitats (MÜLLER 2005; VAN DER NAT *et al.* 2002).

Highly specialised flora and fauna colonize this special environment. Specialisation goes together with sensitivity to small changes due to humans impact. River regulation, gravel exploitation and pollution compromises these environmental setting and so the habitats which now are in danger of extinction (MÜLLER 2005).

The European Union recognised this issue and integrated alpine rivers habitats in the Flora Fauna Habitat (FFH)-directive "on the conservation of natural habitats and of wild fauna and flora" (EC 2007). This directive focuses on the conservation of European endangered habitats and the creation of a network of protected areas called "NATURA 2000".

In Table 1, FFH habitats found in the active floodplain of Tagliamento River are listed. The Habitats were assessed during a field survey (LIPPERT et al. 1995, MÜLLER et al. 1993, MÜLLER et al. 2004 cited in MÜLLER 2005), in which vegetation and river morphology was surveyed on eight different representative sites (Figure 7). Six habitats of European importance were observed along the stream course. Two, 7240* and 91E0*, are even priority habitats meaning highly endangered of extinction (MÜLLER 2005).

Comparing Table 1 with Figure 7, coherence of the network is pointed. FFH habitats occur continuously over a large part of the stream, forming a 152 km^2 corridor over the alpine and continental biogeografic regions (MÜLLER 2005).

During last 700 years, rivers in Europe have been under extensive regulation and engineering, so that most braided rivers disappeared (FRANCIS *et al.* 2009). The Tagliamento is an exception, being free of severe engineering and regulation measures so that ecosystem components (e.g. intact riparian woodlands, large populations of species capable of vegetative reproduction) and processes (e.g. dynamic hydrology, flow variability, sediment transport, tree entrainment, deposition and establishment) still interact in ancestral natural way forming a wide island and bare dominated floodplain (FRANCIS *et al.* 2009). This gives the Tagliamento also from hydromorphic view a special weight.

The study reach between Cornino and Flagogna (location 4 in Figure 7 Chapter 2.1) was chosen for this research. Detailed characterisation of the study site is integrated within the here presented methodological steps.

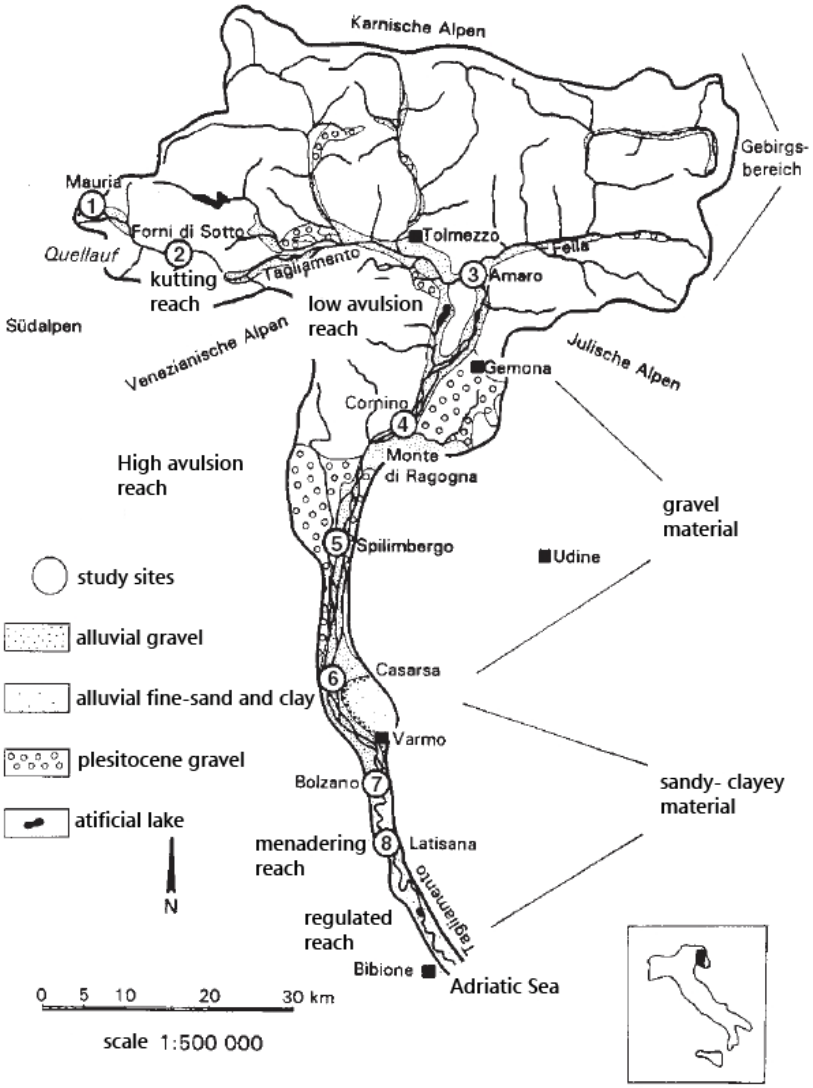

Figure 6: Geology, reach type and study sites of MÜLLER (2005) at the Tagliamento (personal translation)

Table 1: FFH floodplain habitat location, observed by (EC 2007; MÜLLER 2005)

Habitat name	**FFH Code**	**Study site num./location**
Alpine rivers and the herbaceous vegetation along their banks	3220	2- Forni until 7-Bolzano
Alpine rivers and their ligneous vegetation with *Myricaria germanica*	3230	2-Forni until 4-Cornino
Alpine rivers and their ligneous vegetation with *Salix elaeagnos*	3240	1-Mauria until 7- Bolzano
* Alpine pioneer formations of *Caricion bicoloris-atrofuscae*	7240*	1-Mauria until 4-Cornino
Alkaline fens	7230	1-Mauria until 4-Cornino
Alluvial forests with Alnus glutinosa and Fraxinus excelsior (Alno-Padion, Alnion incanae, Salicion albae)	91E0*	1-Mauria until 3-Amaro and 6-Casarsa until 7-Bolzano

2.2 Application of CAESAR

We present here general steps needed to run the hydromorphic model CAESAR. Two main steps were defined: first, an initial set-up was defined by preparing input data and defining base setting. Afterword, a multi scale calibration and validation approach was chosen to simulate hydromorphic changes over four years.

2.2.1 Initial set-up

2.2.1.1 Initial data preparation

Basic input data are DEM-file (Digital Elevation Model), Q-file (discharge-file), and bedrock-file. Furthermore, definition of grain size classes, proportions and distribution is needed.

The DEM (Digital Elevation Model) has been derived by an airborne LiDAR dataset with resolution of 5m. The dataset has been commissioned by NERC (Natural Environmental Research Council – UK) in May 2005 together with an aerial picture of 1m resolution.

BERTOLDI (unpublished) processed the raw dataset by filtering vegetation.

Generally, the DEM was processed by removing errors such as bridges and sinks. After, the DEM was turned (220°) to get the main flow direction from right to left, which is the main direction of the flow routing process of CAESAR (COULTHARD and DE ROSA 2009; COULTHARD and VAN DE WIEL n.d.).

The bedrock-file, similar to the DEM, is an elevation-file. Where bedrock touches surface bedrock-file has the same heights as the DEM (COULTHARD and DE ROSA 2009). Boundaries of bedrock were defined through aerial picture, DEM and the knowledge gained during a first field trip.

ZILIANI (2009) provided us with water stages of the Tagliamento for Venzone for the time span 2000-2009. Even if the measuring station is around 20 Km stream upward (between Amaro and Gemona Figure 6 Chapter 2.2.1.1), there is no large affluent in-between Venzone and the study reach. Water uptake at Osoppo and water input from Cavazzo Lake are thought to compensate each other.

The half-an-hour water stages were translated to Q using formulas derived by WELBER *et al.* (unpublished). These formulas were derived for three different water height ranges. For each range a different correlation with Q is given.

.

Since discharge data (Q) are a rarely available because not all rivers have water stage monitoring, the resulting dataset was aggregated to mean daily mean values.
Figure 8 shows the resulting hydrograph.

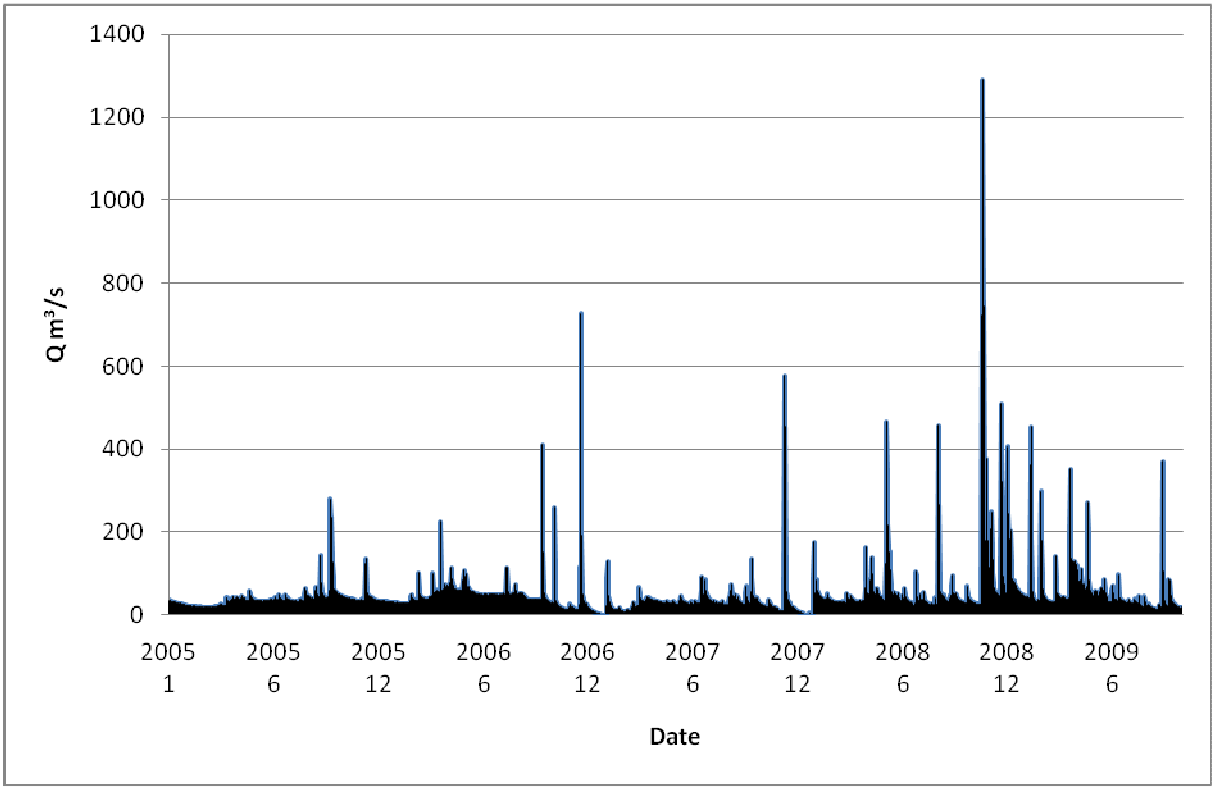

Figure 7: Hydrograph for the Tagliamento river at location of Venzone.

Next, CAESAR allows setting of up to nine different sediment grain-sizes. Each class is defined through the average grain-size (COULTHARD and VAN DE WIEL n.d.).
Granulometry analysis of the study reach (CATANI 2007) and impressions of a first field trip were used to define grain size distribution and proportion. The analysis consists of a combination of sieve analysis to define coarse material (Appendix 2) and a laser analysis for finer parts (Appendix 1). Even if a reference is used, it is assumed that a rough estimation or the same analysis method as in CATANI (2007), are easy enough. To combine these two analysis results, we assumed that the overlapping class “sand” contains finer sediments of the laser analysis.
The US Udden-Wentworth grain size subdivision was used to aggregate the sediment classes into nine classes as shown in Table 2. In this process it is important to keep the fine sediment classes (clay, silt and sand), due to its importance for plant growth and aggregate more coarser classes (gravel, cobble and boulder).

Furthermore, each sett sediment class needs to be defined as bedload or suspended load based on average flow velocity range of the studied river. This is a fixed setting because CAESAR does not change this value based on flow velocities (COULTHARD and VAN DE WIEL n.d.). The fall velocities for suspended load were calculated using Stokes law (Table 2).

Table 2: fall velocity for each grain size

grain size	**%**	**grain size (m)**	**fall velocity (m/s)**
Colloid + clay	0.6	0.0000007	0.0000005
Silt	4.6	0.0000332	0.0009613
Very fine + fine sand	7.9	0.0001563	0.0212891
Medium sand	6.5	0.0003750	0.0360000
Coarse + very coarse sand	3.4	0.0009571	Bedload
Very fine + fine gravel	20.0	0.0050000	Bedload
Medium gravel	20.0	0.0120000	Bedload
Coarse gravel	20.0	0.0237500	Bedload
Very coarse gravel + cobble	17.0	0.0782500	Bedload

2.2.1.2 DEM definition and spin-up settings

Because CAESAR is a cellular automaton, calculation time is very sensitive to the total amount of cells through which water has to be routed (COULTHARD and VAN DE WIEL n.d.). Both extent and resolution influence number of cells.

A sensitivity analysis was done to find a compromise between number of cells and calculation time. A base CAESAR (version 6.1f-10/11/2009) setting suggested by COULTHARD (COULTHARD and DE ROSA 2009) was run on a Intel(R) Core(TM)2 Duo CPU E6550 at 2.33 GHz, a RAM of 1.95 GB and Windows XP professional to study sensitivity.

All settings were kept constant; only the input DEM of the study area changed in size and resolution. The different study area boundaries were based on possibility to define clear and stable water input locations.

The "real" time that CAESAR required to simulate 10 minutes was measured and extrapolated to simulate one day, which is thought to be better comparable.

After choosing an optimal extent and resolution, speed of CAESAR is tried to improve by a simple sensitivity analysis for basic parameters. "*Max erod limit*", "*Slope used to calculate Tau (bed sheer stress)*", "*Min Q for depth calc*" and "*Flow distribution*" were tested because

they had a strong effect on modelled time step and number of cells included in water routing process.

2.2.1.3 Spin-up run

CAESAR assumes at beginning that all cells have the same proportion of initially set sediment classes. The spin-up run creates a heterogeneous distribution and allows the river bed to armour (COULTHARD and DE ROSA 2009).

The Q-file for the spin-up was designed having same proportion of discharge in a year as the study river. Doing so, we were able to reproduce a Q file similar to the hydrograph of the Tagliamento, consisting of two peaks every year. From tests, it appears that adapting the Q-file to the "shape" of the study river hydrograph is best solution. The period over which Q increases or fluctuates influences both location and amount of incision. The grain size distribution is influenced by incision rate, because different water stages reach different location, depending on the channel depth. Due to this it is important to start with maximum Q, lowering down to minimum and back again to maximum in the time span of yearly floods. This allows a general mixing of the grain size of the floodplain before river incises into his bed. After, the river bed has the possibility to armour.

The model was run with the previous defined parameter settings, the hydrograph-similar Q-file and without recirculating sediments (output sediments = input sediments). Lateral erosion is not integrated yet because the goal was to create a heterogeneous gains size file without changing much the floodplain morphology before starting of the later simulation.

The sediment outflow per time period (catchment file) can be set as a saving output, as soon this gets constant, spin-up run is done. The fluctuating Q over time allows a comparison of sediment discharge over each max-Q to max-Q cycle.

2.2.1.4 Vegetation settings

Herbaceous vegetation do not play an important role in braided rivers as the resprouting and the development of seedlings of Salicaceae do (GURNELL, SURIAN and ZANONI 2009; KOLLMANN *et al.* 1999). This was clearly visible during a first field trip. Therefore, we assumed that the grass growing model of CAESAR is similar to resprouting of Salicaceae and development of seedlings.

Generally, vegetation in braided river grows very fast (GURNELL *et al.* 2006; 2009). In Figure 19 in Chapter 3.1.2.1, we can see that floods with a returning period of 2-3 years reach vegetated patches, indicating the time without disturbance needed for development.

We set vegetation development time at 3 years, meaning that in this time frame a 100% grass cover develops.

2.2.2 Multi scale calibration and validation

As soon the base data sets DEM, bedrock, discharge (Q), sediment classes and sediment distribution was prepared we calibrated lateral erosion and its interaction with bed erosion.
The general approach is shown in Figure 8.
The first two years were used to calibrate the erosion parameter. Visual criteria were used for single events, while quantitative data, such as turnover rates, were used to estimate the yearly performance.
The last two years CAESAR results were used for validation, done using aerial pictures and field data, such as sediment flux.

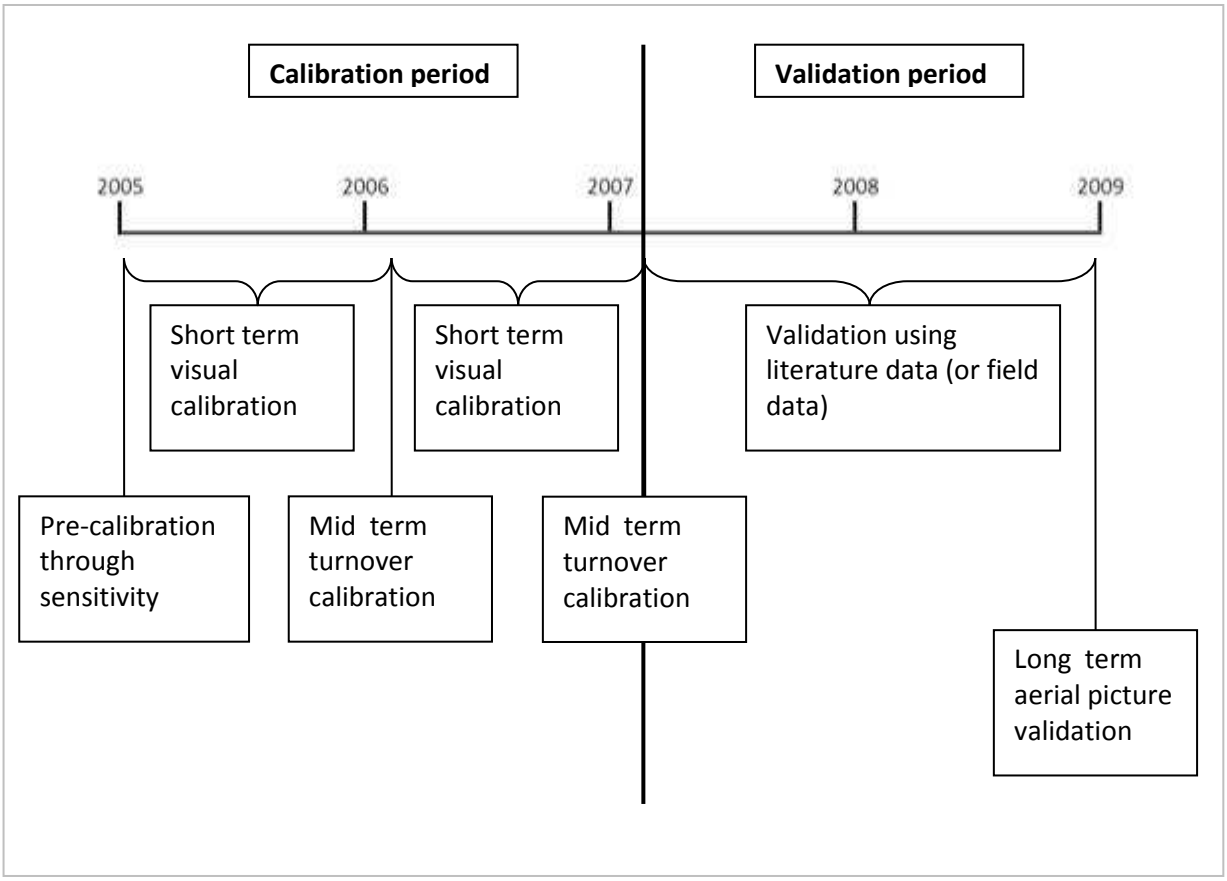

Figure 8: Multi scale calibration validation approach

2.2.2.1 Pre-calibration and sensitivity analysis

For a **pre-calibration**, data are taken from general literature on braided rivers. We included literature of the Tagliamento if considered to be general valid. This is often the case, because the Tagliamento is considered as reference for alpine braided rivers.

GURNELL *et al.* (2009), collected maximum discharge, bed slope and braiding type for different braided rivers (Figure 16 Chapter 3.1.2.1). The specific channel-slope/discharge relationship of the study reach was used to classify the river in a braiding class and so find general processes describing literature (Figure 18 Chapter 3.1.2.1).

Aerial pictures of the same year as the DEM were used to match simulated river pattern to aerial picture flow pattern. This allowed a preliminary setting of sinuosity.

To define the erosion parameter, we used different constant Q with a returning period within one year. CAESAR, run for each Q over five "model" days. We assessed the process rates by comparing indices as total flow (tQ), sediment transport (sed-Q) and lateral turnover rate (% turn). Lateral turnover rate is defined as percentage of floodplain with elevation change outside the initial channel higher than three times the overall mean grain size.

The goal is to find the right preliminary settings of lateral and bed erosion by comparing the indices with literature processes description.

2.2.2.2 Calibration

Feasible model set-ups defined during the pre-calibration, were run using real discharge 2005-2009.

A short and midterm calibration was done by comparing different CAESAR setting outputs with descriptive and quantitative criteria. The criteria are used to evaluate the settings for lateral erosion, bed erosion and sinuosity.

The criteria used were:

Calculation time: time the model takes to calculate one year should be as small as possible. Even if this parameter was included in the definition of the spin-up settings, this parameter is taken again because integrating now lateral erosion.

Sinuosity**:** ZANONI *et al.*(2008) analysed aerial pictures over 50 years for the same reach of the Tagliamento River as BERTOLDI *et al.*(2009) did. This corresponds also to here chosen study area. Both concluded that generally sinuosity, aquatic habitat composition and island to corridor ratio stay constant over time.

Aerial pictures were used to define sinuosity of the river as the ration between flow distances of the main channel(s) divided by the straight bed slope line (defined as the middle of the active corridor).
Sinuosity pattern is tried to keep visually and numerically within this range.

Erosion / avulsion pattern (Process): WARD *et al.*(2002) states that avulsion is the primary process of channel dynamics in braided rivers. Especially in island braided rivers this is the dominant process over lateral erosion. Both avulsion and lateral erosion shape geomorphic features in the floodplain, influencing turnover rate, succession and turnover of the landscape elements such as islands (WARD *et al.* 2002).
The process of avulsion consists of infilling of channels branches and sudden diversion of the flow path in a new (old) channel, while lateral erosion slowly causes channel migrate in one direction (WARD *et al.* 2002).
Literature based on the previously defined braiding type of the study reach, describing these two processes of erosion and avulsion more in detail was used to compare visually and numerically the outcome of CAESAR. Comparing if a certain process happens at a certain discharge was the main focus.

Short term calibration focuses on visual comparison between different model settings of small events within one year. The processes and flow pattern were described through literature. A comparison of different settings of lateral erosion, bed erosion and sinuosity was done primary visually by comparing flow pattern before/after the event. Relative marks were given based on how specific setting fulfil above mentioned descriptive criteria.
For **mid term calibration**, at a time span of one year, sinuosity and turnover rates were used to adapt settings. Here, differently from short term calibration, relative marks were given based on how specific setting fulfil above mentioned quantitative criteria.
Sinuosity ranges were quantified using aerial pictures. Same was done for simulated flow pattern for the year 2005 and 2006.
Also turn-over rates were quantified using aerial pictures. General thought is that disturbance on gravel areas of the floodplain is so high that no vegetation can grow. We can deduce that turnover rate for these areas is less than three years, being this time vegetation needs to reach a 100% cover. By identifying vegetation patches on the aerial pictures, percentage of floodplain turned-over within three years was estimated.

Elevation differences calculated by CAESAR greater than three times the mean grain size were used to calculate the percentage of turned-over area. These values were compared with turnover rate estimated through aerial pictures.
This permits to find best CAESAR settings.

2.2.2.3 Validation

The last two years of simulation time were used for validation. Two different validation steps were done: one based on field work data and a second on aerial pictures.
BERTOLDI *et al.* (2010) analysed morphological changes using topographical surveys after seven flood events at the Tagliamento River. The results were analysed by comparing variables “peak water flow”, “total sediment flux” and “percentage of active width” for each event. The first variable expresses maximum water stage between two surveys. “Total sediment flux” is a dimensionless value using the equation for sediment transport of WONG and PARKER (2006, cited in BERTOLDI *et al.* (2010)). This value expresses potential amount of sediments transported by the peak Q. “Percentage of active width” represents the fraction of the active floodplain where elevation changes more than three times the mean grain size between two surveys (BERTOLDI *et al.* 2010).
We think that the data of BERTOLDI *et al.* (2010) even if difficult to get are necessary for validation.
In detail, final output was saved in 30 days steps. Morphological changes were calculated for the time span between two surveys, whereby morphological changes, as BERTOLDI *et al.* (2010) did, were defined as elevation difference bigger than three times mean grain size used in the settings of CAESAR. Doing so, the percentage of simulated morphological changes was compared to field data.
Second, validation was done by comparing visually simulated flow and vegetation pattern with aerial picture 2009.

2.3 Ecological characterization

The ecological characterization was done independently from the CAESAR outcome, because we had the goal to assess the possible use of CAESAR as predictor for spatial distribution of ecological diversity.
Main technique used to characterize ecological variability was aerial picture evaluation and field work sampling. Following steps were done:

- mapping of different landscape types within active floodplain for simulation end date through aerial pictures;
- mapping new landscape type distribution for survey date;
- field data were taken for every mapped unit. Strategy followed during sampling was to cover variability in term of vegetation type, cover and top grain size of each mapped area.

Even if habitat types were not considered but landscape types, it is thought to be the easiest approach. Habitat types are characterised through plant species composition while landscape units are based on vegetation cover and habit and so easier mappable from aerial pictures.

Table 3: Sampling variables

Sampled data	explanation
Height	Height from a reference point at the floodplain edge, which is thought to be constant over time.
Distance from bare sediments	Bare sediment is seen as a good indicator for the distance from the active part of the floodplain, since the definition of important side channels was difficult.
Topping grain size	The same subdivision as for the CAESAR was used (Chapter 2.2.1.1)
Horizon	Description in terms of grain size until heavy coarse gravel layer. At least 30 cm of pit depth.
Ground water influence	Depth at which red/ox features were visible
Vegetation	We characterised vegetation in terms of height of highest plants, age of oldest plants, degree of coverage and main species compostion.

Moreover, having the goal to fit survey data with the simulation outcome, we can sample landscape units independently from the end date of the simulation if for both dates aerial pictures are available.

As third advantage, does this method fasten and simplify the definition of sample locations.

These variables listed in Table 3 are thought to distinguish the defined landscape types. The first three variables are considered to match with the CAESAR outcome

The heights were processed by removing the river bed gradient of the reach. It is assumed that the gradient of the reach does not change much over time so that the CAESAR output can be used to correct the sampled heights. Correction was done by using the final low flow water depth output of CAESAR, which is seen as indicator for the lowest point. A correction surface was calculated interpolating heights for the points with water depth below 0.05m. This

method allows reducing errors done by CAESAR, such as incision and sudden river slope changes, and independency from the model.
The distances of sampled points from bare sediment were calculated by using ArcGIS. Moreover, to get D50 similar to CAESAR we calculated mean size between soil texture and gravel/stone size tacking in consideration the percentage of stone/gravel content.

Each landscape type was characterised statistically in terms of mean values, standard deviation (STD) and standard error (SE) for the sampled variables. Outliers, defined as exceeding the range of mean plus/minus two times STD, were not included.

2.4 Integrating habitat distribution with CAESAR results

Variables distinguishing landscape types which CAESAR could compute were used in a multinomial logistic regression analysis to calculate the spatial probabilities for landscape unit.
Regression was chosen to identify relations between dependent variables "landscape type", which we want to predict, and a set of independent explanatory variables (Tables 3). Two basic regression methods are available: linear regression and logistic regression. Linear regression is used when the dependent variable can take any value between max and min (i.e. stone/gravel fraction in soils), assuming linear relation between dependent and independent variable. Logistic regression is used if the depended variable can take only a fixed number of values; 1 if present and 0 if absent. This is the case for the dependent variable "landscape types" (HOSMER and LEMESHOW 2000).
Because having more than two classes, a multinomial instead of a binominal, logistic regression was done. The multinomial regression analysis is a combination of binominal regression analysis (Schwab 2010).

First step in this analysis is the logit transformation. This allows identifying coefficients (β) for the function explaining the relation between one class of dependent and the independent variables.

$$Logit_a = \beta_1 x_1 + \beta_2 x_{2\,+\ldots+}\ \beta_0$$

The Logit is a parameter that ranges from -∞ to +∞, is linear and continuous and integrating desirable properties of linear regression. This parameter shows how much analyzed classes differ from a reference class ($logit_r=0$) based on independent variables. Interpretation of differences between classes, and so the logits, is case specific. (HOSMER and LEMESHOW 2000)

We defined the coefficients for the Logit function through the "multinomial logistic regression" tool of SPSS. The Logit was calculated spatially explicit using ArcGIS raster calculator.

The Logit was used to deduce the probability for a certain class. The formula

$$Prob_a = e^{Logita} / (e^{Logita} + e^{Logitb} +1)$$ (TEMME 2010)

compares the difference that classes have with the reference class, and computes the overall probability for a landscape type at a certain location. The "+1" in the formula is for the reference $Logit_r=0$ ($e^{Logitr} =1$).

The formula was used in ArcGIS. In a final step, landscape types were allocated by assigning the type with the highest probability to each cell.

3 Results

As in the methodological chapter, we will first show results for the application of CAESAR, followed by the ecological characterisation and finish with the integration of the statistical model within CAESAR results.

3.1 Application of CAESAR

As explained in Chapter 2 (Figure 3) the application of CAESAR is subdivided in small steps. The starting point is the definition of an initial set-up by a sensitivity analysis and spin-up run to create spatial heterogeneous grain size. Afterwards, CAESAR is calibrated and validated using a multi scale approach.

3.1.1 Initial set-up

Input data were processed as shown in Chapter 2.2.1.1 before settings for CAESAR are defined in the following.

3.1.1.1 DEM definition and spin-up settings

Four possible study area sizes were defined. The decision was based on the possibility to define clear and stable Q input points (Figure 9).

The four study area-DEMs were aggregated over the cell-size, to obtain resolutions of 5m, 10m and 15m. Table 4 shows how size and number of DEM cells change over the “study area size” and resolution.

The extent of the study area has a minor effect on cell number for the DEMs with a resolution of 10m and 15m, while on the 5m DEM large changes occur.

CAESAR was run with some base settings to define which of the DEMs is best for studies purpose. In detail, CAESAR was run in ”reach mode”, lowering “*initial discharge*” to 10 m/s, higher “*Initial # of scans*” to 25 and select “*TAU based on velocity*” to calculate shear stress (COULTHARD and DE ROSA 2009). Moreover, a constant input-Q of 50 m³/s was used. This corresponds to the mean yearly Q of the Tagliamento at Venzone.

The formula of the trend line in Figure 10 shows a power of 1.6, meaning that the calculation time rises faster than the number of cells. Combining Figure 10 with Table 4, we can clearly see that calculation time is controlled rather by resolution than by the length of the reach.

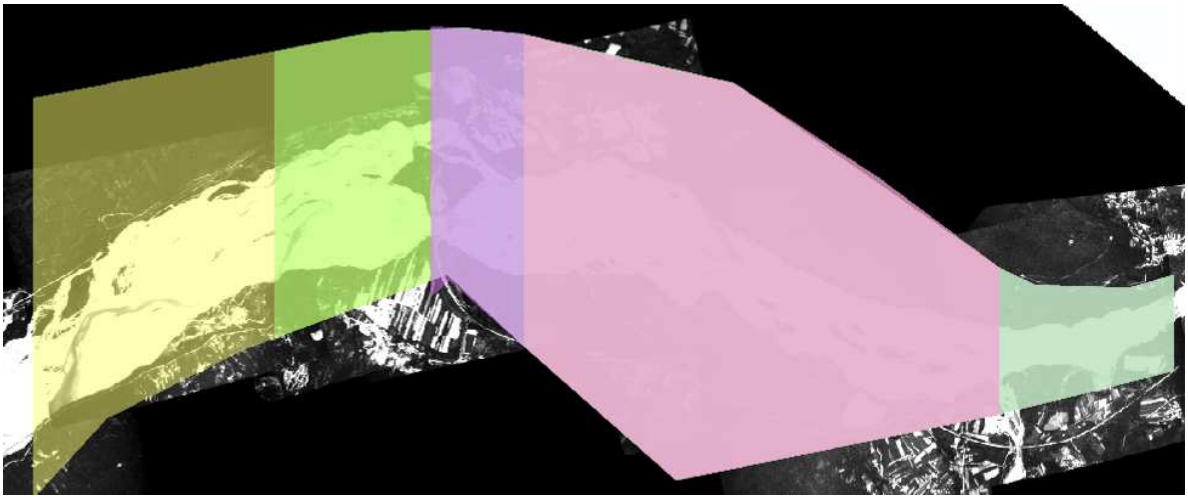

Figure 9: Extent of different study area sizes

1: brown+green+violet+pink+blue

2: green+violet+pink+blue

3: violet+pink+blue

4: violet+pink

5: pink

Table 4: Description of the DEMs used for sensitivity analysis

Study area	Length (km)	05m DEM X*Y	05m DEM num. cells	10m DEM X*Y	10m DEM num. cells	15m DEM X*Y	15m DEM num. cells
1	9.1	1820*752	1368640	910*376	342160	607*251	152357
2	7.2	1434*722	1035348	717*361	258837	478*241	115198
3	5.9	1184*722	854848	592*361	213712	395*241	95195
4	4.5	905*725	656125	454*363	164802	303*242	73326
5	3.8	760*712	541120	380*356	135280	254*238	60452

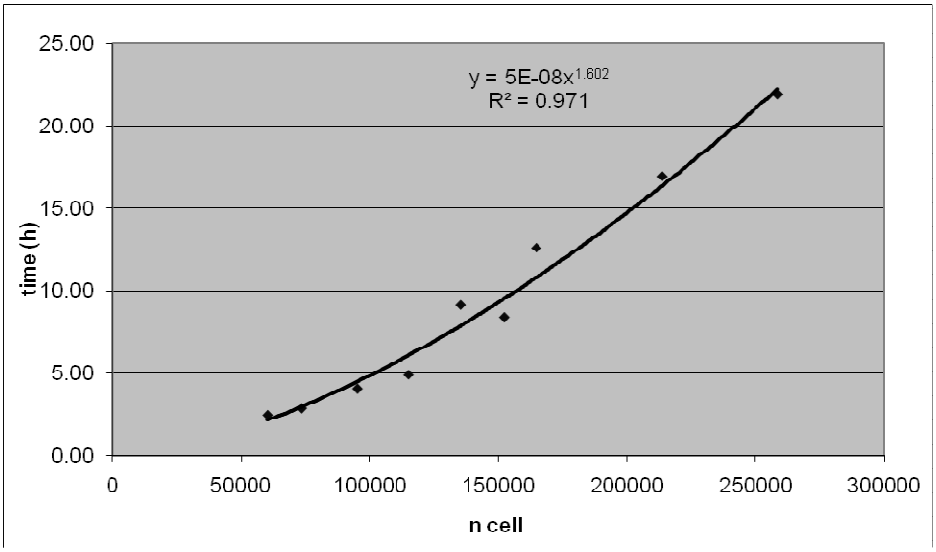

Figure 10: CAESAR calculation time as a function of number of cells in a DEM.

Based on this analysis we choose as the best compromise between calculation time, resolution and size, reach 4 (4.5 km) with a resolution of 10m.

Next, a sensitivity analysis was done by changing model settings that were thought to influence calculation time. The settings of "*erod limit*" and "*Tau calculation method*" were found to have a major impact on the calculation time, while "*Min Q for depth calc*", "*Water depth threshold*" and "*Flow distribution*" showed a relatively smaller impact (Appendix 4). Table 5 shows the settings selected within this step.

Table 5: Summarized model setting found

Parameter	Set model value
Erod limit	0.05
Tau calculation method	Velocity (limit = 1)
Min Q for depth calc	0.0001
Water depth threshold	0.0001
Flow distribution	2

3.1.1.2 Spin-up run

A Spin-up run was carried out to create an initial DEM and grain size distribution file. The general settings for CAESAR shown in Table 5 were used.

A Q input file similar to the Tagliamento hydrograph, with floods returning period of 182 days was designed (Figure 14). In this file, the discharge starts with 1290 m³/s, lowering down to a minimum of 0.34 m³/s after 91 days and increases again, resulting in a yearly bimodal hydrograph.

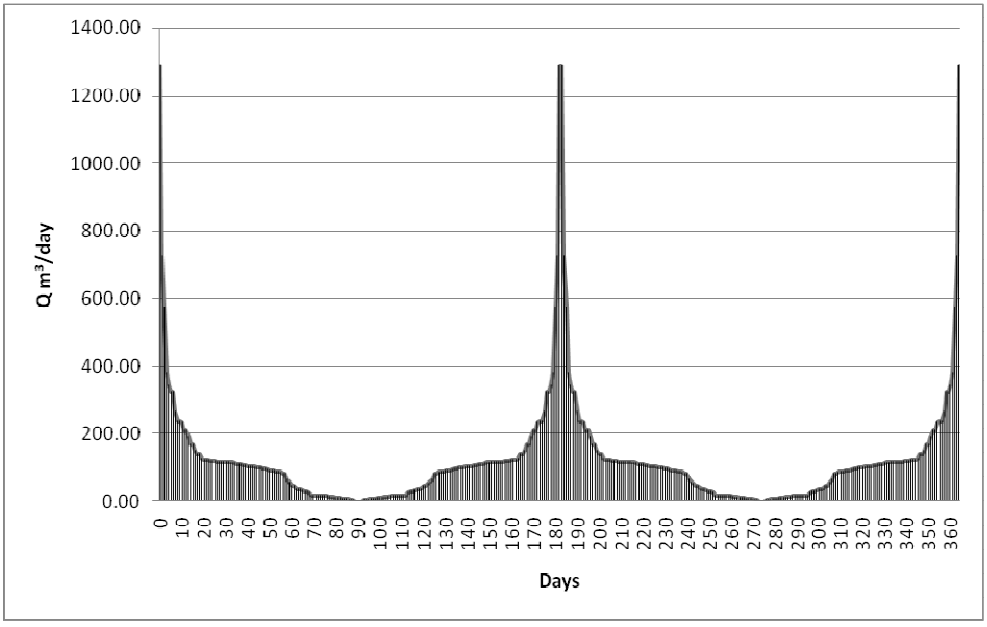

Figure 11: Spin-up hydrograph

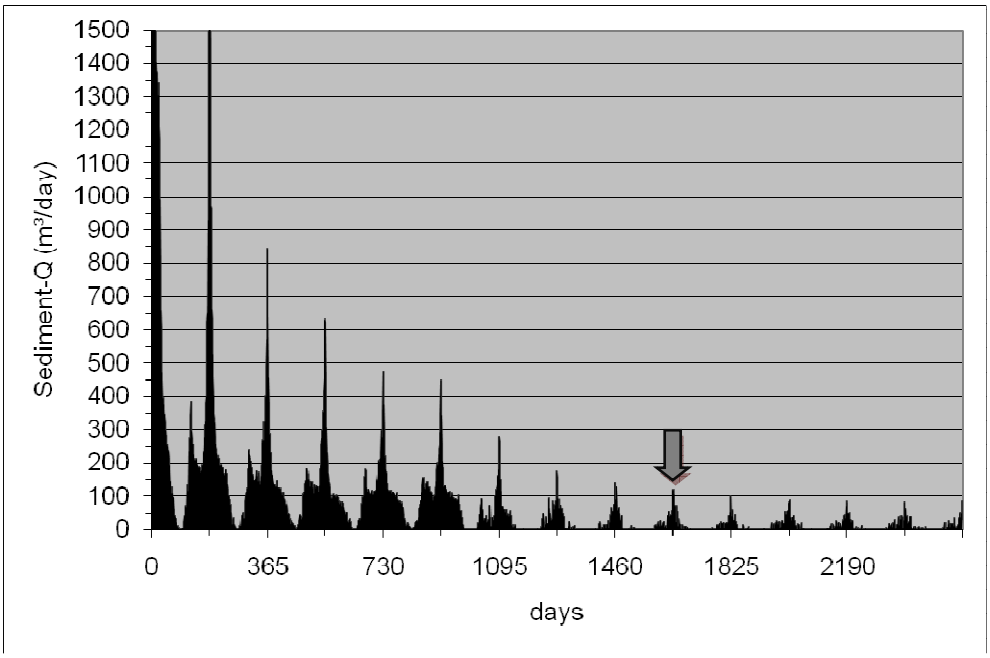

Figure 12: Spin-up sediment discharge over 2555 days

Figure 12 shows the recorded sediment output per day. As soon as the sediment output becomes constant over more flood cycles (every 182 days), spin-up is finished. The model starts with 23586 m³/day of sediments (in the graph this value is cut-off), lowering until the peaks become more constant (128 m³/day) after day 1643.

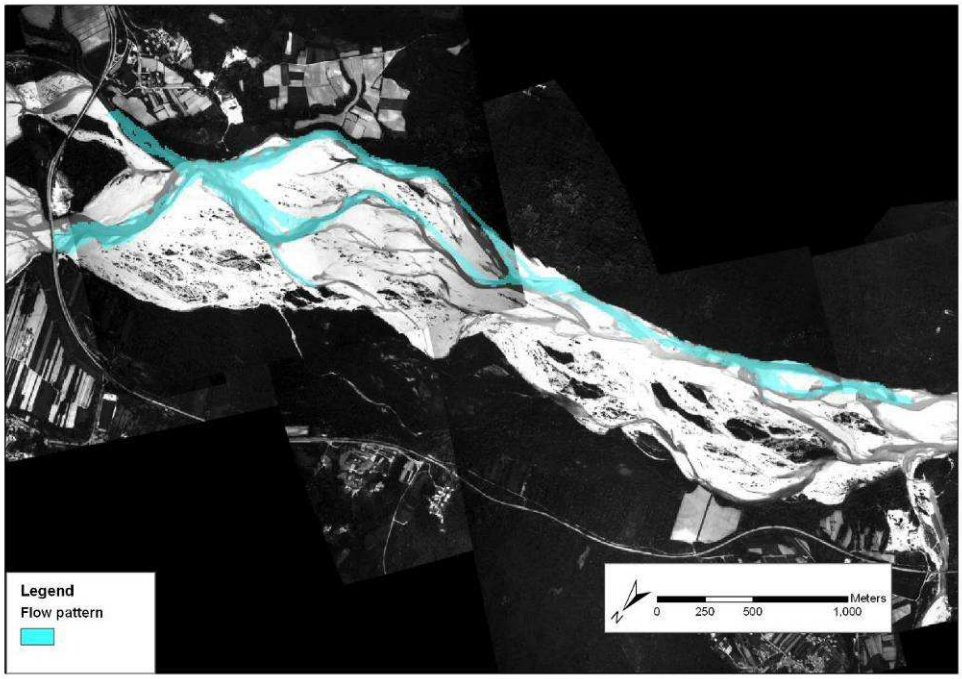

Figure 13: Flow pattern after spin-up run (day 1643)

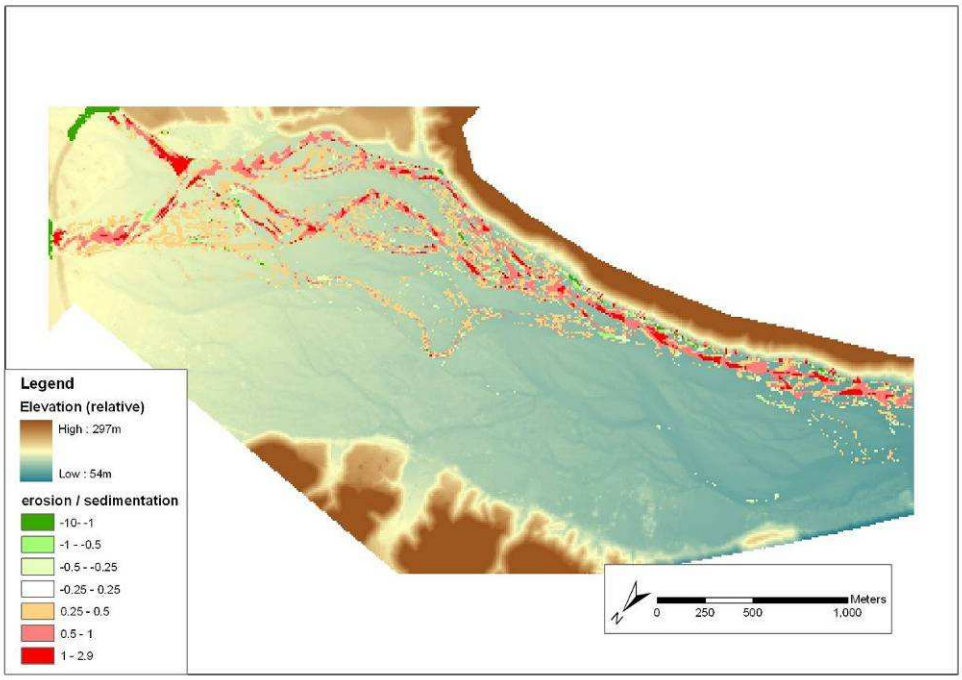

Figure 14: Elevation and erosion pattern after spin-up run (day 1643)

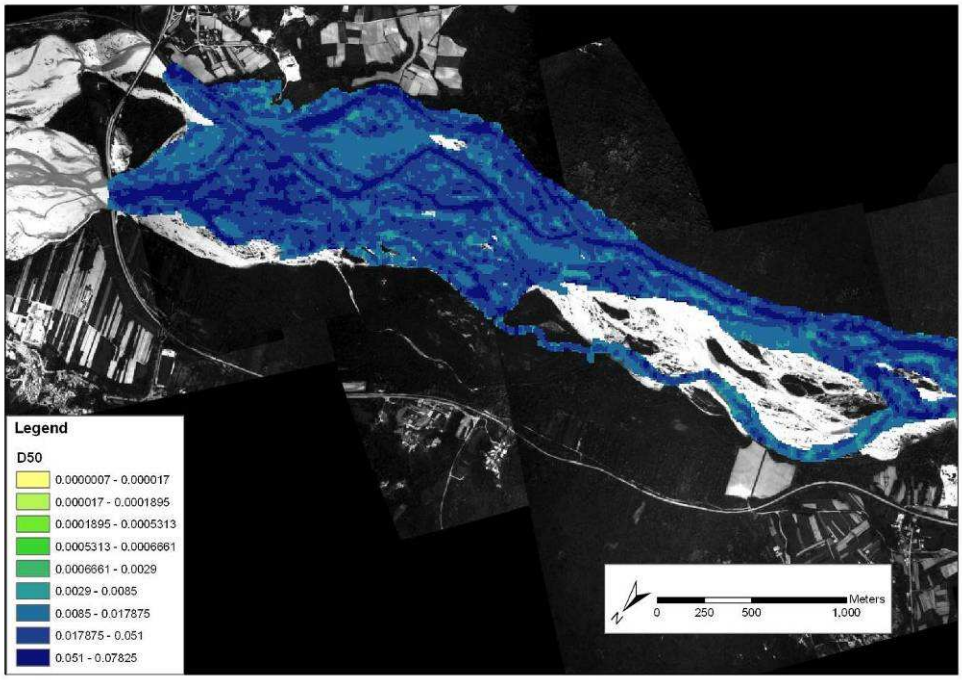

Figure 15: aggregated (3*3) D50 after spin-up run (day 1643)

Figure 13-14-15 show the spin-up results of respectively flow pattern, elevation and D50 (mean grain size). As we can see, the flow pattern at low flow (30m³/s) follows the channel of the aerial pictures 2005.

The DEM changed morphology primary due to incision of the main channel. It can be considered that the spin-up did not change considerably the input floodplain morphology for the later simulation. In the D50 distribution it can be seen that coarser material concentrates in the river bed (blue), while finer material is deposited on higher areas of the floodplain.

3.1.2 Multi scale calibration and validation

For the model setting definition we followed the method proposed in Figure 8 (Chapter 2.2.2).

3.1.2.1 Pre-calibration and sensitivity analysis

In Figure 16 of GURNELL *et al.* (2009), max-Q of the Tagliamento for the years 2005 to 2009 was added with a red cross (05->09 = 280, 727, 577, 1290, 455 m³/s). Bed slope (0.004) is assumed to be constant over the years. We can deduce that the study reach is located on the boundary between the type 1 "braided gravel bed channel only" and type 2 "wandering & braided gravel bed channels, sand bed braided channels". Furthermore, the boundary line between the two types defines the threshold for single thread channels.

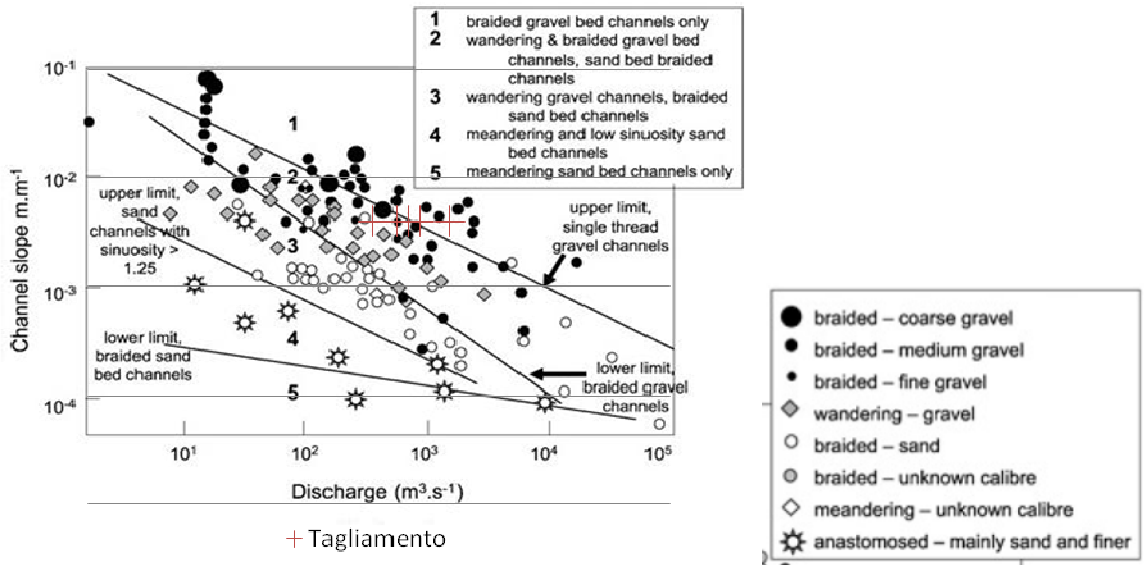

Figure 16: Braiding characterization of Tagliamento river. (data sources: LEOPOLD and WOLMAN, 1957, FERGUSON, 1987, KNIGHTON and NANSON, 1993, BEECHIE et al., 2006, cited in GURNELL (2009))

Looking at the aerial pictures of the study area (Figure 16) it becomes clear that the study reach is divided into two parts, confirming the graph. The western part has more vegetated islands and a single thread channel, while the eastern part has more patched vegetation and at least two main branches.

In general the two defined braided river types are characterised by:

- Braided gravel-bed: high stream power, variable discharge, erodible banks, wide shallow channels and a wide active zone (with some vegetation);
- Wandering gravel-bed: lower stream power and sediment load and frequently vegetated, leading to greater sediment aggradation and more stable channels.

(FRANCIS *et al.* 2009; GURNELL and PETTS 2006)

Knowing the braiding type, criteria for the calibration of the processes of avulsion and lateral erosion can be defined by using literature.

BERTOLDI *et al* (2009) summarised the processes for the Tagliamento based on discharge (in the original water height at Villuzza is used - Figure 17). The study area analysed by BERTOLDI *et al* (2009) integrates the studied reach.

Even for the Tagliamento, Figure 17 can be considered as general valid reference schema for comparable rivers. Braided rivers should have a similar curve between returning period and discharge. Even if sediment supply and quality change and hydrograph range differs, the listed process will happen at the defined return period of a certain Q, otherwise the river cannot be braided. Based on this, processes can be fit to the same position on the curve even if Q is different.

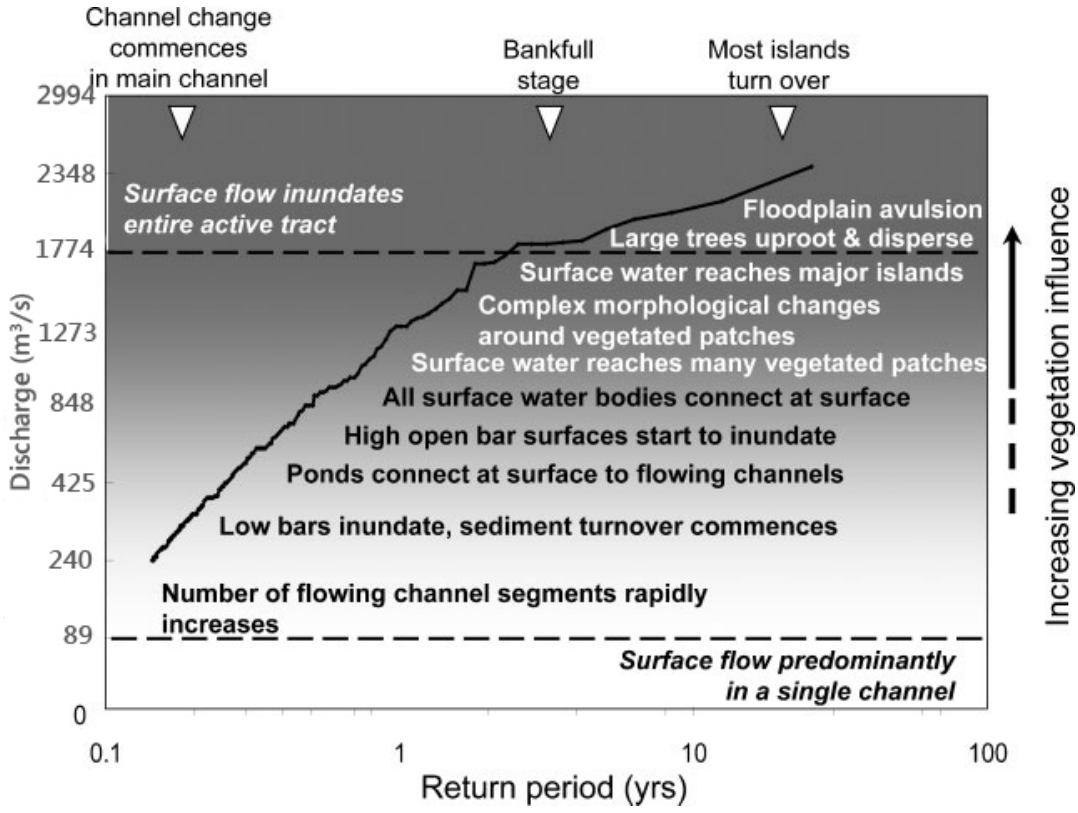

Figure 17: Processes defined by returning period and discharge (original water stages were translated into discharges using the formulas of WELBER *et al.* (unpublished)) (BERTOLDI *et al.* 2009)

Out of Figure 17 we generally define that :

- Low flow = flow in one channel
- Lower floods / flow pulses = primary lateral erosion, small changes in turnover and channel pattern.
- High floods = primary avulsion, big changes in channel pattern and high turnover rates.

(BERTOLDI *et al.* 2009; GURNELL *et al.* 2009; WARD *et al.* 2002)

Now, that processes and pattern are clear for the study reach, a sensitivity analysis for the lateral erosion settings was carried out.
Different settings of *lateral erosion*, *velocity limit to calculate tau* and *edge smoothing values* were tested. Different Q (10-30-50-100-300-1500 m^3/s) were used to assess whether CAESAR simulates the correct behaviour. These Q-values were chosen due to their returning period within one year (BERTOLDI *et al.* 2009).
As an example, four combinations of different settings of CAESAR are compared in the Table 6.

Table 6: Pre-calibration run settings

	T3	T10	Tx	Tx2
Edge value	80	80	80	80
Lateral erosion	3	10	10	3
TAU_vel	2	2	1.75	1.75
Calculation time (h) for 15 days and 25 days	2 -	2.15 9.65	1.45 4.95	1.33 4.66

Visually, *edge smoothing value* of 80 was identified as best option. This option does not create many meanders keeping the flow straighter. The alternatives proposed in Table 6 might change in the later calibration steps.

In order to determinate the most realistic CAESAR settings, Figures 18-19-20 compare discharge (Q), total sediment transport (sed-Q), and percentage of the streambed that has eroded or deposited more than 0.25m (%turn) for the four combinations.
Figure 18, shows that at low discharges turnover increases slightly with increasing Q, while above threshold of 50 m^3/s the graph becomes steeper. This might be due to the fact that flow lower than 50 m^3/s hardly exceeds the set velocity limit, so that the lateral erosion parameter controls the amount of lateral erosion. At Q higher than 50 m^3/s, velocity increases until set limit. This is visible when comparing for instance T10 and Tx, which differ only in set

velocity limit to calculate tau; at the beginning both rise identical until reaching 50 m³/s. From this point on lateral erosion is influenced by the velocity. Contrary, if looking at the line of Tx and Tx2, which differ in the *lateral erosion* values; both run parallel to each other.
Looking at Figure 19, which compares sed-Q response to Q, similar behaviour can be seen as in Figure 18. The curve is steeper for runs with a high *velocity limit to calculate tau*.
Based on Figure 20 the strength of lateral erosion power can be deduced. The steeper the curve, the more sediments are eroded from the river side and not from the river bed. Turnover rates increase faster than Sed-Q at lower Q, indicating that the dominant process in this lower range is the lateral erosion. However, at higher Q one can see that while sediment-Q increases rapidly, the lateral activity increases only slightly, indicating the dominant process of bed erosion. Bed erosion at high water stages causes avulsion.
This reflects the criteria of braided rivers defined before.

Further on, looking at Figure 17, one sees that between Q 240-425 m³/s, sediment turnover commences. This corresponds with all four model results (Figures 18) which have a strong sharp bend in Sed-Q at 300 m³/s.
Taking now in consideration also calculation time (Table 6), we can say that it increases two times by increasing the *velocity limit to calculate tau* threshold of 0.25.

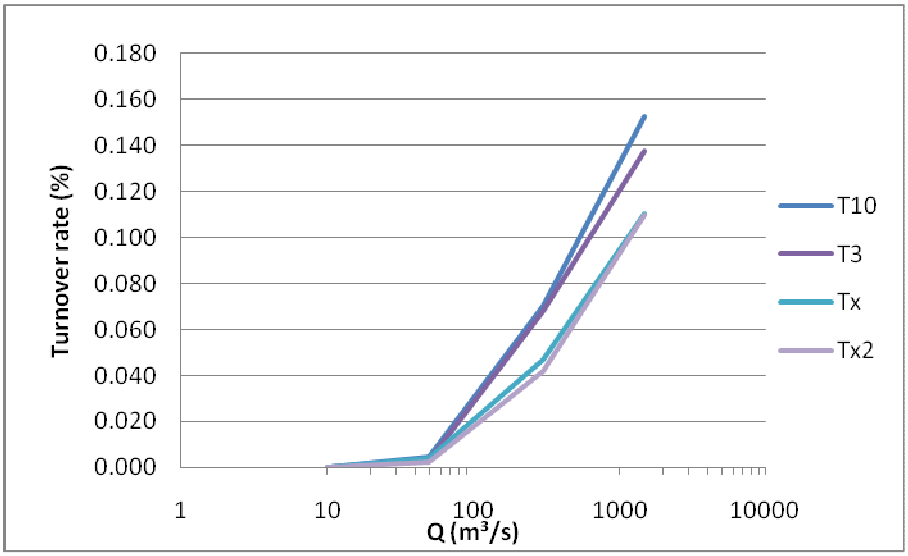

Figure 18: Pre-calibration indices comparison total flow (Q) and lateral turnover rate (% turn).

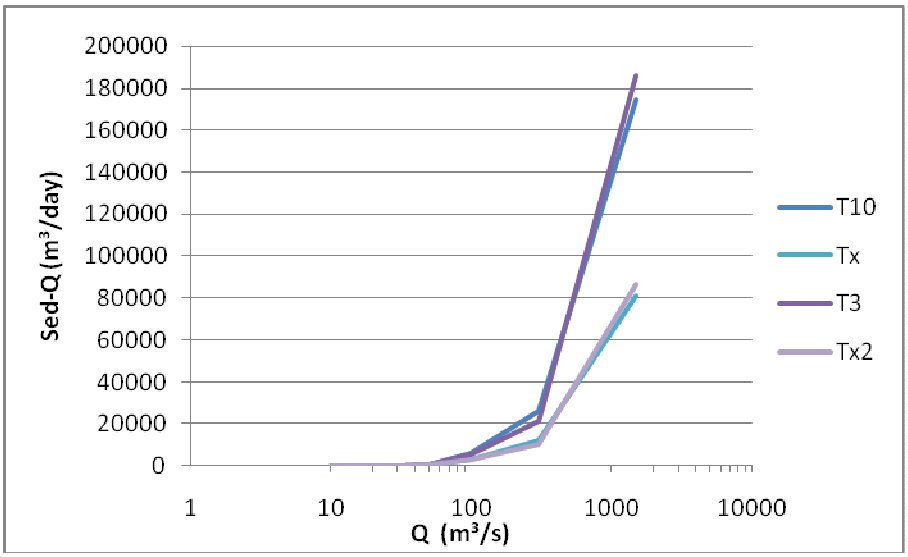

Figure 19: Pre-calibration indices comparison total flow (Q), sediment transport (sed-Q)

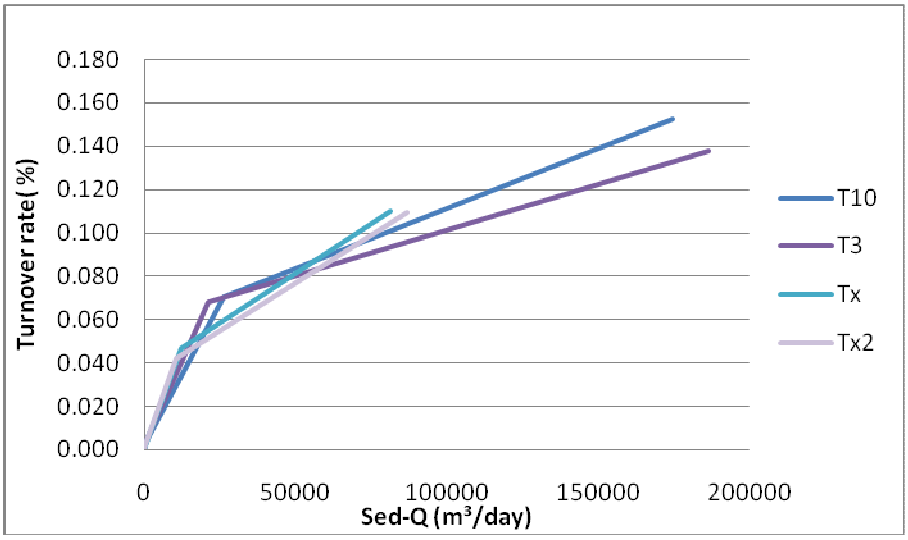

Figure 20: Pre-calibration indices sediment transport (sed-Q) and lateral turnover rate (% turn).

As a conclusion, the best combination of settings in this preliminary step is Tx. The combination yields low calculation time and lateral activity increases more gently with increasing Q. Even if there is not a large difference between Tx and Tx2 a lateral erosion value of 10 is recommended, because lowering incision keeps the channel shallow and wide. However, in the next calibration step T10, Tx and Tx2 were reconsidered, to assess their relative validity with real dataset.

3.1.2.2 Calibration

The best settings of the pre-calibration were applied to real discharge from 2005-2009 and the results evaluated in two steps.

First, a short term calibration was done. Relative marks were based on a visual comparison of different settings for small events. The same process description as for the pre-calibration (page 35) was used for the comparison. The criteria calculation time was used again because if its importance. Doing so CAESAR settings were adjusted, knowing the previously studied sensitivity of each parameter.

Secondly, mid-term calibration was carried out by using quantitative criteria: sinuosity was defined using aerial pictures 2005-2009 and compared to the modelled channel. Turnover rates were estimated by calculating the non-vegetated area of the floodplain, which is thought to be turned-over at least every three years (the time that vegetation needs to develop). It was estimated that 94% of floodplain is turned-over in three years, resulting in 31% and 62 % turn-over respectively after the simulation year 2005 and 2006.

Table 8 shows the comparison of criteria for both calibration steps.

Table 7: marks for criteria used for short- and mid-term calibration

Criteria	Run 6 (T10-TAUvel 1.5)		Run 7 (Tx)		Run 8 (Tx2)	
	05	06	05	06	05	06
Calculation time (h) for ½ Yr. and 1 Yr.	8 26.6	 66.75	16.16 61.83	- -	14 48	- -
Erosion / Avulsion Low flow = one channel lateral erosion avulsion wide shallow channel	 3U-2M-1L a a a	 3BU-2M-1L a b a	 3U-BM-2L c c b	 - - - -	 2U-2M-1L b b c	 - - - -
Sinuosity upper (1.27-1.21) lower reach (1.04-1.10)	1.23 1.05	1.18 1.05	1.28 1.04	- -	1.32 1.10	- -
Turnover rates year 05 (31%) and 06 (62%)	26.8%	40.15	46.5%	-	32.8%	-

Low flow: U= upper channel; M = middle channel; L = lower channel; B= braided; numbers = channel number.
Lateral erosion: does it happen only predominantly at low flow? Is it too much?
Avulsion: does it happen during floods? Is it too much?
Wide shallow channels: are they present in the upper reach?
Marks: a = good b = mid c = bad relative to each other

The settings of Run 7 (Tx of the pre-calibration) had a high calculation time and performed relatively bad compared to the other two model runs over the first year. Lowering *lateral erosion* (Run 7 compared to Run 8), calculation time goes down by about 1/3 and also the performance becomes relatively better (Table 8).

Regarding Run 6, in which *velocity limit for the Tau calculation* is lowered relative to the combination of setting of T10, the calculation time and performance are best.
Therefore, the parameter set for Run 6 was selected and run until year 2009.

3.1.2.3 Validation

In validation, CAESAR was run for the time period 2005-2009, with the settings defined through the previous calibration.
Comparing the modelled flow with the flow pattern of the aerial pictures 2009 (Figure 21), a quite good fit can be seen. Even though the pattern does not fit 1:1, it follows the more active part of the floodplain. In addition, water flows in a single channel in the eastern part and splits in the western part as in the aerial pictures. However, in the first part of the modelled channel the river incises laterally much more than the real river (red line). Following the flow pattern one can asses other examples in which the channel incises laterally in the bedrock.
The most probable reason is the wrong boundary setting of the bed-rock, which excludes this area. Other error sources could be the 50% split water input source of the model around the eastern island and the low set *edge value* in the lateral erosion settings which control sinuosity of modelled channel.
Also in the west simulated flow passes between the two islands, while in the aerial pictures the main channel is shifted to the south. Still, CAESAR routed the flow within the most active part.
Overall, not expecting a complete match with reality from a reduced complexity model, this can be considered as a good result.

It was difficult to assess the performance of the vegetation index (Figure 22). In general, the eastern vegetation values are lower (around 0.2- 0.4), while the western values are higher (close to 1). The upper part is occupied by the most dynamic area of the floodplain, flooded regularly also with lower flow pulses.
Overall, the estimation of the vegetation pattern is possible. Problems arise from difficulties in setting vegetation parameters such as development time and critical shear stress. The linear sub-model for vegetation of CAESAR is designed for grass growth, while vegetation in our study reach develops from willow bushes until the final succession stage of wood (e.g. on islands). This, in combination with short modelling time which is less than one succession cycle (20 ears), makes it difficult for the CAESAR user to differentiate more vegetation structures.

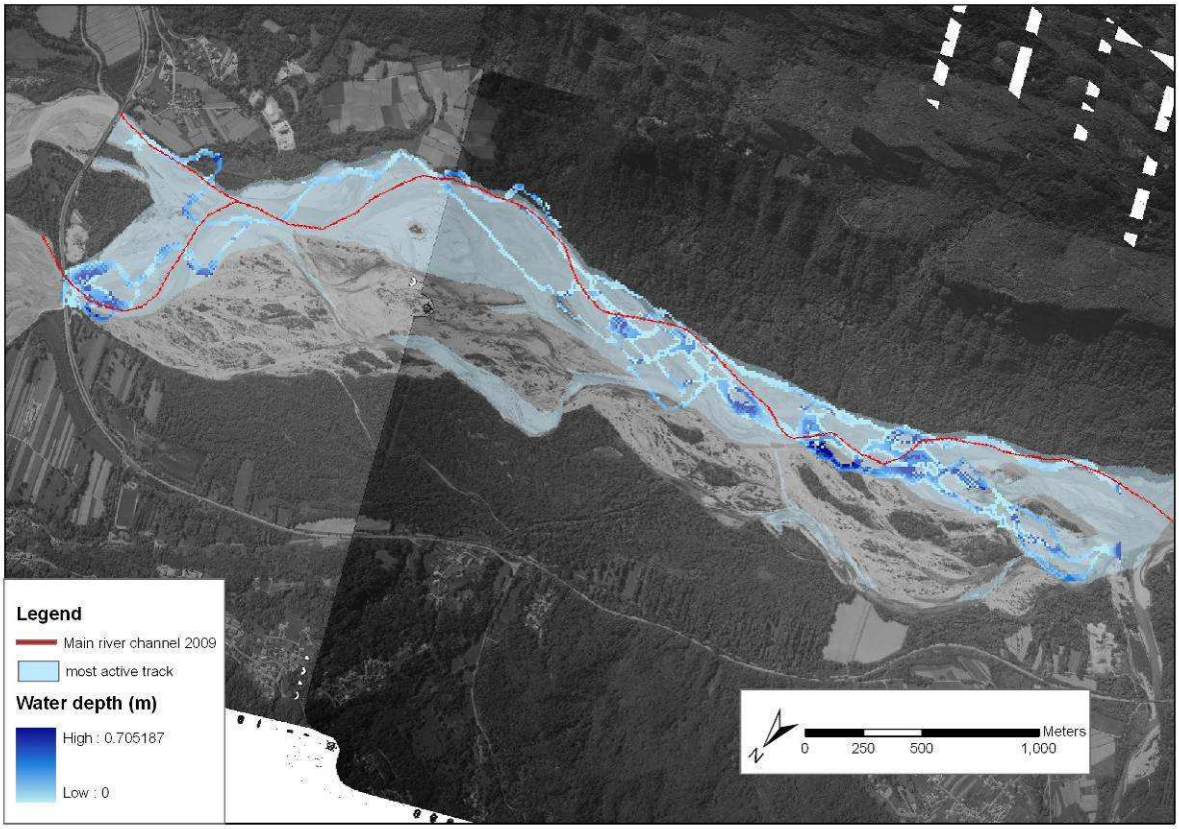

Figure 21: Flow pattern of the model at the end of the simulation (2009)

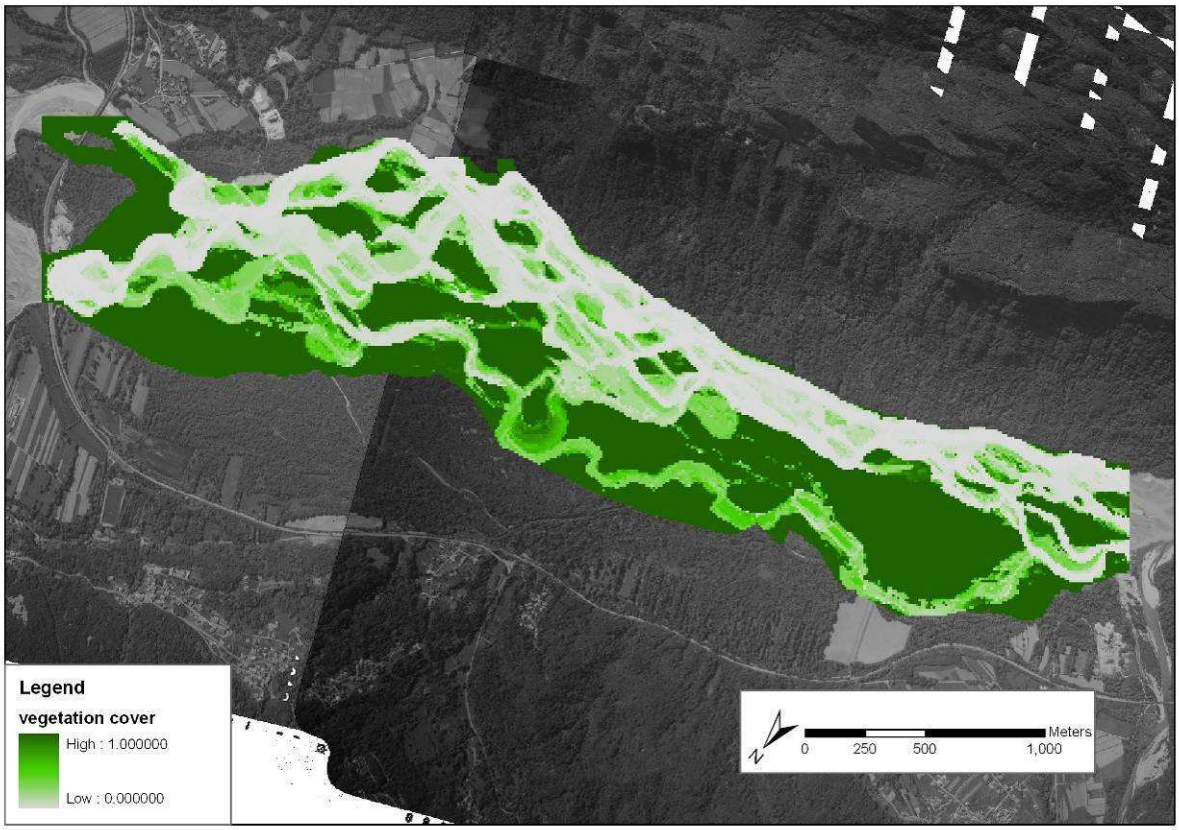

Figure 22: Vegetation cover development for grass at the end of the simulation (2009)

The result shows where grass has the opportunity to grow until 100% cover, based on dynamic properties of each cell. This is assumed to be similar with resprouting or seedling development of willows.

Generally, vegetated areas of the aerial pictures fit with the vegetated areas of the index (compare Figure 21-22).

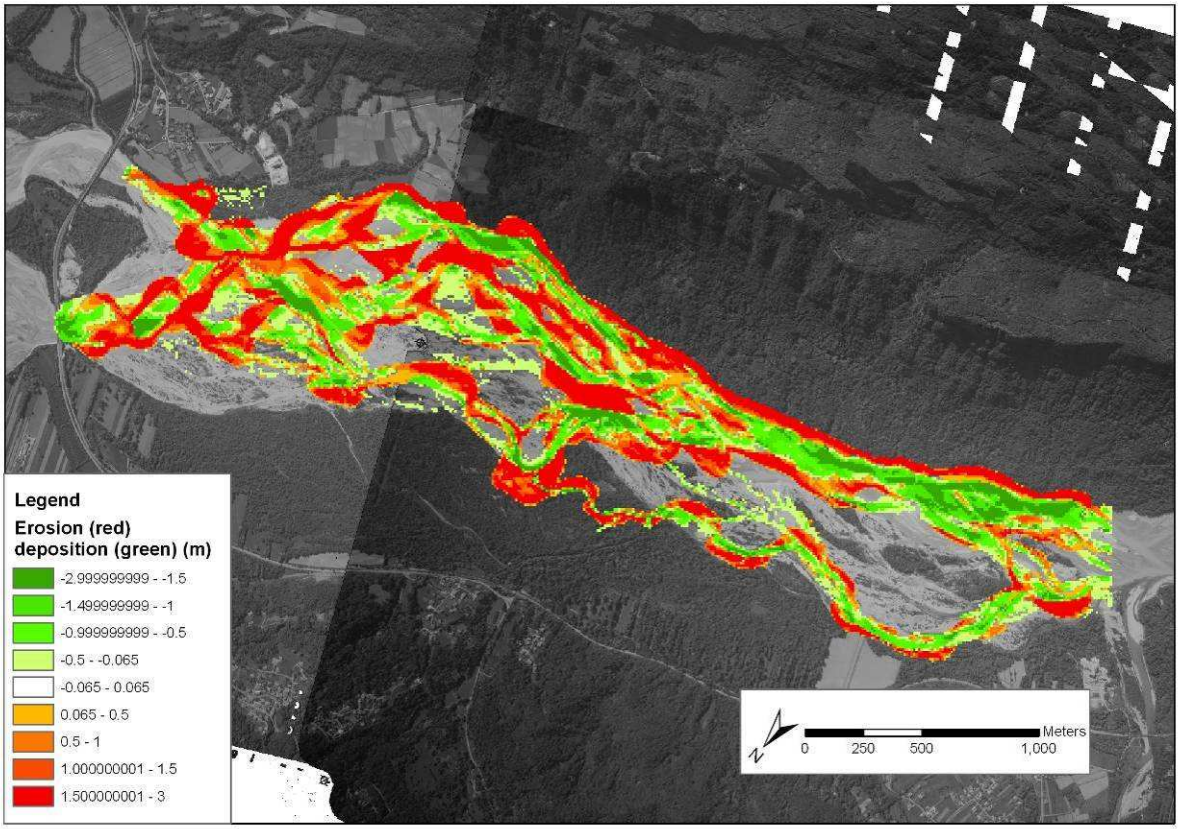

Figure 23: Erosion sedimentation pattern of the model at the end of the simulation (2009)

Looking now at Figure 23, the final erosion pattern (red) and sedimentation pattern (green) can be seen. Lateral erosion patterns clearly show the moving meanders and the filling of old channels. Especially for secondary channels this is visible. In general, the eastern part is more active having a higher planar turnover, while the western part has a more stable central area and channels shift less.

As explained for the flow pattern, highest errors are made on the southern border of the floodplain due to uncertainty while creating the bedrock file, so that in some places the river incised laterally in the mountain removing up to 32 m of material. The resulting DEM integrates these errors so that we can consider that it does not fit 1:1 to reality. Nevertheless, from a broader scale, it reflects stability of different zone of the floodplain.

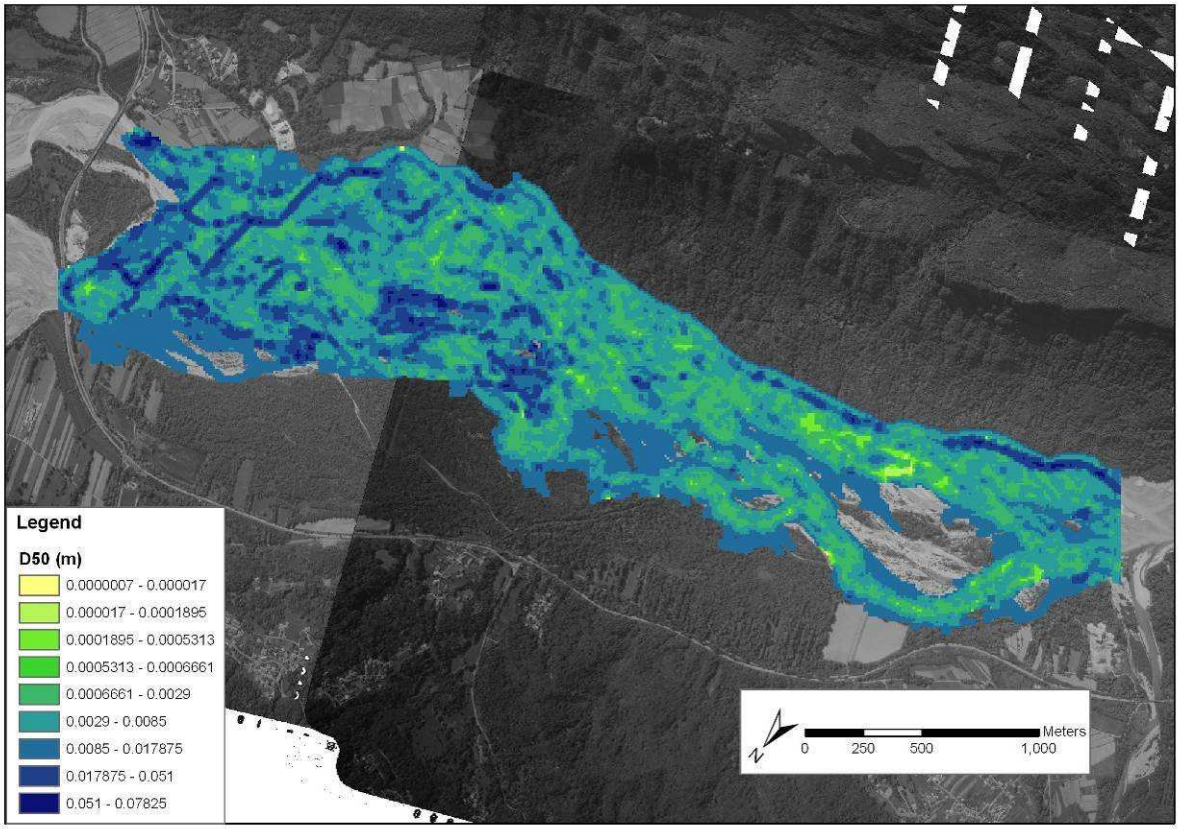

Figure 24: Averaged (3*3) D50 of the model at the end of the simulation (2009)

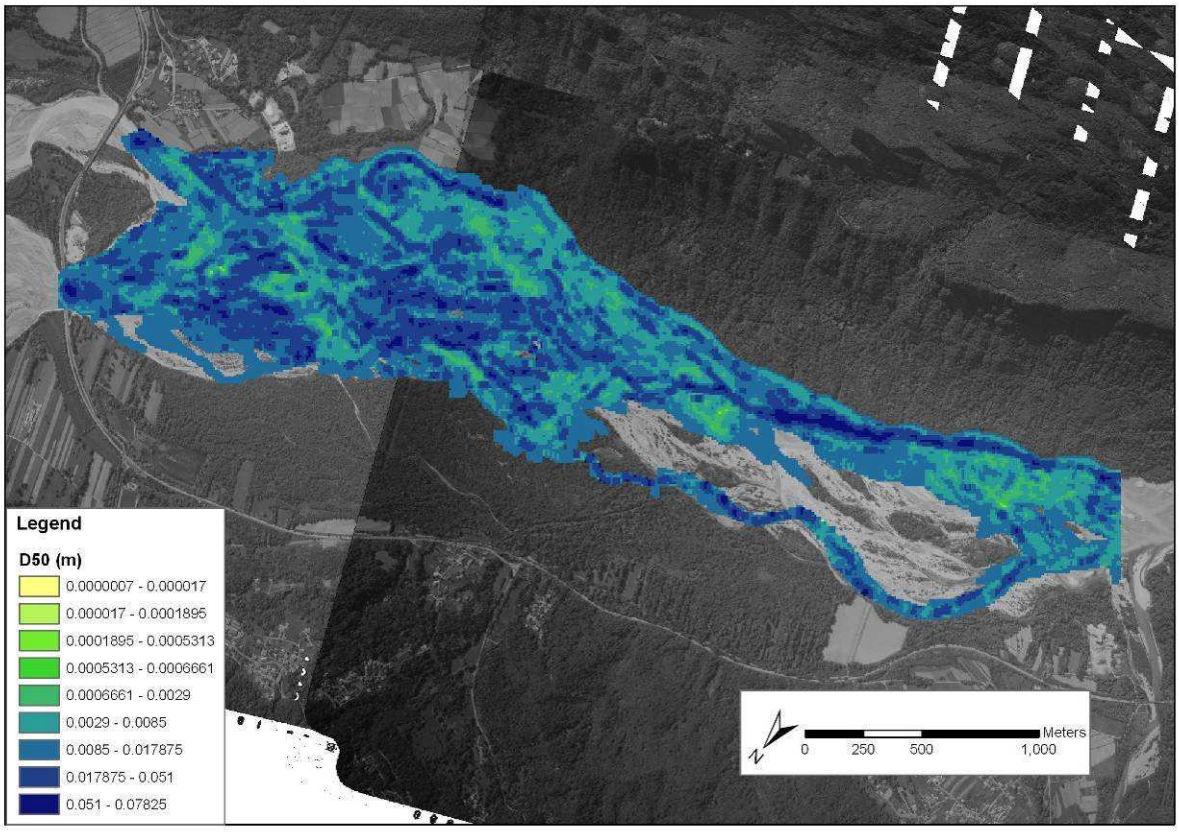

Figure 25: Averaged (3*3) D50 of the model at half of the simulation (2007)

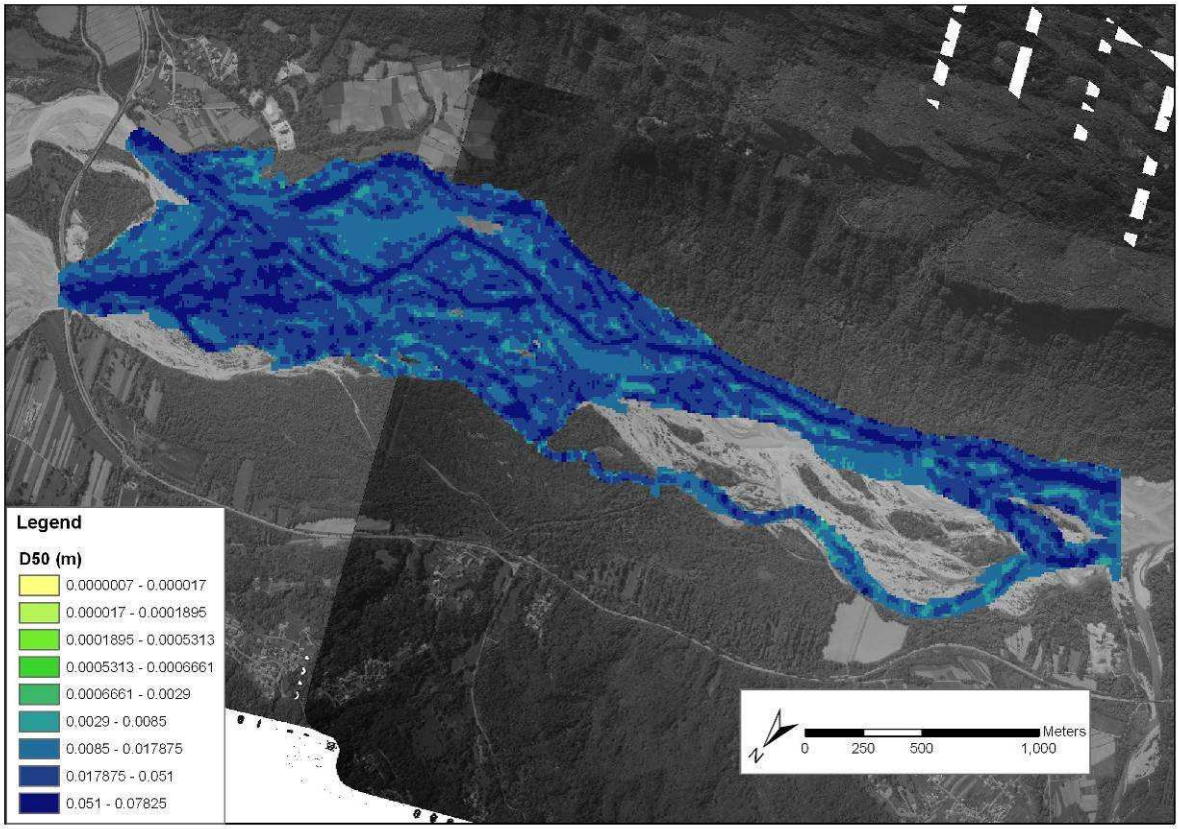

Figure 26: Averaged (3*3) D50 after spin-up run (2005)

Finally, in Figure 24 the simulated aggregated (3*3 cells) D50 sediment size is shown. The result was aggregated to get a better visual comparison by eliminating smaller variations.

The sediment size is coarser along the main channel. Especially in the left and right part of the figure, bed armouring can be seen, while the middle channel did not armour due to rapid shifting flow over the past simulated years.

The right part has a large area (transparent) which was not flooded over the simulation time. This shows different channel stabilities of the right and left part of the study reach.

Comparing now visually the result with the starting D50, D50 looks coarser in 2005 (Figure 26) that in 2009 (Figure 24). The grain-size distribution 2007 is coarser than in 2009 and finer than in 2005. This is also confirmed by Figure 27 which shows an overall decrease of mean D50 over the simulation time from 0.032 m in 2005 to 0.008 m in 2009.

Furthermore, from a visual comparison one can see that the flooded area (extend of D50) enlarged, based on areas where morphological changes occurred during the simulation.

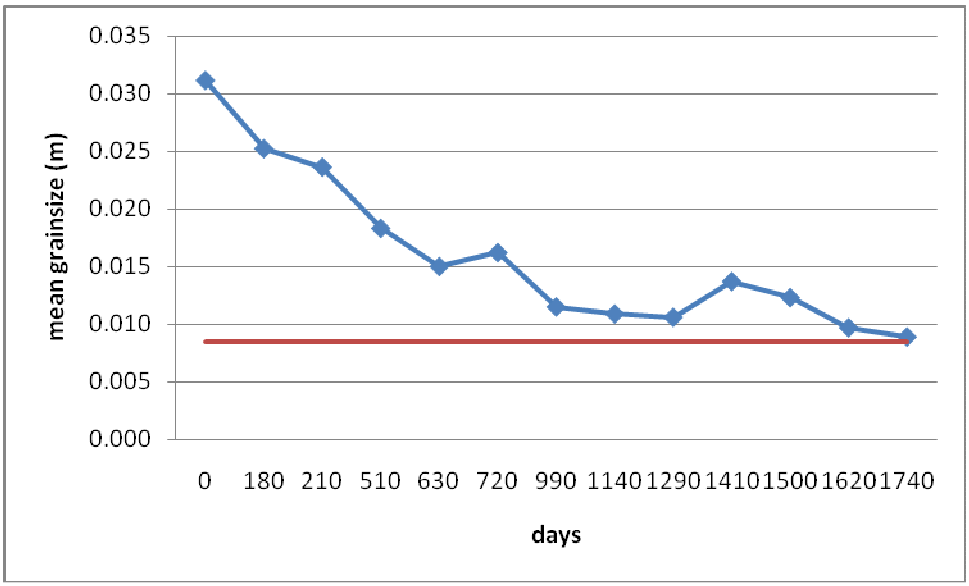

Figure 27: Development of the general mean D50 of the study area over the simulation period.

To understand the decreasing mean D50, sediment discharge (m^3/day) per water discharge (m^3/day) was computed. In Figure 28 the overall sediment discharges per cubic meter of water increases rapidly until day 200. After, high oscillations can be observed, indicating the adaptation of the sediment discharge to hydrograph fluctuations. Moreover, one sees that the finer the sediments, the more the concentration increases in time. The clay fraction (green line) increases faster than coarse sand (yellow line) and gravel (orange). This is reasonable, because finer sediments are transported easier than coarser sediments and accumulated in the ricirculated water.

Combining the previous data, it can be explained that the increasing sediment discharge is due to the effect of the spin-up run and the later integration of lateral erosion. During the spin-up run, easy erodible sediments where flushed away so that a new deposition in the study area was not possible. This causes average D50 to increase until 0.0032 m.

All through the later simulation, lateral erosion incised in new sediment layers that were not turned over during the spin-up, adding finer material to the ricirculated water (CAESAR assumes a sediment layer every 20 cm with a grain size distribution as defined in the settings).

Looking now at Figure 27 one can asses that the simulation integrates for almost the entire period, the adaptation of the overall mean D50 to 0.0085 m which corresponds to the initial set D50. The adaptation phase is visible until day 1740 to 0.0087 which is close to the set D50 grain size distribution.

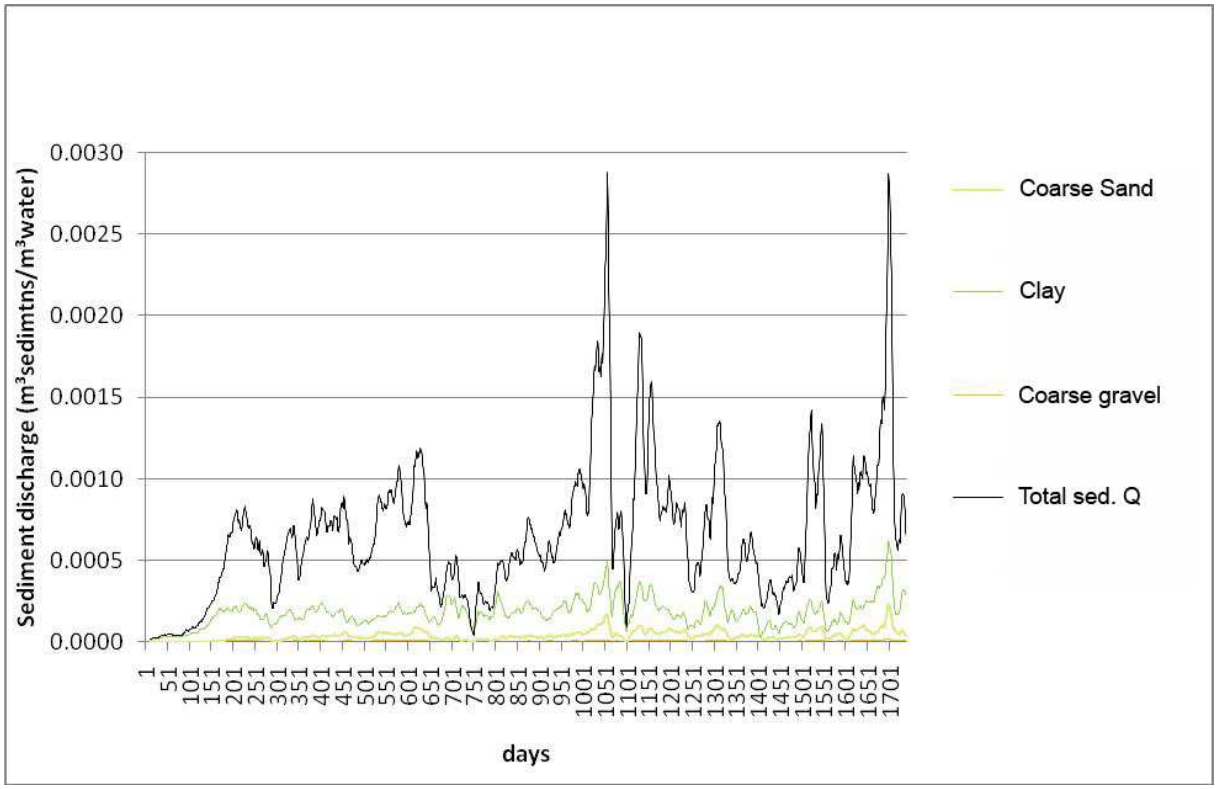

Figure 28: Sediment discharge per m³ water over simulation time.

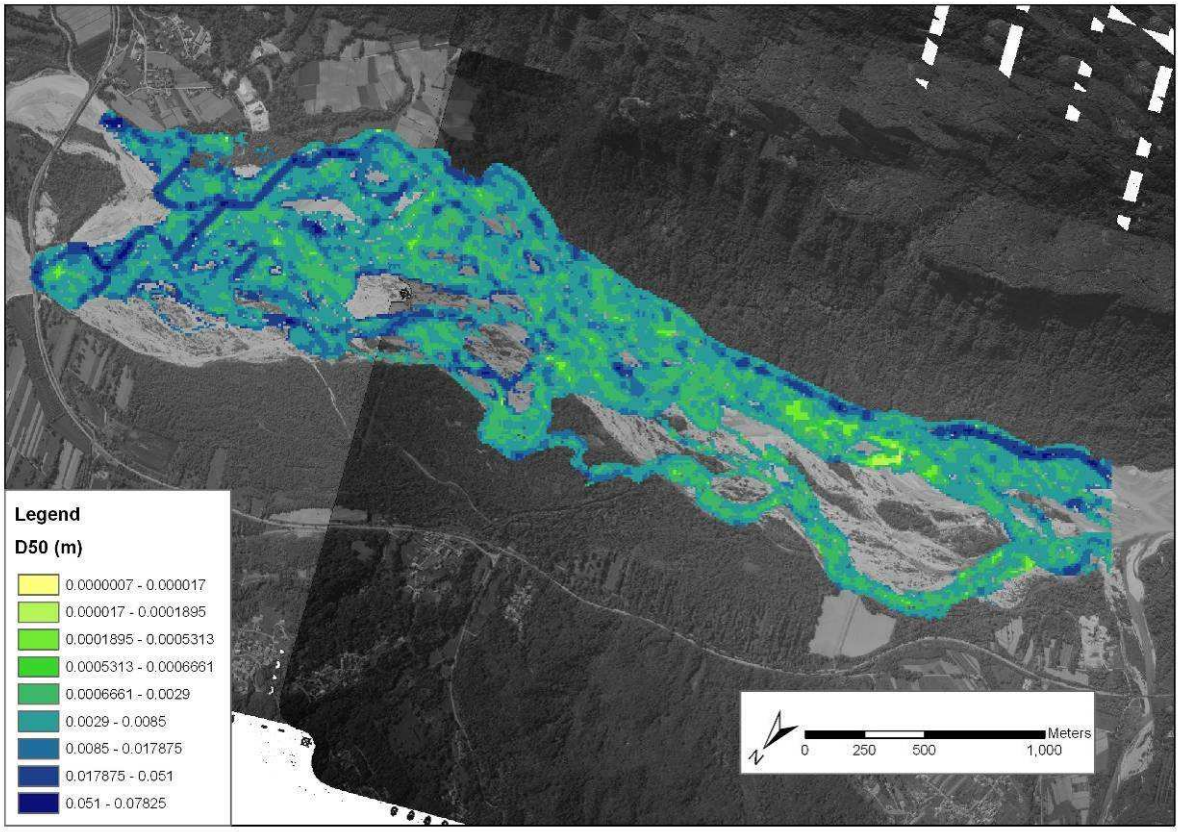

Figure 29: Final D50 distribution (2009)

Looking now at the D50 distribution in relation with the elevation one can assesses that on higher spots the D50 gets coarser, while in secondary channels and areas close to the main channel finer sediments deposited. This effect was caused by the above explained failed spin-up run so that it can be considered as a modelling error. Coarse material on high spots is still the falsified D50 of the spin-up which was not turned over during the simulation.
A comparison of D50 within the study area is only possible in areas that were turned-over during the simulation as shown in Figure 29. In all other areas the D50 is unrealistic.

A second validation was done using morphological survey data from BERTOLDI *et al.* (2010). Even though the data were taken a few kilometres stream upward, error is considered negligible. The survey data used are shown in Table 8.
One can notice that the simulation saving dates do not match with the survey dates of BERTOLDI *et al.* (2010). Nevertheless, in most of the cases differences are about a few days, which is negligible when considering that time span between two surveys is a few months.

Table 8: Description of the validation surveys (BERTOLDI *et al.* 2010).

Event	Peak water-level (m)	Discharge (m^3/s)	Flood duration (h)	Model duration (h)	Event date	Survey date	Model date (model day)
0	-	-	-		-	17/06/2007	19/06/2007 (900)
1	0.71	137	4	24	28/09/2007	15/10/2007	18/10/2007 (1020)
2	2.03	577	50	48	25/11/2007	13/12/2007	16/12/2007 (1080)
3	1.10	177	17	24	13/01/2008	03/04/2008	17/03/2008 (1170)
4	1.62	466	93	96	19/05/2008	29/07/2008	15/07/2008 (1290)
5	2.67	458	24	24	15/08/2008	17/09/2008	13/09/2008 (1350)
6	3.04	1290	247	240	30/10/2008	26/11/2008	12/12/2008 (1440)

The graphic below (Figure 30) compares “percentage of active width” with “peak water level”. “Percentage of active width” indicates the fraction of the floodplain where elevation changes more than three times the mean grain size. BERTOLDI *et al.* (2010) defined a mean grain size of 0.04m, while in this study the mean value of 0.065m (0.021m*3) was used, corresponding to the mean set grain-size classes of CAESAR.

Comparing the results, one can see that over the entire survey time (triangles in Figure 30) the model overestimates the flood plain active width at lower peak discharges and underestimates the effect at higher peak discharges. The events 3 to 5 show the lowest errors, while events 1 and 6 show the largest. Active width for the water level of 2.65m is similar to the water stage of 2m. This can be explained due to the short duration of the event with a comparable high water stage (Table 8).

red= triangles blue =dots

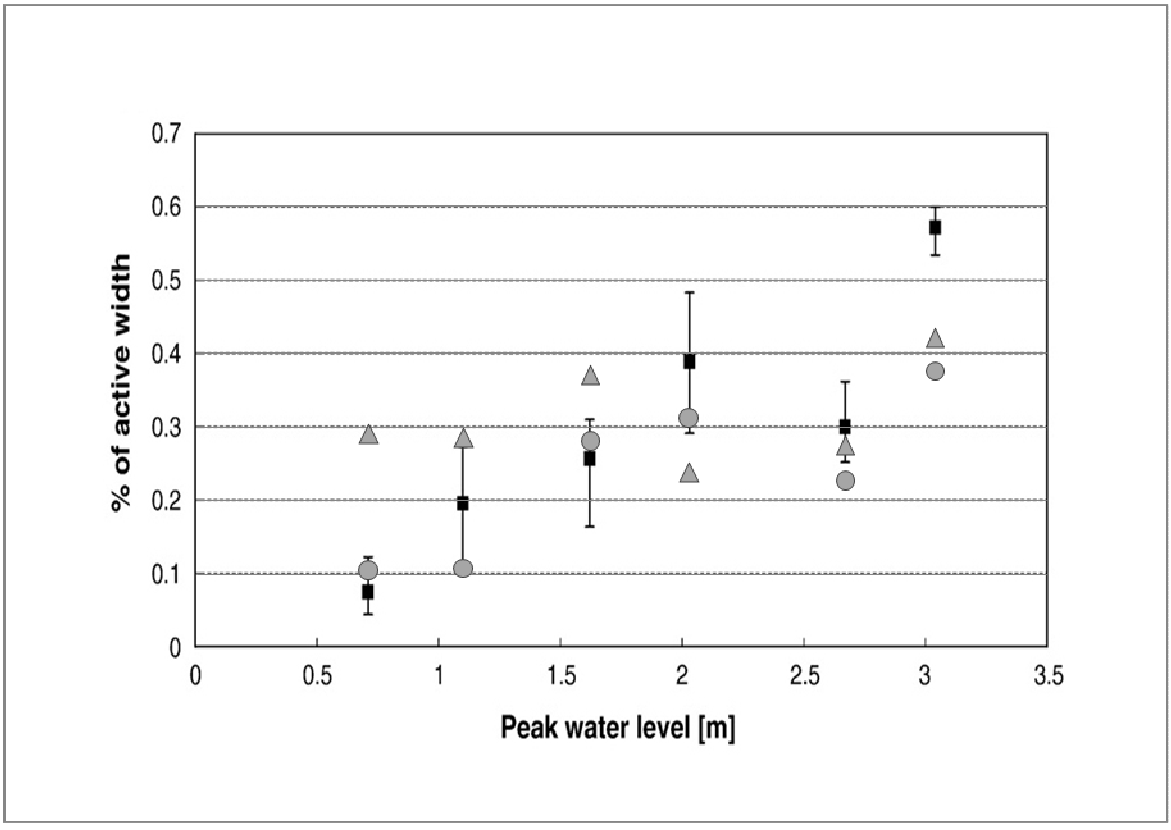

Figure 30: Comparison of the percentage of active width related to the peak water level at Venzone:

Triangles: total percentage active width of the model output over the entire survey period.

Dots: total percentage active width of the model output over maximum flood period.

Black: field survey data (BERTOLDI *et al.* 2010).

The additional flooding time in the model may induce larger turnover rates than in reality. Therefore, the effect of single flood events, which BERTOLDI *et al.* (2010) declares as main actors for morphological changes within two surveys, was compared. CAESAR was run again over 30 days ending with the surveyed floods. Knowing the duration of the event (Table 8), the elevation difference that occurred within this time frame was calculated. Comparing the duration of the simulation with the duration of the real flood (Table 8), one can assess large time differences for the first (0.71 m water height) and third flood (1.10 m).

The results of the single flood events are shown in Figure 30 with the dots. These correspond more to the surveyed data. Considering also the standard error bars, simulation follows better the field data until water levels of 2m (580m³/s). Only for very high floods CAESAR underestimates the active width. Nevertheless, CAESAR should reproduce activity between surveyed dates and not of the single event.

The results suggest high activity during low flows and a quite low activity during high floods. The erosion processes during floods performed relatively well (dots), only the cumulative effect of low flow period in-between the events has too high activity (triangles). Especially for the event at water level of 2m, which has a percentage of active width that is larger if the single event is considered than the activity over the entire surveyed period, this effect is visible. The cause is a missing calibration for low flow.

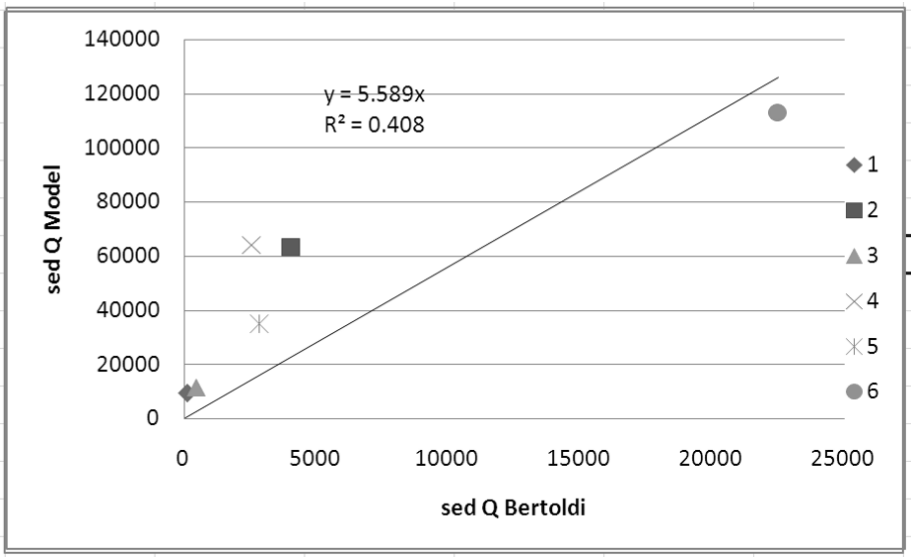

Figure 31: Relation sediment flux from BERTOLDI *et al.* (2010) and the model output.

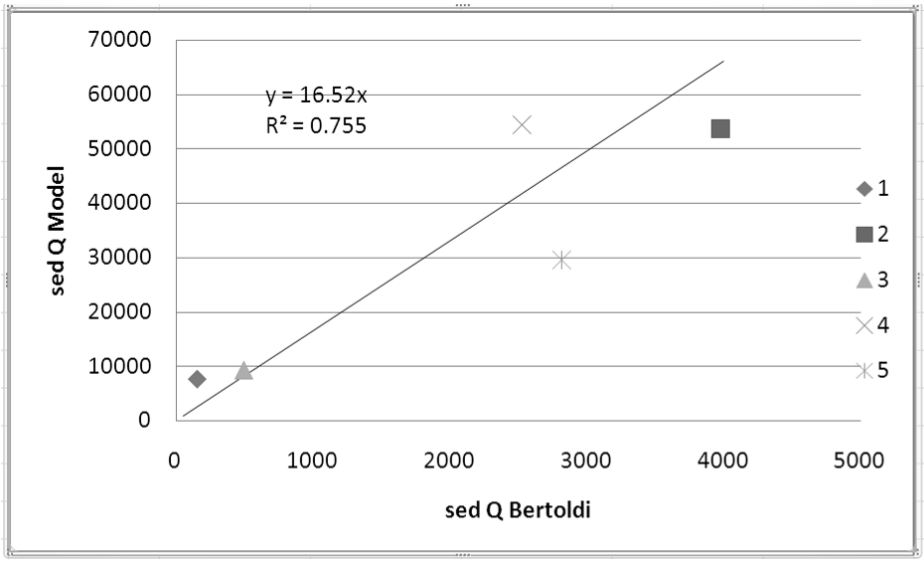

Figure 32: Relation sediment flux from BERTOLDI *et al.* (2010) and the model output without flood 6.

Table 9: R and R^2 for the correlation between model and BERTOLDI *et al.* (2010) sediment flux calculation.

Missing events	R	R^2
no 6	0.869	0.755
no 4	0.841	0.707
no 2	0.778	0.606
no 5	0.657	0.432
all points	0.639	0.408
no 3	0.496	0.246
no 1	0.472	0.223

BERTOLDI *et al.* (2010) calculated the dimensionless potential sediment flux per flood and compared this with the percentage of active width.

In Figure 31, the sediment flux of BERTOLDI *et al.* (2010) was compared with the one calculated by CAESAR for each event. The results show that R^2 (0.0408) is rather low, indicating no significant correlation. For some events the simulation dramatically over/ underestimates the sediment fluxes.

To define which event has the highest error, correlation was recalculated by removing event by event. In Table 9 one can see that the highest significant R^2 is given when event 6 is removed from the correlation analysis.

Table 10: Reliability of the validation events.

Event	Bertoldi Sed-Q	Model Sed-Q	Problems of the data
1	50	8624	Large simulation time than reality (Table 8)
2	400	9880	
3	2500	62259	Large simulation time than reality (Table 8)
4	2800	33446	
5	4000	61531	Large flashy Flood
6	22500	111074	Bertoldi measure is an outlier (mean +- 2SD), the models one not.

Table 11: Comparison of the different regression formulas excluding some events with BERTOLDI *et al.* (2010) reference data

	Event 1	3	4	5	2	6	
al points X=Y/5.589	1543	1768	11139	5984	11009	19874	
Reference minus calculated	-1493	-1368	-8639	-3184	-7009	2626	
fraction of error	30.86	4.42	4.46	2.14	2.75	0.88	7.6
without 6 X=Y/16.52	522	598	3769	2025	3725	6724	
Reference minus calculated	-472	-198	-1269	775	275	15776	
fraction of error	10.44	1.50	1.51	0.72	0.93	0.30	2.6
Only 4, 2 X=Y/14.33	478	547	3449	1853	3409	6154	
Reference minus calculated	-428	-147	-949	947	591	16346	
fraction of error	9.56	1.37	1.38	0.66	0.85	0.27	2.3

Also when removing events 4 or 2, correlation increases significantly. Still, events 2 and 4 can be considered the more reliable ones, as shown in the Table 10, because they have the lowest probability of measuring mistakes.

This suggests that CAESAR computes the highest error for the 6th event.

For a closer assessment, the formulas of the previously analysed regression lines (formulas in Figures 31-32) were used to "translate" the simulated sediment discharges into the unit-less sediment flux of BERTOLDI *et al.* (2010). These values were then compared with the reference values of BERTOLDI *et al.* (2010) as shown in Figure 33- 34 below. Table 11 allows a more detailed comparison.

Based on Figure 33, one can assess that including all points (dark gray) largest absolute errors are made for events 4 and 2. If event 6 is removed from the regression line calculation (white), only event 6 shows a large absolute error. Also values of the regression formula

created only with event 4 and 2 (light gray) behave similar to the previous one, only with a steeper gradient.

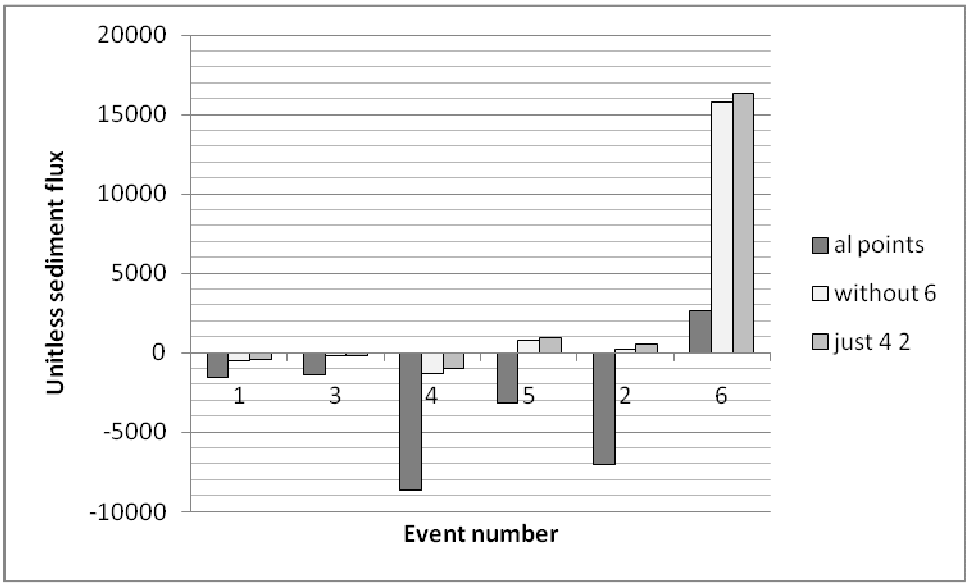

Figure 33: Absolute error relative of the translated model values into the BERTOLDI *et al.* (2010) system using different regression line.

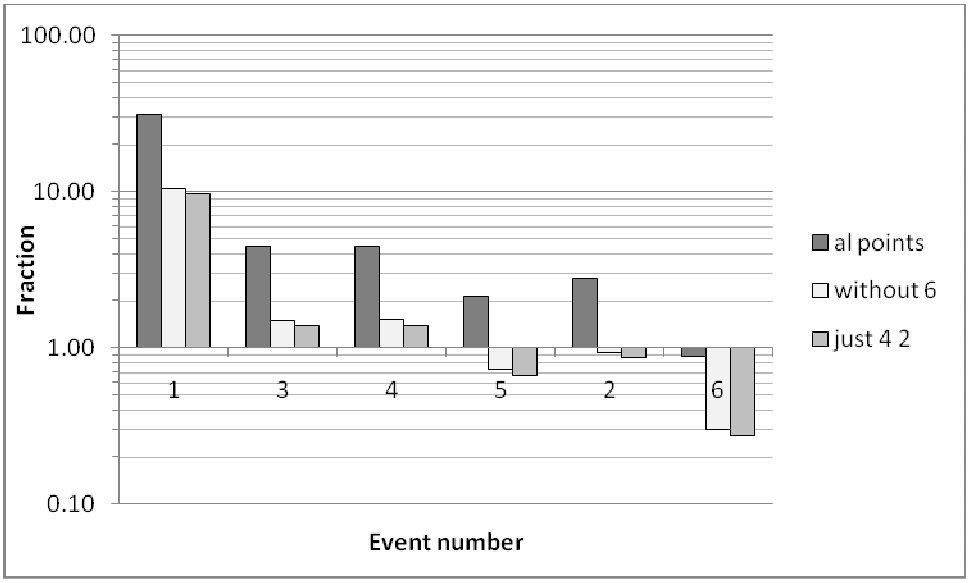

Figure 34: Fraction of the error relative of the translated model values into the BERTOLDI *et al.* (2010) system using different regression line

To asses better where CAESAR computes largest errors, the fraction of error relative to reference values was calculated. The results are shown on a logarithmic scale in Figure 34. Based on this graphic it becomes clear that CAESAR overestimates 30 times the sediment flux of the first event and underestimates 0.3 times the largest flood if the regression formula

including all points is used (dark gray). The fraction error for the other events ranges between 3 and 4 times the reference values. The overall mean fraction error is 7.6 (Table 12).
When comparing the fraction error by excluding event 6 (white) in the analysis we can assess that this lowers down dramatically. The fraction error for the first event goes down from 30 to 10, while for the events 4 to 5 vary in the range 1.50 to 0.72. Only event 6 increases fraction error form 0.88 to 0.30.
Over all mean fraction error excluding the sixth event decreases from 7.6 to 2.6 (Table 11). When using the formula including only point 4 and 2 because the most reliable, mean fraction error decreases even until 2.3.
The results, excluding event 6 and by using only events 4 and 2, show the same error pattern as shown in Figure 30 (peak water level compared to percentage activity). This suggests that CAESAR completely misses the sediment discharge for event 6.
In summary combining the quantitative validation results, lateral activity and sediment discharge should be lower for flow pulses and lower floods, while both should increase for extreme flood events.
Even if the low flow processes are overestimated and peak floods are highly underestimated, one can assess that especially the elevation and the flow pattern can be used for further integration with prediction of landscape type distribution. The vegetation parameter can also help by defining the dynamic properties of each raster cell if taking in consideration that the calculation is especially valid for grass growth. The sediment distribution (D50) is only valid in the areas turned-over during the simulation time, so that a comparison for the entire floodplain is difficult.

3.2 Ecological characterization of the landscape types

In the following, the results from the fieldwork carried out in the period 24-31 march 2010 are presented.
The following steps were done as described in Chapter 2.3:

- mapping of different landscape types within the active floodplain for the model end date by using aerial pictures;
- mapping the new landscape type for the sampling date;
- taking field data for every mapped unit. Here, the sampling number should cover the variability in terms of vegetation type, vegetation cover and top sediment size of the mapped area.

3.2.1 Spatial distribution of the landscape types

Based on the aerial pictures 2009, landscape types were mapped for the date in which CAESAR simulation ended. The landscape types were mapped visually at the scale of 1:5000 using mainly the criteria vegetation cover and habit. Four different units were defined: bare sediments, large scale patchy (LS patchy), small scale patchy (SS patchy) and wood. Figure 35, shows the appearance of the different units.

Afterwards, occurred morphological changes for the time range 2009-2010 were mapped from the hill in the south of the study area. Subsequently, landscape types were mapped for the sampling year 2010.

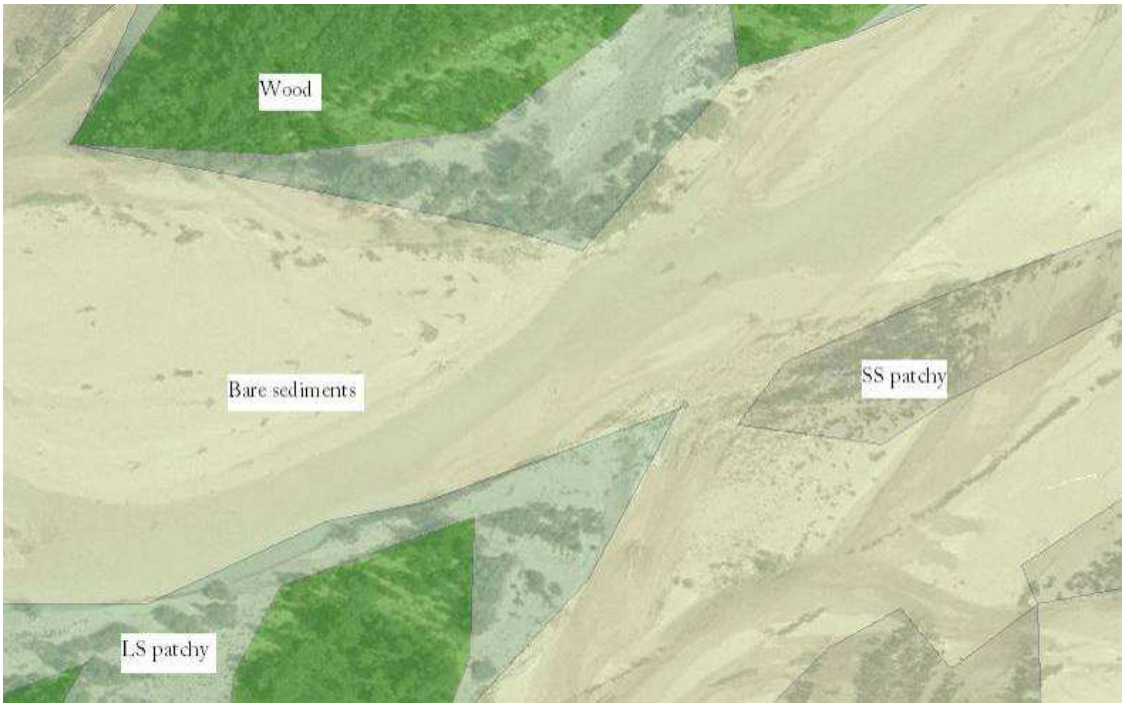

Figure 35: example of mapped landscape types.

Figures 36-37 show the distribution of landscape types for the simulation end-date 2009 and the sampling year 2010. Not many changes occurred in this period. Most are found for sediments and LS patchy vegetation, which change spatial distribution especially at the northern border of the floodplain and change slightly overall percentage of total surface. Still, bare sediments increase the relative percentage while LS patchy decreases (Table 13).

Wood and SS patchy do not change considerably in terms of both spatial distribution and overall percentage, but looking at the relative percentage in Table 13 changes are visible. The lowest relative percentage of change of wood indicates the higher stability of this landscape.

The main channel shifts closer to the southern border of the floodplain and looses sinuosity, developing a more straight flow.

Table 12: Percentage of mapped landscape units 2009 and 2010

Landscape types	**2009 %**	**2010 %**	**Relative increase %**
Wood	10.2	10.6	4.2
Sediments	50.7	54.3	6.7
LS patchy	34.3	30.6	-11.0
SS patchy	4.9	4.5	-8.5

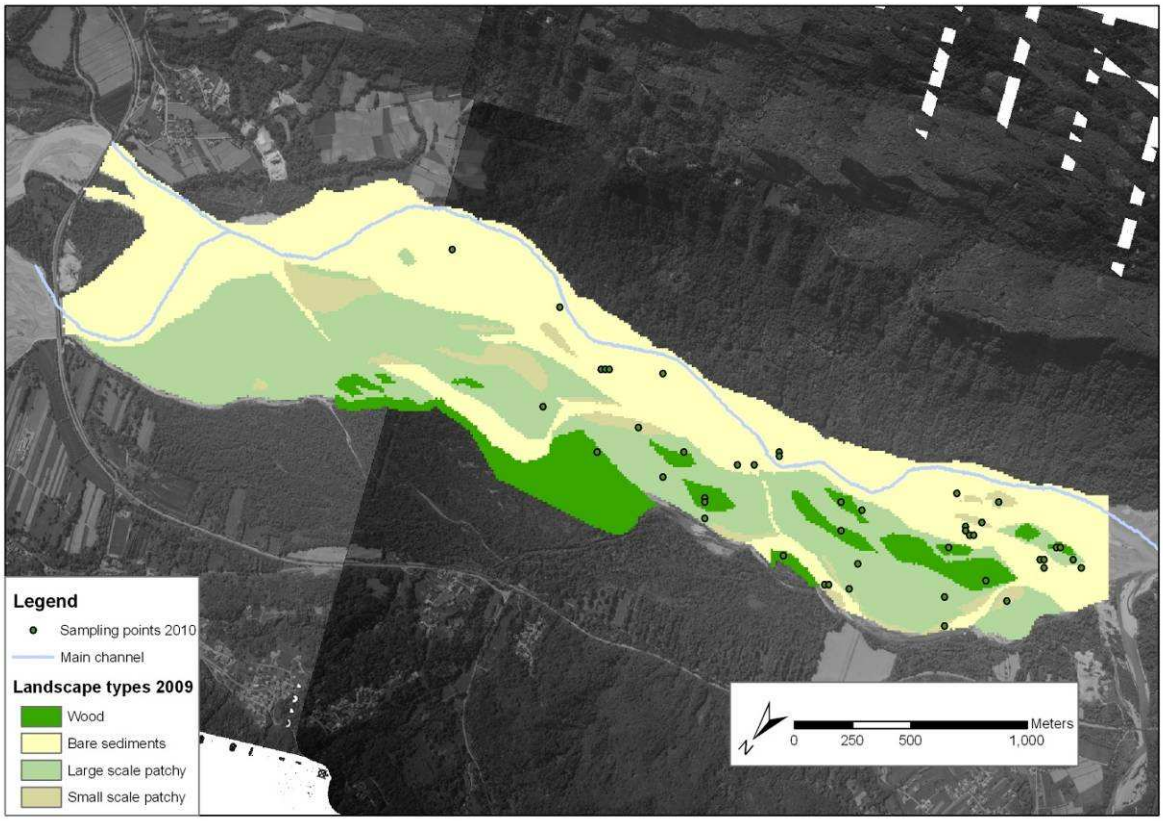

Figure 36: Mapped landscape types and main channel 2009. Moreover, the sampling points taken in 2010 are shown.

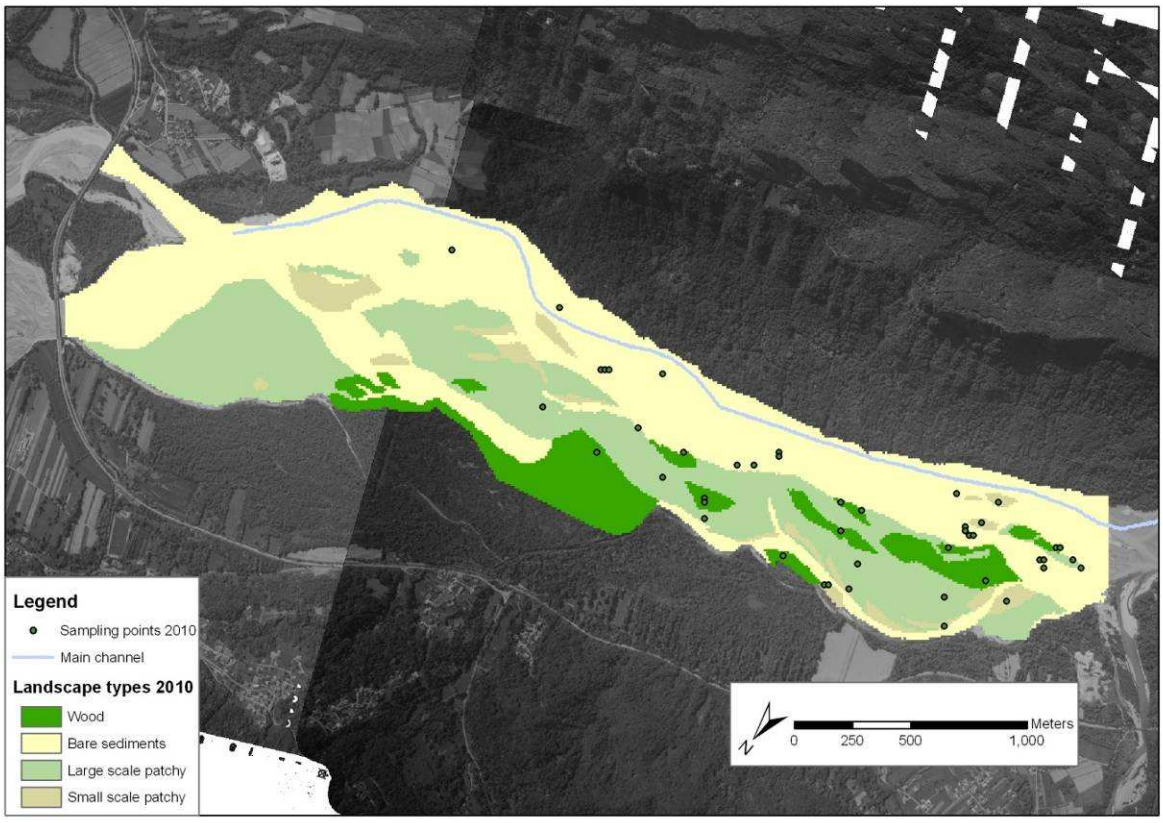

Figure 37: Mapped landscape types and main channel 2010. Moreover, the sampling points taken in 2010 are shown.

3.2.2 Characterization of the landscape types

Due to time constrains, no samples were taken in the eastern braided gravel-bed sub-reach (Figure 40). Hence, the resulting ecological description is more representative for the western wandering gravel-bed sub-reach (Chapter 3.1.2.1).

We will give a summary description of the landscape types based on the presented diagrams (Figure 41-49) and the vegetation survey (Table 13). The diagrams show the mean value and standard error (SE) of the surveyed variables for each landscape type. Below each diagram, standard deviation (STD) is additionally listed.

3.2.2.1 Bare Sediments

This landscape type is characterised by a missing vegetation cover (Figure 38-40), indicating high dynamic properties. The thickness of the fine substrate is rather low (11cm; STD 15.9cm) compared to the other landscape types and often combined with high stone/gravel content (42-50%; STD 52.7-27%) (Figures 42- 43). This is also shown by the mean grain size, which is medium gravel (STD clay-gravel). Sand-fans were often observed overlaying a stone/gravel base layer. Elevation above main channel is around 0m (Figure 45) with large STD (1.83m), showing again large morphological diversity of this unit, including fans and incised lower areas. The groundwater influence was mostly not visible because of the coarse and fresh material. Still, in few cases red/ox processes were visible close to the surface (0cm; STD 18.3).

This landscape type is located around the main channel and indicates secondary channels were water flows due to higher flow pulses.

3.2.2.2 Large scale patchy (LS patchy)

This unit is characterised by patches divided by a few meter of bare sediments. Vegetation is located higher (up to 1m) than the surrounding coarse sediments on 3-10m large fine sediment fans. Every patch is characterised by a few 5 years old Salix spp. bushes (mainly S. eleagnos and S. purpurea) (Table 13, Figure 39-40). Also small Populous can be found. The height is around 6m (Figure 38).

The heterogeneity of this landscape unit is also shown in the thickness of fine sediment (35cm; STD 33.2cm), Stone/gravel content (15%; STD 30.7) and grain size (fine grave; STD clay-coarse gravel).

The elevation above channel shows that this unit develops on spots higher than the landscape type “bare sediment” (1.9m; STD 1.74). The data only include measurements on sediment fans, so that the mean values are only representing fans but not the gravel bed in-between.

The distance from landscape type bare sediment (Figure 46) covers a wide range (61m; STD 44.8m).

The described variables indicate better development conditions for plant growth and fewer disturbances on sediment fans than for landscape type bare sediments. Due to the higher position, less floods and flow pulses disturb this unit. Still, coarse sediments between patches indicate that floods with high stream power role over this unit. Only good and deep rooted willows which protect the fine sediments are able to resist. The deeper fine sediment layers enhance plant growth; on the other hand is the layer growing due to the protective effect of willows, having so a self enhancing system. Due to this, draught in summer might be a problem for plant growth in this landscape type. GURNELL *et al.* (2001) described this process in his conceptual model.

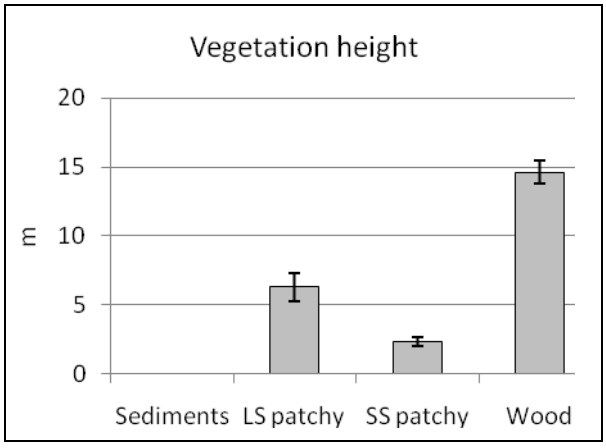

Figure 38: Ecological characterisation: Vegetation height

Std: sed = 0; LS=3.9; SS=0.9; wood= 2.8

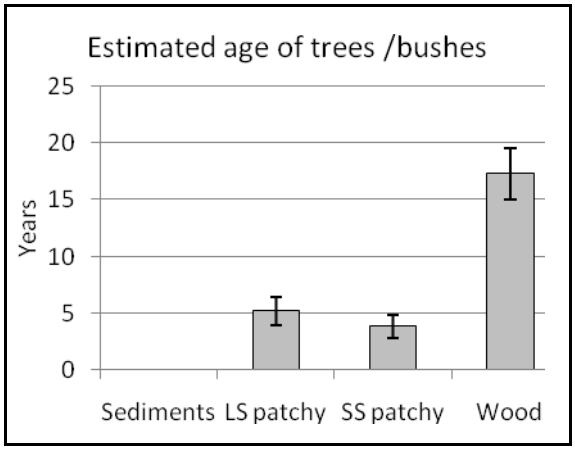

Figure 39: Ecological characterisation: Estimated age

Std: sed =0.00 ; LS=1.24; SS=1.00; wood=2.22

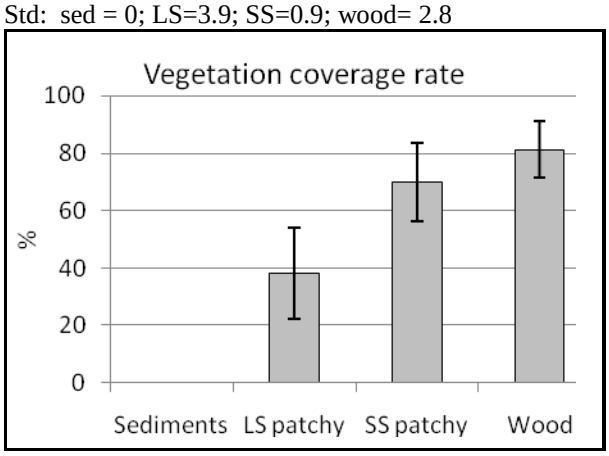

Figure 40: Ecological characterisation: Vegetation coverage rate

Std: sed = 0.0; LS= 33.7; SS=18.7; wood=19.1

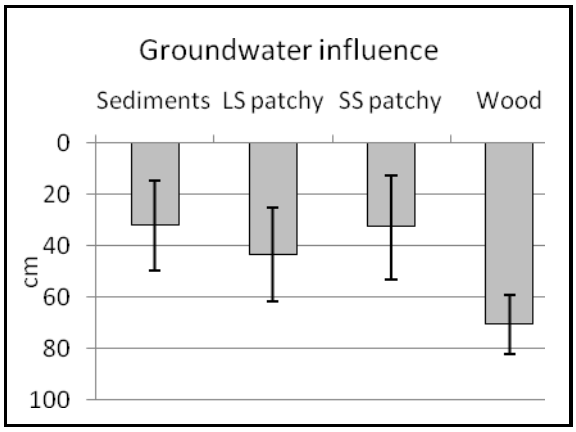

Figure 41: Ecological characterisation: Groundwater influence

Std: sed = 18.3; LS= 15.6; SS=21.2; wood=18.5

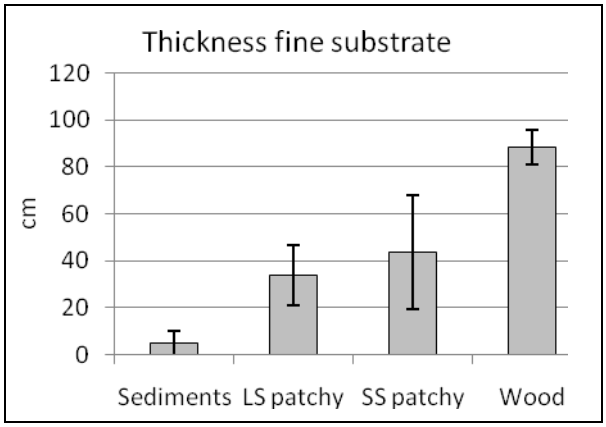

Figure 42: Ecological characterisation: Thickness fine substrate

Std: sed = 15.9 ; LS= 33.2; SS= 32.8; wood=14.7

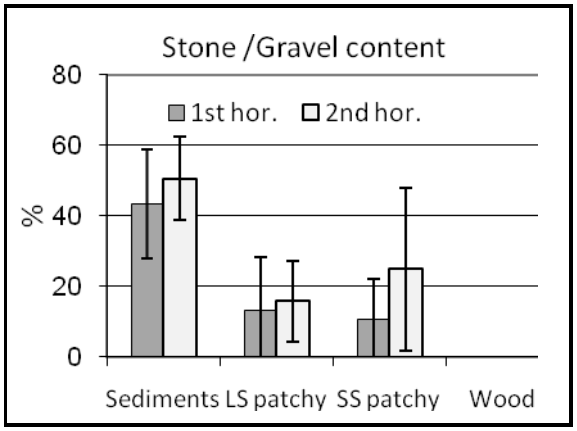

Figure 43: Ecological characterisation: Stone/Grave content

Std . 1st /2nd hor: sed =35.3/27.0 ; LS=30.7/23.3; SS=13.7/31.5; wood= 0.0/0.0

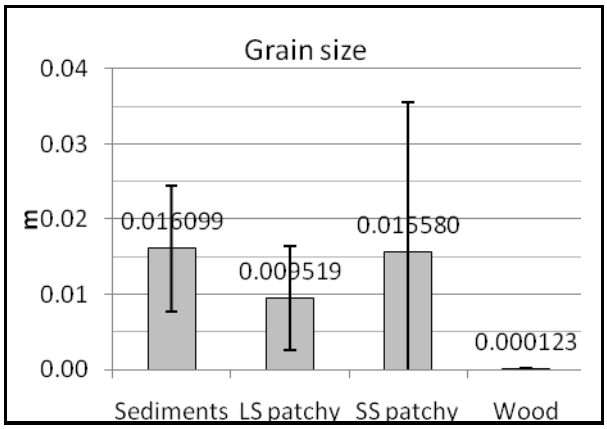

Figure 44: Ecological characterisation: Grain size

Std: sed = 0.016; LS=0.019; SS=0.027; wood= 0.000048

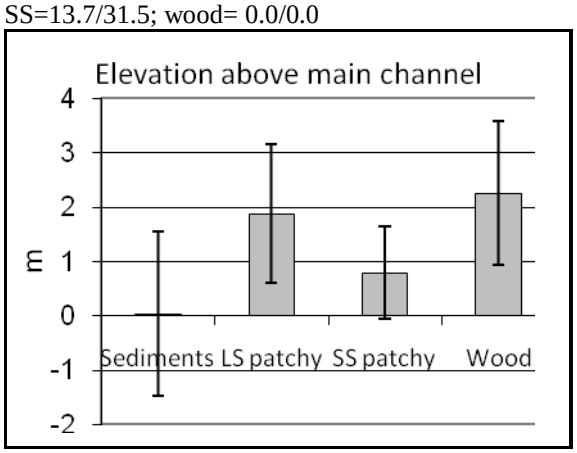

Figure 45: Ecological characterisation: Elevation above main channel

Std: sed = 1.83; LS=1.74; SS=1.03; wood= 1.61

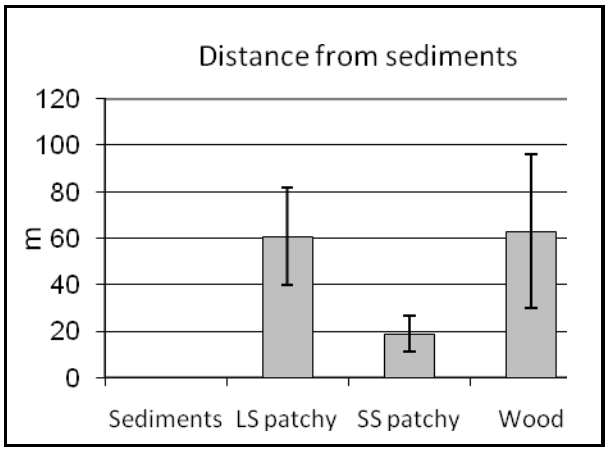

Figure 46: Ecological characterisation: Distance form sediments

Std: sed =0.0; LS=44.8; SS=10.6; wood= 64.0

Table 13: Vegetation description for landscape types

Vegetation species		SS patchy	LS patchy	Wood
Salix ssp.		11	11	13
	S. ssp.		6	7
	S. purpurea	7	3	
	S.eleagnos	4	2	
	S. triandra			6
Populus ssp.			7	12
	P. ssp.		5	6
	P. alba		2	6
Calamagrostis pseudophragmitis		3	3	1
Equisetum		2		
Alnus		2		
Populus ssp.		1		
Taraxacum ruderalia		1		
Myricaria germanica		1		1
Hippophaë rhamnoides		1		
Tussilago farfara			2	
Petasites			1	
Taraxacum ruderalia			1	
Trifolium			1	
Buddleja davidii			1	
Fraxinus			1	
Robinia pseudoacacia			1	
Pinus ssp.				6
Hedera helix				5
Betula ssp.				3
Rubus fruticosus				3
Equisetum ssp.				2
lonicera				1
Ligustrum vulgaris				1
Alnus ssp.				1
Hippophaë rhamnoides				1
Primula elatior				1
Juniperus				1
Fraxinus excelsior				1
Corylus avellana				1
Epilobium dodonaei				1

3.2.2.3 Small scale patchy (SS patchy)

In contrast to LS patchy, this landscape unit is characterised by small patches of vegetation (or even constantly covered), divided by less than one meter coarse sediments. The unit develops on flat fine sediment surface or on small sediment fans. The sediment fans are only few decimetres high and up to one meter large, which differentiates them from the previous unit. The vegetation is characterised by young (4 years old) and buried resprouting willows (mainly S. eleagnos and S. purpurea) reaching 2m height (STD 0.9m) (Figure 38-39). In contrast to LS patchy no poplars grows here, but Calamagrostis pseudophragmitis (Table 13).
Due to smaller gaps, the coverage rate (70%; STD 18.7%) is larger than for LS patchy vegetation (Figure 40).
The fine sediment layer is slightly larger (40cm; STD 32.8cm) than for the previous introduced landscape types, but with a larger range (Figure 42). This is also shown by the grain size, which is medium gravel, with the largest STD ranging from clay to coarse gravel (Figure 44).
The stone/gravel content of the 1st horizon (10%; STD 13.7) is slightly lower than for LS patchy, while for the second (25%; STD 31.5) the opposite is the case (Figure 43).
Looking at the height above main channel (Figure 45) and distance from bare sediments (Figure 46), this unit is generally found closer to bare sediment. Both, height (0.8m) and distance (20m) have relatively low STD of respectively 1m and 10.6m.
The results indicate similar dynamic properties as for LS patchy. Because slightly closer to the most dynamic landscape unit it suggests that SS patchy vegetation is flooded more often than LS patchy vegetation. On some sites plants and finer sediments buried by coarse gravel layers were found, which supports this idea. Contrary the finer grain size and higher thickness of fine sediments indicate that the stream power of floods or flow pulses is lower. Nevertheless, it is difficult to assess difference in dynamic properties between SS and LS patchy vegetation.

3.2.2.4 Wood

Wooded islands consist of the oldest (17 years; STD 4.1) and highest (15m; STD 2.8) vegetation (Figures 40-41). Also the coverage rates reach highest value of 80% (STD 19.1; Figure 42). Salix ssp. (including S. triandra) and Populus ssp. are the main trees in this landscape type. Also Pinus ssp. and Betula ssp. are present, but in a minor proportion (Table 13).

Thickness of fine substrate is largest when compared to other units, with a mean value of 90cm (STD 14.7). No gravel/stones are present in the first two horizons (Figure 42-43)
The mean grain size is silt (STD clay-fine sand) and is the finest if compared to the other landscape types (Figure 44).
Elevation is slightly higher (2.2 m; STD 1.6) than for LS patchy vegetation, but this again might be due to measurement errors explained above.
Also distance from bare sediment has the same value (63m) as LS patchy, only the range is larger (STD 64).
The elevation from the channel, the thick fine sediment layer and the relatively old trees show that this unit is the most stable. There is not a certain distance from main channel, indicating that conditions for development of wooded islands cannot be found by the actual channel flow pattern but in the shifts of these over the at least last 20 years. It is clear from the maps that, the closer wooded islands are to main channel, the higher the probability to be laterally eroded during a large flood.

3.3 Integrating habitat distribution with CAESAR results

In the validation Chapter (3.1.2.3) of CAESAR spatial variables have been assessed which can be used for prediction of the spatial pattern of landscapes units as: elevation, river flow pattern and vegetation index. Looking at the ecological characterisation of the landscape types (Chapter 3.2.2), variables matching to the spatially defined model output can be found.
The D50 output (grain size distribution), was not suitable due to processing errors during the spin-up run (Chapter 2.1.2.2).
The final DEM calculated by CAESAR had to be corrected for the bed slope of the reach (Chapter 3.2.1). The same correction surface, as used for the height measurements in the ecological description, was subtracted from the final simulated DEM.
The vegetation index indicates where willows (first step in succession) do not have the conditions to grow due to high disturbances (Chapter 2.1.2 and 3.1.2.3). The index was applied, without multinomial regression analysis, to classify the non-vegetated landscape type bare sediments. Based on that, the distances from bare sediments could be calculated, as done for the ecological characterisation.
In summary, the vegetation index of CAESAR was applied to classify bare sediments, while for the vegetated landscape types a multinomial logistic regression analysis was performed using the variables “elevation above main channel” and “distance from bare sediments”. In

the multinomial logistic regression analysis only variables mainly indicating dynamic properties were used, since grain size could not be used due to processing error during the spin-up run (Chapter 2.1.2.2).

First, the ratio of cases to independent variables was ensured to be at least 10/1 (SCHWAB 2010). In this study 19 cases and two independent variables were available, so that the used statistical method is almost appropriate (9.5/1).
Following, the Logit transformation was performed using the "multinomial logistic regression" tool of SPSS. The landscape unit wood was chooses as reference category.
The overall fit of the statistical model expressed by the significance in Table 14 is rather low, indicating that the chance that this statistical model does not explain more variation than the standard model is 12.9%.
To ensure to not have numerical problems among independent variables, standard errors of the coefficient (B values in table 15) were assessed to be smaller or equal to the value of two as indicated by SCHWAB (2010). The significance of B values (coefficients) is, as for the overall statistical model, rather low. In Table 15-16 one can see that the significance of the coefficients of independent variables are better for distinguishing SS patchy from wood than LS patchy from wood. Nevertheless, all coefficients have a low significance, indicating that contribution in distinguishing these two classes from wood is rather low.
To assess the overall utility of the multinomial logistic regression, classification accuracy is evaluated. The SPSS computed R^2, estimating strength of correlation between measures and estimates, is not considered to be a good measure of accuracy for the classified data. The classification accuracy is seen as better (SCHWAB 2010). In Table 17 the classification accuracy is 57.9%, which is higher than the by chance accuracy of 41%. The chance accuracy is defined as squared sum of the ratio of cases for each class (SCHWAB 2010).
Giving an interpretation of the coefficients of each independent variable we can follow that, with increasing height, the probability to find LS patchy and SS patchy compared to wood decreases. For SS patchy this tendency decreases faster than for LS patchy; the coefficients of the first landscape units are four times higher than for the second.
The distance from sediments has a minor effect on prediction, because the coefficient is lower than for the first independent variable. Also in this case we can assess that with increasing distance, relative to the class of wood, the probability for both SS patchy and LS patchy decreases.

The results correspond with the findings of the ecological characterization in Chapter 3.2.2 (Figure 45-46), making this a reasonable outcome.

Table 14: Statistical model; fitting information

Model	Model Fitting Criteria	Likelihood Ratio Tests		
	-2 Log Likelihood	Chi-Square	df	Sig.
Intercept Only	41,644			
Final	34,502	7,142	4	,129

Table 15: Statistical model; likelihood ratio tests

Effect	Model Fitting Criteria	Likelihood Ratio Tests		
	-2 Log Likelihood of Reduced Model	Chi-Square	df	Sig.
Intercept	39,052	4,550	2	,103
elevation above main channel	37,734	3,232	2	,199
distance from sediments	38,892	4,390	2	,111

Table 16: Statistical model; Parameter estimates

V2[a]		B	Std. Error	Wald	df	Sig.	Exp(B)	95% Confidence Interval for Exp(B)	
								Lower Bound	Upper Bound
LS patchy	Intercept	,614	1,237	,246	1	,620			
	elevation above main channel	-,175	,382	,209	1	,647	,840	,397	1,775
	distance from sediments	-,002	,011	,023	1	,881	,998	,978	1,019
SS patchy	Intercept	2,319	1,304	3,162	1	,075			
	elevation above main channel	-,717	,456	2,469	1	,116	,488	,200	1,194
	distance from sediments	-,036	,024	2,223	1	,136	,965	,921	1,011

a. The reference category is: Wood.

Table 17: Statistical model; Classification

Observed	Predicted			
	Wood	LS patchy	SS patchy	Percent Correct
Wood	3	2	1	50,0%
LS patchy	2	4	1	57,1%
SS patchy	0	2	4	66,7%
Overall Percentage	26,3%	42,1%	31,6%	57,9%

Using the coefficients B in Table 16, we wrote the Logit transformation as follows:

$Logit_{LS}$ = 0.614 - 0.175 * "*elevation above main channel*" - 0.002 * "*distance from sediments*"
$Logit_{SS}$ = 2.319 - 0.717 * "*elevation above main channel*" - 0.036 * "*distance from sediments*"
$Logit_{wood}$ = 0

The spatially explicit Logits were calculated using the "raster calculator" of ArcGIS. The same independent variables as for the statistical model were applied: "elevation above main channel" and "distance from bare sediments". The cell specific probability for each landscape unit was calculated using the formula below.

$$Prob_{LS} = e^{Logit\ LS} / (e^{Logit\ LS} + e^{Logit\ SS} + e^{Logit\ wood})$$
$$Prob_{SS} = e^{Logit\ SS} / (e^{Logit\ LS} + e^{Logit\ SS} + e^{Logit\ wood})$$
$$Prob_{wood} = e^{Logit\ LS} / (e^{Logit\ LS} + e^{Logit\ SS} + e^{Logit\ wood})$$

Finally, each cell was classified with the landscape type with the highest probability. It is important to notice that the probabilities calculated here are not the absolute for each landscape type, but are the probabilities that one landscape type has relative to the other ones based on differences in Logit. In particular we cannot assess how large real difference between the probabilities is; we can only say that there is a difference between the probabilities of N%.

Figure 47 shows the resulting classification. The overall accuracy of correct classified cells compared to mapped landscape types 2009 is 55.4%. However, if calculating the accuracy of the three classes classified by the statistical model (excluding bare sediment classified with the vegetation index) it decreases to 37.3%.

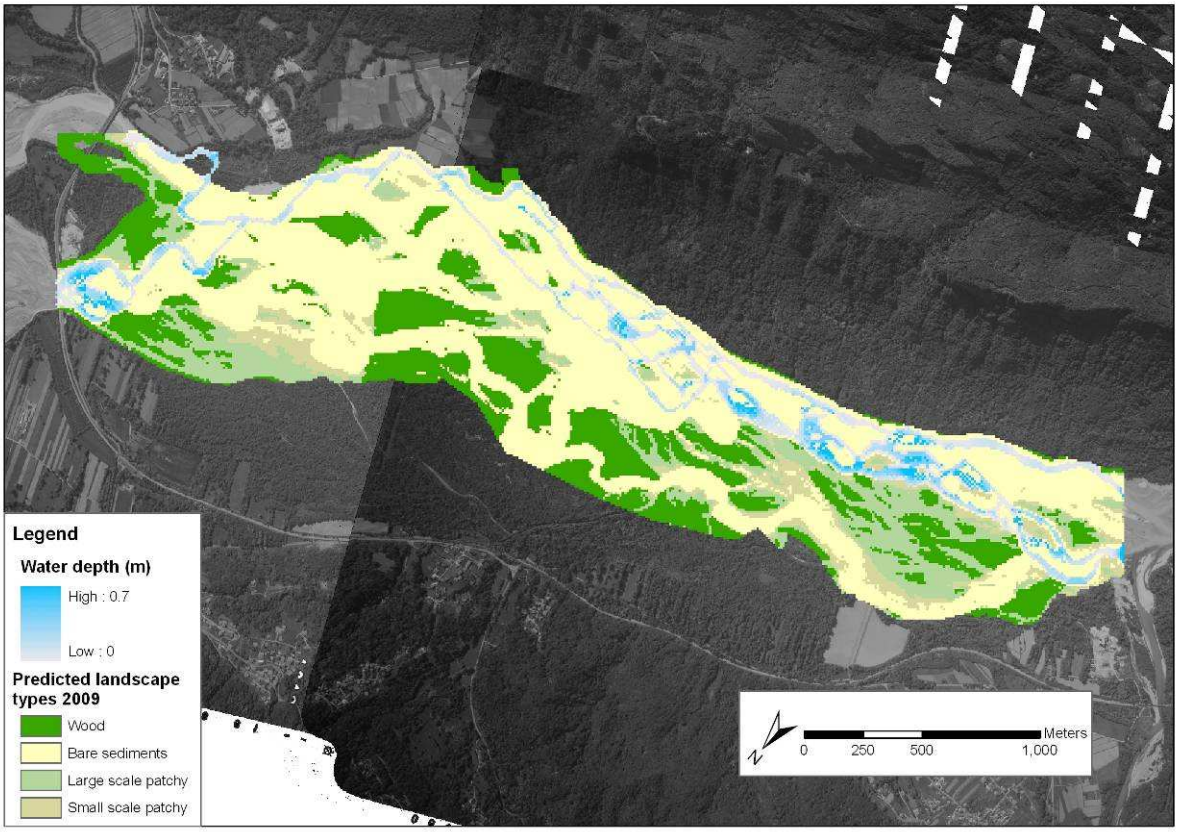

Figure 47: Map of predicted landscape types 2009

4 Discussion

Following, the results of the different steps taken in this approach are discussed and related to the overall goal of predicting landscape types. Issues concerning the implementation of the next methodological step were already discussed in the results chapter. Here the focal point is an overall discussion focusing on issues interacting over several steps of the here proposed approach.

4.1 Application of CAESAR

We can identify a few errors made in the setting of CAESAR.

The bed-rock boundaries defined through aerial pictures and DEM, should be improved by an easy field work to define more accurate boundaries where erosion is allowed to happen.

A more serious problem rose from the wrong spin-up setting of CAESAR. The problem was connected with the out-flushing of fine sediments, so that the overall mean D50 increased. During the later simulation 2005 to 2009, lateral erosion incised in new sediment layers. The new layers have the initial set mean grain size distribution with a higher percentage of finer parts than the D50 after the spin-up. This led to fine sediment supply and so to a decrease of the mean D50 until the set initial mean. Therefore, the final grain size distribution could not be used for the prediction of landscape types (Chapter 3.3 and 4.3).

Almost no literature can be found related to the spin-up run, especially not for our scale of interest. For the reach scale, focus is on a more detailed flow pattern than for the catchment scale. The higher resolution of the DEM, allows a better simulation of small river bed processes such as avulsion and sediment entrainment and so for connected features such as channel shifts and islands formation (VAN DE WIEL *et al.* 2007). Because morphology of the floodplain is a sensitive key driving factor for river flow and connected processes, it is important that not many morphological changes occur during the spin-up. This is important so that results of the later simulation are still comparable to the reality.

The here proposed method using a bimodal spin-up hydrograph without integrating lateral erosion, guaranties grain size heterogeneity without large morphological changes. Nevertheless, contrary as we did, recirculation of sediments also during spin-up is recommended to not falsify the mean D50.

As a second issue, independently from the previous, it was shown that a longer time period than four years should be simulated. Main problem was that heterogeneous grain size

distribution can only be calculated for areas which were turned-over during the spin-up and the simulation. If this time is too short, areas are not turned over and have still the initial set mean grain size, which cannot be used for later prediction. In the case of the Tagliamento floodplain turnover would be about 20 years, which is the turnover rate of islands (GURNELL and PETTS 2002).

The validation of processes showed that lateral activity and sediment discharge are overestimated during flow pulses, while both are underestimated for extreme flood events (Chapter 3.1.2.3).

This suggests that, in a later study, *lateral erosion* parameter should be set lower, *velocity limit for tau calculation* set higher and *edge value* raised close to 100. Only interaction with bed erosion should be checked, which might be higher if lateral erosion is lowered. Further, it should be taken in consideration that computational time would increase considerably.

Especially the quantitative validation showed to be difficult. The transect of BERTOLDI *et al.* (2010) is a difficult dataset, but showed to be necessary for validation. Further, the transect was located a few kilometres stream-upward on a reach similar to the eastern part of our study area. Nevertheless, comparing only the eastern part with the validation dataset no higher fit with the CAESAR output could be achieved.

In order to identify the right settings, turnover rates should also be calculated over shorter time ranges than only for one year. Doing so, activity during periods of low flow can be compared to periods with height floods.

One step further would be the integration of survey data, which allow quantification of processes such as erosion and deposition. Using these data for calibration and not only for validation (sediment flux), ensures a better setting, because more criteria that the model needs to fulfil are available.

The vegetation sub-model of CAESAR is seen as good, because it integrates basic feedbacks between vegetation and hydromorphic processes.

The set shear-stress represents the upper limit of stream power that vegetation can handle. Also back-growth of vegetation if under water, accounts for the flooding frequency vegetation can handle. Both, flood magnitude and frequency, are important parameter influencing vegetation development and aggradation (FRANCIS *et al.* 2009; GURNELL *et al.* 2001) and is predicted through the vegetation index.

We could see its good performance out of the high accuracy of bare sediments. Only bare sediments, the only non-vegetate landscape unit, could be classified based on this index,

because knowing were grass has no opportunity to grow due to high dynamic properties. The vegetated landscape units could not be classified by this index because of the missing differentiation in further succession stages.

An improve of the linear grass growth model to a slightly more complex one, integrating next succession steps in vegetation structure (scrubs and trees) would give another tool for predicting vegetated landscape types. It is clear that landscape types cannot be defined only through this index, but if combined with further ecological site conditions, it gives additional spatially defined information where vegetation has the opportunity to reach the succession stage of wood.

Moreover, also interaction between vegetation and hydromorphic process would be considered in a better way, as for instance VAUGHAN *et al.* (2009) and GURNELL and PETTS (2002) ask.

PERONA *et al.* (2009a) developed a model similar to the here proposed one, which is able to "estimate the probability of having a given area of exposed sediment and water on the basis of the statistical properties of stream flow".

He applied this model to a reach of the Maggia River, located in the Swiss Canton Tessin, to evaluate the impact of dam construction. Similar to our case, PERONA *et al.* (2009b; 2009a) subdivided the vegetation in classes based on the evaluation of aerial pictures and one field survey. The three defined classes (grass, scrubs and trees) were simulated by a deterministic model, were the growing rates were estimate by areal pictures. Transitions between two succession stages are defined through transition rules (PERONA *et al.* 2009b; PERONA *et al.* 2009a).

Vegetation is reset by stochastic flood disturbances, whereby flow was characterised in terms of probability of magnitude and frequency. On not flooded areas vegetation is growing by the previous defined rate (PERONA *et al.* 2009b).

This simplified model, which needs to calibrate only two parameter (vegetation growth rate and threshold of Q above which floodplain turnover begins), has been shown to be able to predict impact with an absolute error less than 5% (PERONA *et al.* 2009a).

Nevertheless, this model is for an analytical evaluation, while here the attempt was made to be spatially explicit, showing within the reach potential development areas of endangered habitats. Moreover, PERONAs *et al.* (2009a) approach describes geomorphic processes statistically; dependent on this, vegetation is allowed to grow. CAESAR contrary simulates the effect of different riverine process and integrates interactions between vegetation and

morphology. Still, the deterministic vegetation growth model, which can be calibrated based on aerial picture, shows the possibilities of improve that CAESAR has to predict spatially explicit vegetation patterns over more succession stages.

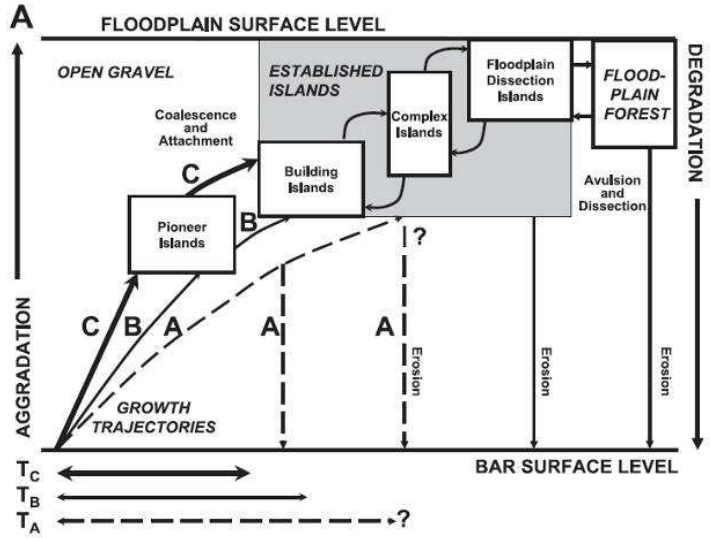

Figure 48: Development time of the different island types; TA: development time from seedlings; TB development time from death wood; TC: development time from leaving wood. (GURNELL and PETTS 2006).

The different vegetation succession stages, which change in height and cover, have a different impact on the hydraulic roughness and resistance to bed and lateral erosion. Additionally, growth rate is influenced by physical disturbance. The higher succession stages are less vulnerable to physical action such as burring or removal by floods.

The more vegetation growth, the higher hydraulic roughness gets and so the aggradation rate. An idealized line can be drawn where sediment supply is in equilibrium with the vegetation growth (Figure 48). Below this line, nutrient amount needed for the growth provided by fine sediments is the limiting factor. In contrast, high amounts of sediments might burry vegetation (GURNELL and PETTS 2002).

This scheme could be used as reference for improving the vegetation growth model of CAESAR, by integrating changing critical shear stress coefficient and roughness of the surface based on the succession stage. To calibrate the vegetation sub-model more accurate research is needed to set the upper limit of shear stress.

CAESAR does not include resistance to lateral erosion due to the effect of roots. Also here, the integration of a factor in dependency of vegetation succession stage would give an additional eco-hydromorphic feedback.

The possibility of integrating different trajectories based on dispersed propagules and dead or living wood, shown in Figure 48, is seen as too complex and not at the scale of this research. At lower scales (1-5m DEM) an integration of "large woody debris" is seen as too complex, because of the need of an additional sub-model.
Anyway, for the scale of this study more general feedbacks are enough to predict river island formation (FRANCIS *et al.* 2009).

The integration of other variables that showed to be good predictors for landscape diversity in the ecological characterisation is too complex and would require much more calculation power. For instance is *thickness of topsoil layers with fine sediments* difficult to integrate. Because CAESAR assumes 20 cm think sediment layers, it would require long simulation time to turnover even the lower layers so that a heterogeneous D50 could be predicted also in depth. We thick that at least one floodplain turnover cycle (20yr.) is needed and still it is not sure if the depth of 90cm, important for islands prediction (Figure 42 Chapter 3.2.2), can be reached.

Independently from the results, the presented methodological steps are seen as a good method for the CAESAR application. The input data preparation is relatively easy, even if data such as discharge and grain size distribution are hardly available. Especially, discharge data are most difficult to get, while grain size data can easily be sampled. Also the sensitivity analysis to define the study area size, DEM resolution and preliminary settings of CAESAR is seen as easy method to join computational power and research requirements. The spin-up run method has also its potential if some issue are taken in consideration, as explained before.
The multi scale calibration is a good approach to find the right settings of CAESAR, even though some more quantitative short term steps should be integrated to define better the processes of avulsion, lateral erosion and bed erosion.
The validation using aerial pictures is an easy way to evaluate flow pattern and vegetation growth. The use of quantitative data, such as sediment fluxes and morphological changes are difficult to get but showed to be necessary to validate the simulated processes.

4.2 Ecological characterization

Comparing the mapped landscape types and their characterisation through field data with the described islands type in GURNELL *et al.* (2001) (Figure 2 Chapter 1.2), we can define in which landscape type specific island types develop.

As shown in Figure 2, bare gravel corresponds with the landscape type bare sediment. Moreover, SS patchy corresponds to the diffuse/patchy class, which grows out of propagules. If taking in consideration that LS patchy integrates large coarse sediment areas, we can combine this landscape unit with areas where pioneer islands of the conceptual model occur. This landscape type corresponds to areas where islands develop mostly out of the engineering action of large woody debris. The classes defined in the conceptual model as building islands, complex islands and floodplain dissection islands are aggregated without distinction in the class of wood (EDWARDS *et al.* 1999; GURNELL *et al.* 2001). A further distinction of these island types can be done by analysing the history of island formation during the entire simulation run and the use of the indicator of relative height difference to floodplain level proposed by GURNELL *et al.* (2001). Nevertheless, this would require longer simulation time, large GIS evaluation of the simulation history and more precise height processing technique for removing the rive gradient.

The landscape types were mapped for the years 2009 and 2010. Additionally, we mapped the landscape types for 2005 and <2005 (exact date unknown). Doing so, we can assess if the simplified conceptual model of GURNELL *et al.* (2001) is applicable to the landscape type concept of this research. The connection is strengthening the comparability of the two scales and, further gives some good evaluation possibilities of future scenarios being islands considered indicators for hydromorphological integrity of the river (TOCKNER *et al.* 2003).

Table 18, shows the percentage of the study area with a certain development chain over time in terms of total percentage and relative percentage of each succession chain to the sum of all succession chains ending in the same landscape type (example: LS patchy developing into sediments relative to the sum of all chains having for 2010 the landscape type sediments).

Figure 49 shows the spatial distribution of the succession chains. The code is designed as follows: number 1 = bare sediments, 2 = SS patchy, 3 = LS patchy and 4 = wood. The position of each number reveals in which year a certain landscape was mapped, so that the 2010 = X000, 2009 = 0X00, 2005 = 00X0 and <2005 = 000X.

Only the succession chains with a percentage larger than 1% were taken, so that boundary errors can be considered as negligible. 81.54% of the surface was taken in consideration.
Based on the analysis, almost 30% of the floodplain stays constant over time as bare sediment and following the southern border of the floodplain. Even if highly dynamic, it is highly constant from the spatial point of view because 56.28% of total sediment cover of 2010 has always been bare sediments in the past. A small overall (1.79%) but large relative percentage (40.47%) develops from bare sediment through establishment of propagules to SS patchy as shown in the conceptual model of GURNELL *et al.* (2001) in Figure 2. This development chain is located next to long term constant bare sediment area.

Table 18: Successions chains for the study area
Code: 1 = bare sediments, 2 = SS patchy, 3 = LS patchy, 4 = wood
2010 = X000, 2009 = 0X00, 2005 = 00X0, <2005 = 000X

Code 2010←2003		Relative % to end stage	Total %	Aggr. %
1111	Sediments	56.28	29.54	29.54
(2211)	Sediments→ SS patchy	40.47	1.79	1.79
(3332)	SS patchy → LS patchy	11.38	3.66	3.66
1113	LS patchy → Sediments	7.75	4.07	
1311	Sediments→ LS patchy →Sediments	3.75	1.97	
1131	Sediments→ LS patchy →Sediments	6.64	3.48	
3311	Sediments→ LS patchy	9.68	3.11	
3313	LS patchy →Sediments→ LS patchy	3.56	1.14	
3331	Sediments→ LS patchy	2.72	12.60	26.37
3333	LS patchy	17.19	5.53	5.53
4443	LS patchy →Wood	9.79	1.07	1.07
4444	Wood	66.86	7.31	7.31
1114	Wood →Sediments	8.77	4.60	4.60
1112	SS patchy →Sediments	3.15	1.66	1.66
SUM		-	*81.54*	-

3.66 % develop from SS patchy to LS patchy. The main process is the aggradation and the attachment (GURNELL *et al.* 2001). In the map below, these areas concentrate in the northern part. 26.37% has a relative rapid change between bare sediments and LS patchy (in the conceptual model pioneer islands) by regenerating living wood or propagules establishment in the lee of dead wood. Often this unit is reset to bare sediment by large and powerful floods.

This shows the second path for development of pioneer islands without diffuse/patchy vegetation (EDWARDS *et al.* 1999; GURNELL *et al.* 2001).

In Figure 49, these succession chains interchanging LS patchy and sediments are subdivided into two categories: light green is primary bare sediment and the darker green stays primary LS patchy. As we can see the light green areas are closer to the constant main channel (code 1111), which have the opportunity of resprouting in less active years. Contrary the darker green areas of this alternating class, are situated further away from the main channel or close to side channels where woody debris have better opportunities to resprout (FRANCIS *et al.* 2009).

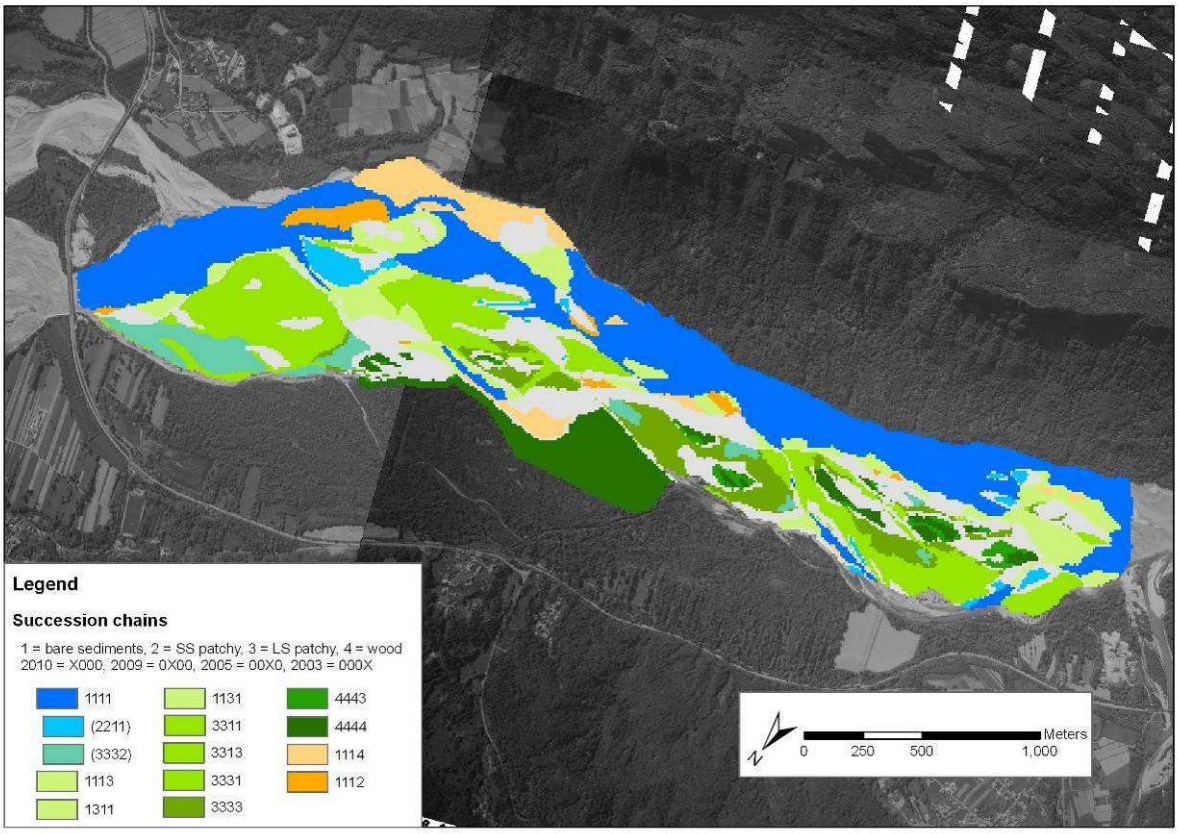

Figure 49: Spatial pattern of successions chains for the study area

5.53% overall and 17.19% relative change stays constant over time as LS patchy, while a small percentage (1.07%) develops further into wood (islands). The main process for the later one is aggradation, attachment, avulsion or dissection of the floodplain (EDWARDS *et al.* 1999; GURNELL *et al.* 2001).

A small overall percentage (7.31%) stays constantly wood over the entire period. The relative change of 66.86% is the highest, indicating the relative stability of this landscape type if

compared to the other. 4.60% of wood are reset to bare sediment. Main process for the resetting of islands is due to lateral erosion next to the main channel (EDWARDS *et al.* 1999).
In the map (Figure 49), we can clearly see the attachment process: chain 4443 is located in-between two different areas that stay constantly wooded over time. Moreover, we can see that mostly chain 4443 is surrounded by chain 3333 (constantly LS), indicating the dynamic gradient of the different landscape units.

To define whether the subdivision of landscape types supports the evaluation of human impact on endangered habitats, we tried to match FFH habitat found at the Tagliamento River with the defined landscape units. Here, we tried to go one step further than the simplified subdivision into island types, which do not take into account vegetation diversity.
The early date of the field survey presented difficulties in distinguishing different willow species and other key species listed in the FFH interpretational manual. A clear combination of FFH code and landscape units was so difficult to define. Still, we tried to define some matches based mostly on the morphological description. The vegetation survey is only used as supplementary indication.
The FFH habitat 3220 “Alpine rivers and the herbaceous vegetation along their banks” is characterized by herbaceous or suffrutescent plants (EC 2007).
The subtype 24.221 is characterized by herbaceous plants as Chondrilla chondrilloides, Erigeron acris, Epiolobium dodonaei and Scrophularia canina. The best conditions are found on gravel banks which are stable for at least the second year and are slightly above annual mean water level. The vegetation cover hardly exceeds 5% (MÜLLER 2005).
Even we could not define vegetation on bare sediments because of early date of the field work, this habitat is very likely present in this landscape unit.
The vegetation for the subtype 24.222 is Calamagrostis pseudophragmites with seedlings of Salix and Myricaria germanica (EC 2007). It develops along secondary channels where finer sediments deposit and ground water is close to the surface (MÜLLER 2005).
We can fit this habitat to the landscape type SS patchy, were we found the previous defined vegetation composition as shown in Table 13 (Chapter 3.2.2). Also the development around secondary channel is shown in Figure 46 (Chapter 3.2.2).
The habitat 3230 “Alpine rivers and their ligneous vegetation with Myricaria germanica” has also been found in the study area (MÜLLER 2005). This habitat develops from habitat 3220 through the development of willow seedlings into low shrubby vegetation (EC 2007). The ecological conditions in which this habitat develops are similar to the previous habitat. To

develop into a higher vegetation stage a large fine sediment layer is needed for the nutrients support. Moreover, groundwater is relatively high, providing water in the dry summer season. With optimal conditions this habitat can reach a high cover rates (MÜLLER 2005).

Also this habitat can be found in the landscape unit SS patchy. The large STD for the thickness of fine sediment and the low groundwater level, indicate that this landscape unit integrates both FFH habitat, 3220 (subtype 24.222) and 3230. Also the vegetation analysis of SS patchy shows species listed in the FFH manual (EC 2007), which are at an age between 1-3 years.

Further, FFH habitat 3240 "Alpine rivers and their ligneous vegetation with Salix elaeagnos" can be found. This habitat is characterized by thickets or wood of Salix ssp. and Hippophae rhamnoides (EC 2007). This habitat develops on higher gravel spots than the previous habitats and in the Tagliamento often it is combined with Populus x Canadensis. Low flow conditions can lead to a drying-out (MÜLLER 2005).

The sampled species (Table 13 Chapter 3.2.2) and the elevation above main channel indicate that this habitat can be found in the LS patchy landscape unit. Also lower ground water level (Figure 41) in combination with less fine substrate thickness and observed high stone/gravel content indicate that this landscape unit has higher probability for drying out than the other previous ones.

There is a second association of the habitat 3240 in which Salix eleagnos dominates. The vegetation is located on more dynamic locations showing often traces of abrasion. Due to high physical disturbance vegetation height is max 1.5m, which focuses more on the development of roots (MÜLLER 2005). Differently from the previous association of habitat 3240, we can find this one in the landscape type of SS patchy because developing larger homogeneously covered areas and because being on more dynamic locations.

The priority habitat 7240* "Alpine pioneer formations of Caricion bicoloris-atrofuscae" and 7230 "Alkaline fens" are small habitats that form around water pools fed by rising groundwater and slow flowing gullies (MÜLLER 2005). These habitats are difficult to match with one landscape type due to its small extension and special conditions of development. Still, even if not mapped as single unit, it is known that both are present in the study area (MÜLLER 2005).

The landscape type wood is not clearly compatible with FFH habitat described by MÜLLER (2005). Problem is that woody FFH habitats are largely defined through the species composition and not through geomorphic attributes as the dynamic floodplain FFH habitats.

Due to scarce vegetation data, attribution of FFH habitats to landscape type wood becomes more difficult.

The FFH priority habitat 91E0* “Alluvial forests with Alnus glutinosa and Fraxinus excelsior (Alno-Padion, Alnion incanae, Salicion albae)” develops on more stable areas of the floodplain. The woody areas defined in this study are clearly the more stable within the floodplain and also vegetation data indicate that the association Salicetum triandrae and Salicetum albae are possible on this landscape type. Nevertheless, the scarce vegetation data cannot confirm the doubt MÜLLER (2005) has concerning its occurrence in the study reach.

Table 19 summarise briefly the attribution of FFH habitat and associations defined by MÜLLER (2005) to the landscape types of our study.

In summary, we can assess that SS patchy and LS patchy are good indicators for the occurrence of endangered FFH habitats, even though within the landscape type itself a better distinction is not possible. More samples in combination with a better vegetation description are needed to characterise environmental conditions in which this habitat exists within its unit. This allows a further subdivision of landscape units in habitat distribution, as done for the landscape distribution. Especially, the landscape class wood would profit out of more detailed vegetation analysis.

Table 19: Landscape type attributable FFH habitat

FFH habitat	Sub-type	Association	Landscape type
3220	24.222	*Chondrilletum chondrilloidi*	Bare sediments
	24.222	*Calamagrostietum pseudophragmitis*	SS patchy
3230		*Salici-Myricarietum*	SS patchy
3240		*Salix eleagnos*	SS patchy
		Salici-Hippophaetum rhamnoidis	LS patchy
7240*		*Caricion bicoloris- atrofuscae*	-
7230		*Caricetum davallianae*	-
91E0*		*Salicetum triandrae*	Wood?
		Salicetum albae	Wood?

.

For the methodological approach, we saw that a characterization of the defined landscape types is easily possible, showing the relation between vegetation cover and patchiness visible through aerial pictures and the ecological variability sampled in the field.

This approach allowed the mapping of landscape units based on aerial photographs. Big advantage of this approach is the independence of the year of sampling to characterize the landscape units and the year to which the CAESAR simulation ends.

For our purpose decision to take landscape types is feasible because we had the DEM with a resolution of 10m and the biotopes, such as single vegetation patches, mostly of smaller extent, making prediction of these difficult. Still, the size of the smallest mapped unit of SS patchy (mostly 20m large), is at the limit of prediction.

Disadvantage of landscape types is that vegetation associations might be distributed over more than one landscape type, because vegetation differs in age and habit but not in species composition. Due to the weak species characterization this cannot be excluded. Anyway, the results showed that different landscape types can include the same FFH habitats because integrating vegetation associations differing in habit.

Moreover, CAESAR only integrates eco-hydromorphic feedbacks on higher landscape level as explained in Chapter 4.1. The prediction of single pioneer islands for which woody debris plays an important role (FRANCIS *et al.* 2009; GURNELL *et al.* 2001), are difficult to implement into a simulation at lower scale.

The choice for landscape types is so adapted to the here chosen scale of CAESAR.

The largest source of error occurring during the sampling is if variance of each defined landscape unit is not covered. This happened in this research with the LS patchy landscape unit, where only the sedimentation fans were sampled and not the bare sediments in-between (Chapter 3.2.2.2). This had consequences for the characterization and the later multinomial logistic regression analysis, which gets falsified.

Moreover, before sampling, minimum sampling number should be defined to carry out significant statistics. This prevents, as happened in this study, that the ratio cases to independent variables misses even the lower boundary for multinomial logistic regression analysis (Chapter 3.3). The reason is the relative few elevation measures, so that only a small set of samples could be used. This shows that the focus should also be placed on key variables which are known to match to CAESAR data.

4.3 Integrating habitat distribution with CAESAR results

Table 14 (Chapter 3.3) shows a low significance of the statistical model with independent variables compared to the model without independent variables. Also the significance of the B coefficients for each independent variable is low (Table 15 Chapter 3.3).

The significance would increase if more samples and independent variables would be added to the multinomial logistic regression analysis. Nevertheless, the defined variables were the only spatial available calculated by CAESAR.

LS patchy and wood are difficult to distinguish in terms of “elevation above main channel” and “distance from sediments” because both have similar mean value and STD. Comparing the distribution of the two variables on a scatter plot for LS patchy and wood as shown in Figure 50, we can see that there is a large overlap. This shows the difficulty in distinguishing these two landscape types. Nevertheless, it is expected that removing sampling errors in LS patchy (Chapter 3.2.2.2) would improve differences between these two units.

If comparing now the variable “grain size” to “elevation above main channel” we can improve the differentiation of LS patchy and wood. Figure 51 shows that the sample distribution between LS patchy and wood has less overlap, leading into a better prediction. Contrary, we can assess that for this combination of independent variables SS patchy has a higher overlap with LS patchy.

Knowing this, a multinomial logistic regression analysis including the third independent variable “grain size” was tested. Even though, more samples would be needed to reach at least the cases to independent variables ratio of 10/1, it should give an indication if the statistical model improves significance.

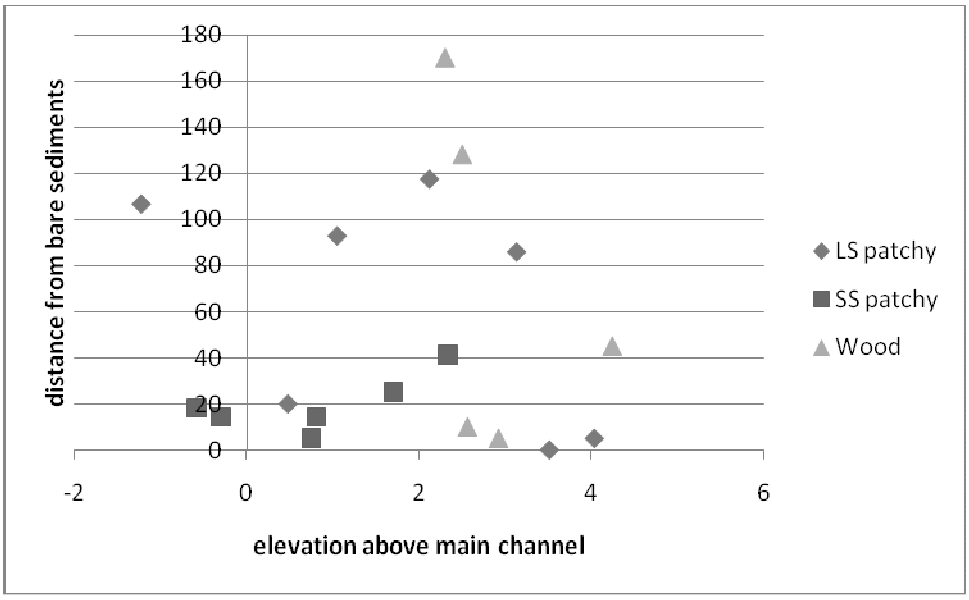

Figure 50: Comparison of the variable distance from bare sediments and elevation above main channel.

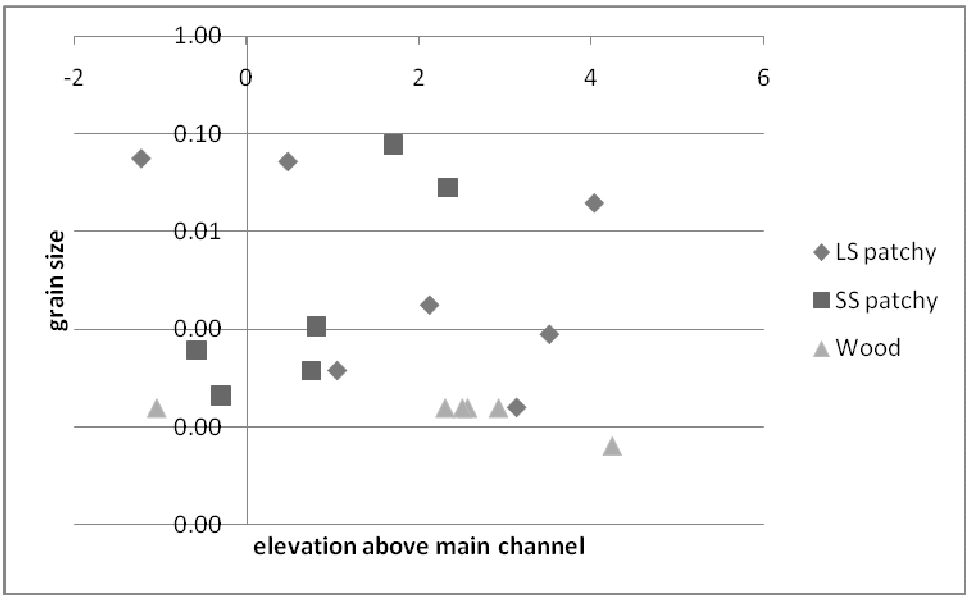

Figure 51: Comparison of the variable grin size and elevation above main channel.

In the following tables we can see that the statistical model improves its overall significance from 0.129 to <0.001. This shows that, even the number of cases is low the chance that this model does not explain more variation than the standard model is almost 0%. Moreover, also the significance of each independent variable increases (compare Table 16 with Table 22), shown by the improved significance from 0.119 to 0.062 for the variable "elevation above main channel" and from 0.111 to 0.071 for the "variable distance from sediments".

Also the overall classification accuracy increase from 57.9% to 84.2%, which is a great improve. Especially the classification of wood improves considerably its performance (Table 22).

Overall, even if the number of cases is quite low so that more independent variables cannot be included, the here presented results show that by including "grain size" into the analysis, the performance of the statistical model is improved considerably.

Table 20: Improved statistical model; fitting information

Model	Model Fitting Criteria	Likelihood Ratio Tests		
	-2 Log Likelihood	Chi-Square	df	Sig.
Intercept Only	41,644			
Final	14,480	27,164	6	,000

Table 21: Statistical model; likelihood ratio tests

Effect	Model Fitting Criteria	Likelihood Ratio Tests		
	-2 Log Likelihood of Reduced Model	Chi-Square	df	Sig.
Intercept	26,467	11,987	2	,002
elevation above main channel	20,045[a]	5,565	2	,062
distance from sediments	19,782[a]	5,303	2	,071
mean grain size	34,528	20,049	2	,000

Table 22: Improved statistical model; Classification

Observed	Predicted			
	Wood	LS patchy	SS patchy	Percent Correct
Wood	6	0	0	100,0%
LS patchy	1	5	1	71,4%
SS patchy	0	1	5	83,3%
Overall Percentage	36,8%	31,6%	31,6%	84,2%

CORONA *et al.* (2008), calculated the probabilities using a multinomial regression analysis for land to change from farmland to forest based on different data which can be easily get through the interpretation of aerial pictures. Such data, as for instance “distance from sediments in the past years”, “elevation above channel from a previous DEM” or “elevation difference between two dates”, could be integrated to explain landscape distribution by adding transition probabilities.

Moreover, multinomial regression for transition from one landscape type to another was compared to ordinal regression by RUTHERFORD *et al.* (2007). Ordinal regression showed to be easier in application and in indentifying more efficiently key variables. Additionally, RUTHERFORD *et al.* (2007) states that this method is favourable if changes into another land unit can be identified as ordinal process.

The integration of probabilities of one landscape type into another could be an additional tool which could be integrated as second additional statistical model.

4.4 Assessment of the prediction

Comparing the results of the prediction (Figure 47) with the mapped landscape types (Figure 36) we can assess that most errors were done for the eastern sub-reach. The green areas in Figure 52 show the correct classified cells whereas the red areas the wrongly classified ones. Moreover, intense colour stay for the performance of the statistical model, while light colour for the classification of bare sediments by the vegetation index of CAESAR.

If we only take in consideration the lower part of the reach, overall prediction accuracy rises from 51.4% to 69.8%. This can be considered as a great improve.

Looking at the performance of the statistical model one can see in Figure 53 that there is almost no match (intense green and red) for the eastern reach. The large errors of the statistical model are due to the two different braiding types of the studied reach (Chapter 3.1.2.1). Having sampled only the downstream reach, as shown in Figure 37, the statistical model is only able to represent the spatial distribution of landscape types of the western sub-reach. If we take in consideration only landscape types classified through the statistical model, the classification accuracy of the western reach is 46.0%, which is almost nine percent points higher than the accuracy of the entire reach for the same classes (37.3%).

Even if samples would cover the entire reach we would recommend to split the statistical model based on the two sub-reaches. This is necessary due to the hydromorphic differences, which might cause changes in the β factors of the Logit transformation.

The vegetation index of CAESAR instead, is a better classification tool, having accuracy for bare sediments of 66.8% for the entire reach. Nevertheless, also in this case larger errors appear in the eastern sub-reach (light red Figure 53). Feasible reasons might be the water input source for the CAESAR simulation which is constant over time and chosen to be split equally around the island (Chapter 3.1.1). This does not correspond to reality because water discharge shifts in power and amount in time from one side of the island to the other. The model did not do so, so that we can consider the first kilometre influenced by this source of error; after it gets negligible.

If considering only the landscape type bare sediments, classification accuracy of the western reach is 75%, which is a large increase if considering accuracy for the entire reach of 66.8%.

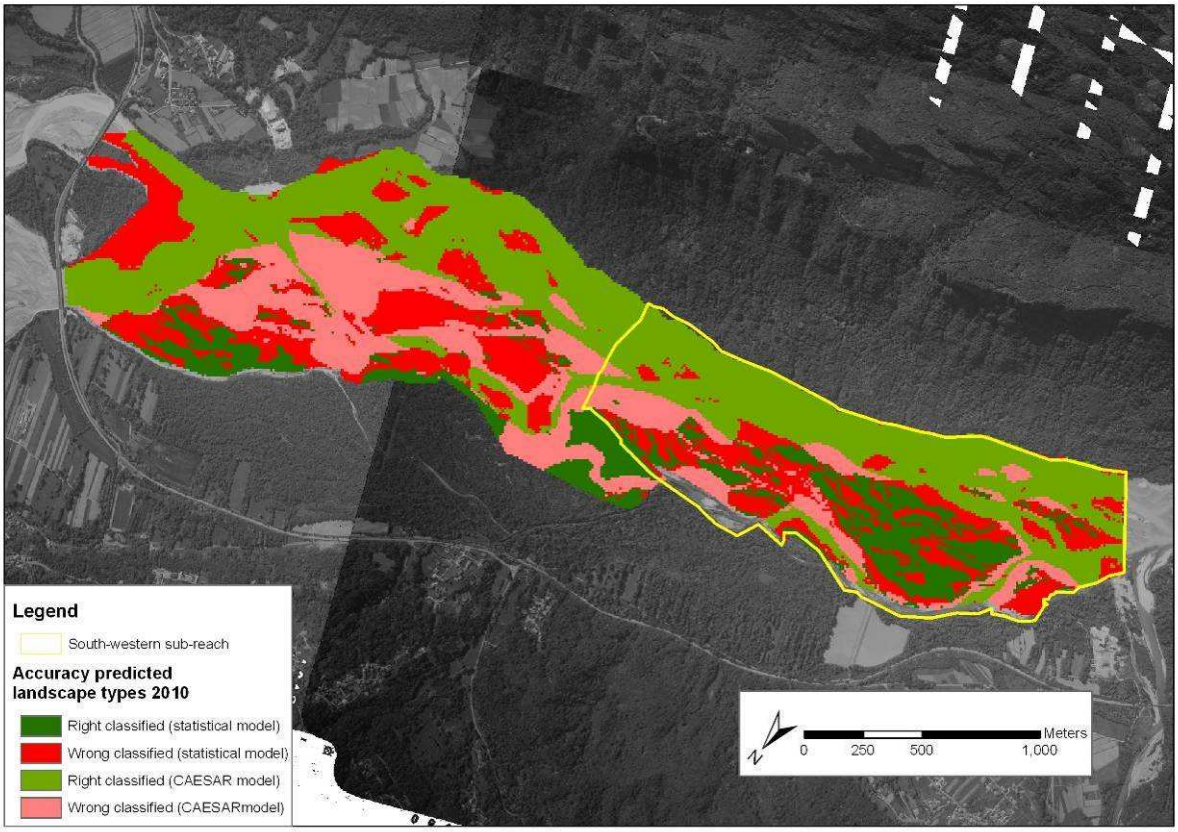

Figure 52: Accuracy (user) of predicted landscape types 2009

For the previously mentioned argues only the western reach will be considered for the next steps.

Next, we can look at the classification accuracy of each single landscape type in terms of producer and user accuracy (Table 23-24). The producer accuracy allows us to interpret how many cells were classified right based on the mapped validation data. Here we can assess the performance of the classification method for each landscape type class. Contrary the user accuracy; in this case we can assess how large the possibility is that a certain predicted class is truly the indicated one.

Looking at the producer accuracy (Table 23) we can assess that landscape unit bare sediment has a high value indicting CAESAR simulated well the vegetation index.

Looking at the performance of the statistical model, wood performed best, predicting for 57.00% the right location. Most classification errors were done with LS patchy. SS patchy has a higher match with bare sediment (77.71%) than with itself.

Looking now at the user accuracy in Table 24, we can still see bare sediments as best classified unit. From the total surface predicted there is only a small difference, being 58% the predicted percentage of the floodplain classified as bare sediments and 50% the mapped one.

Table 23: Producer accuracy of the prediction

		Map 2009			
		Sed.	LS patchy	SS patchy	Wood
Predicted 2009	Sed.	86.90	27.22	77.71	12.58
	LS patchy	3.87	36.48	3.71	26.71
	SS patchy	7.50	12.54	15.01	3.72
	Wood	1.74	23.76	3.57	57.00
	tot	*100.00*	*100.00*	*100.00*	*100.00*

Table 24: User accuracy of the prediction

		Map 2009				
		Sed.	LS patchy	SS patchy	Wood	*tot*
Predicted 2009	Sed.	75.04	16.32	6.37	2.27	*100.00*
	LS patchy	11.01	72.12	1.00	15.87	*100.00*
	SS patchy	40.72	47.32	7.75	4.22	*100.00*
	Wood	5.70	54.15	1.11	39.05	*100.00*

Wood has a lower user accuracy (39.05%) than producer accuracy (57.00). The total surface predicted is 15% while the mapped 10%, so that the lower user accuracy is attributable to the large relative surface difference.

LS patchy, converse to the producer accuracy, has a high user accuracy (72.12%). This might be due to the fact that the predicted area (17%) is half of the mapped area (34%).

SS patchy has a low user accuracy of 7.75%. Most of the cases are misclassified as sediments and LS patchy. The total predicted surface (9%) is almost two times higher than the mapped surface (5%).

In summary, the low significance of the parameter “elevation above main channel” and “distance from bare sediments” (Chapter 3.3) is also visible in user and producer accuracy, showing that the statistical model is not really able to predict spatial distribution for this landscape units (Table 23-24). Nevertheless, it is expected that the statistical model increases its performance, if more samples and independent variables, such as grain size, are add to the analysis. This, as shown in Chapter 4.3, appears to increase overall accuracy.

The vegetation index, instead has in both accuracy measures high values. This suggests again as shown in Chapter 4.1 the better prediction potential of the vegetation growth sub-model integrated in CAESAR.

An increase in accuracy could also be done by aggregating the two worst predicted classes and run the multinomial regression analysis again. Surely, a better accuracy can be achieved by merging LS and SS patchy. Nevertheless, aggregation of these two units would make

accreditation of FFH habitats more difficult, and so its use for environmental impact assessment.

Knowing CAESAR as a reduced complexity model, it does not have the aim to predict exact fluvial pattern, but more the general behaviour (COULTHARD *et al.* 2007). This influences the prediction which is based on the spatial distribution of the predicted variables. By increasing scale, reality and simulation get closer so that inaccuracy of the model is averaged out. In the validation of the CAESAR results this got clear (Chapter 3.1.2.3).

Because of this, we can improve accuracy only by increasing resolution. A multiple resolution validation program developed for the CLUE model was used (PONTIUS JR *et al.* 2008). This program compares if, with increasing window size, area of predicted landscape types correspond to the area of mapped landscapes.

Figure 53, shows the fit between the mapped and the predicted units for different window sizes. As we can see, fit increases fast until window size of 21 cells; this means that at a distance of 210m (cell size 10m*windows size 21) accuracy of prediction (R^2) increases from 0.69 to 0.80. After, the fit increases slower.

Table 25 illustrates the differences between predicted and mapped landscape types at different scales. The blue colours indicate high errors, while yellow low ones. It is visible that for all landscape types errors decrease if resolution is decreased.

In Appendix 5, an example for the landscape type cover at a scale of 21 cells is shown to clarify the results presented in Table 25.

To evaluate how much each landscape type improves its fit with decreasing resolution we can only compare the differences between the starting fit at 1 cell resolution with the coarse resolution scales but not the absolute values. Figure 54 shows this comparison.

The landscape type wood and SS patchy perform worst if window size is increased, not improving much their performance. This is due to the small size and the low percentage of cover if compared to LS patchy and bare sediments. By increasing resolution fit does not rise fast because large areas do not include this landscape type, so that at the 1 cell scale the R^2 has already a high fit (R^2 SS patchy at 1 cell 0.87). The few windows including these landscape types improve the R^2.

Not only in Figure 54 but also in the maps (Table 25) this is visible. Large area fit the map at high resolution, because not classified as SS patchy. The few areas that are predicted to be SS patchy almost never correspond to the mapped location, being its accuracy very low.

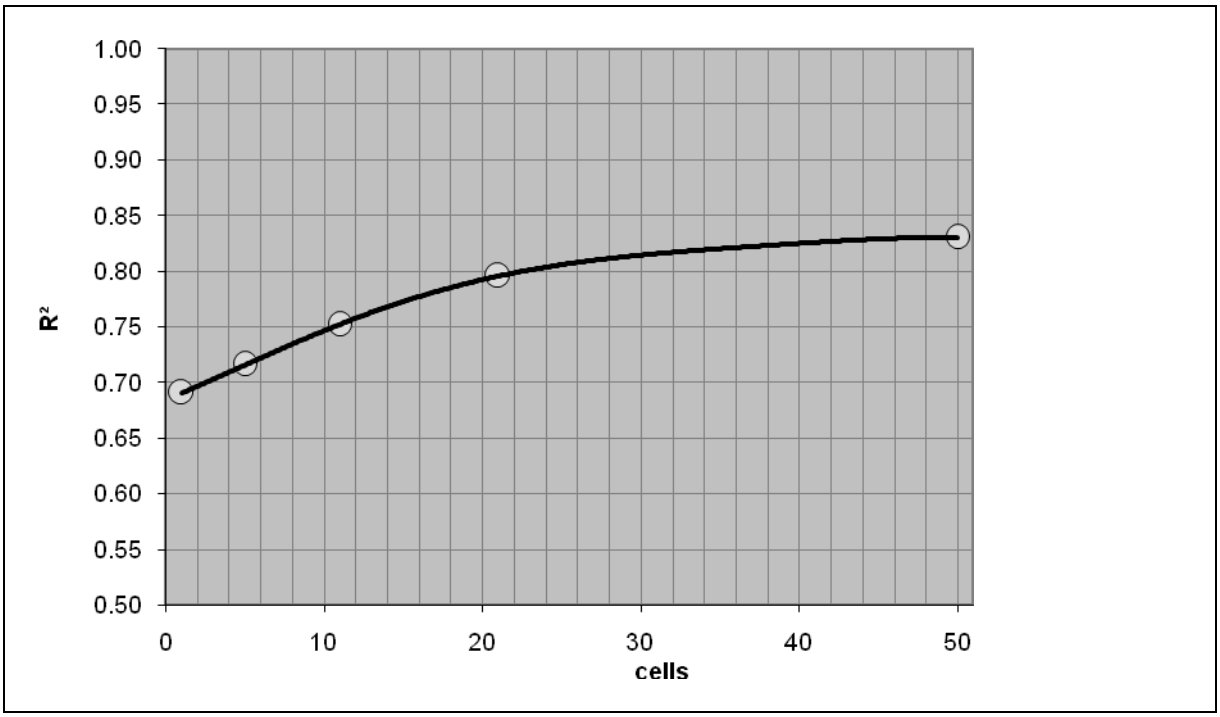

Figure 53: Multiple resolution validation of the prediction. Blue dots show the resolution of the maps of Table 24

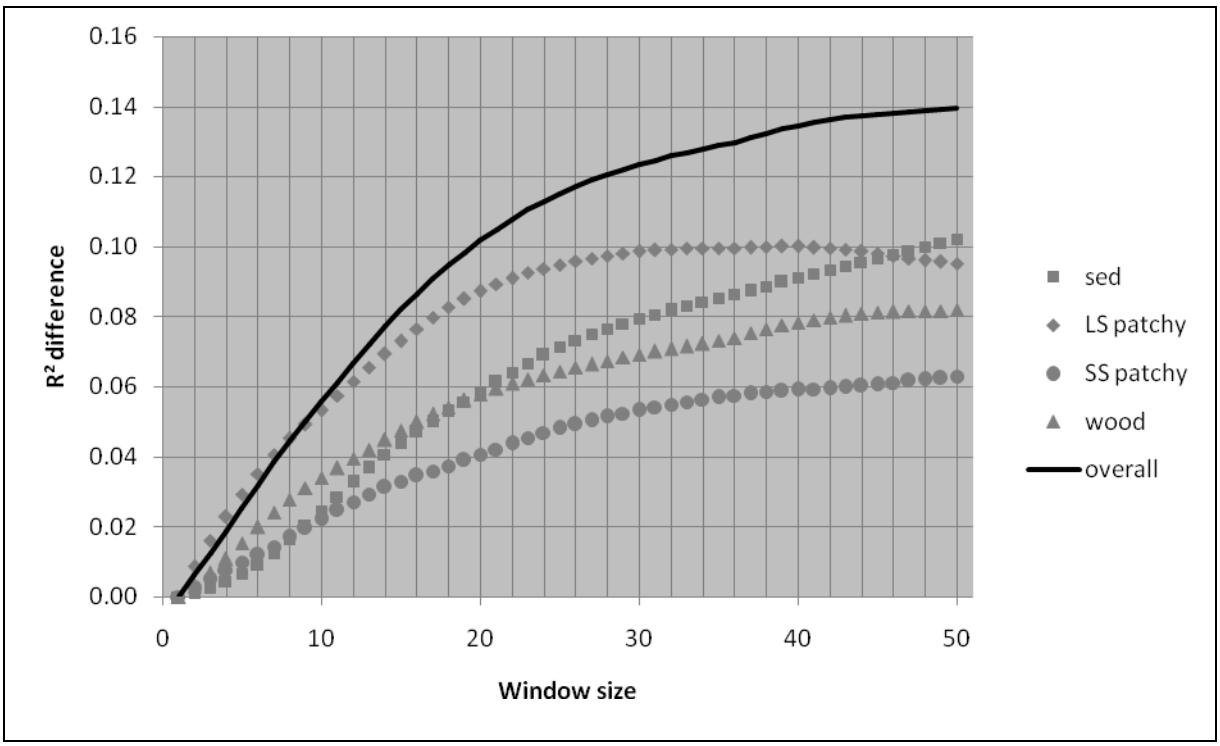

Figure 54: Fit difference for each landscape type.

LS patchy shows large errors in the northern part of the sub-reach (Table 25). Its performance in terms of increasing R^2 is highest, increasing almost three times faster than SS patchy. This indicates that mismatches are more likely to be due to inaccurate prediction of the spatial variables by CAESAR. Anyway, at around resolution of 30 cells, R^2 difference inverts

tendency because of the overall low predicted area of this landscape unit. In Table 25, the same effect is visible due to colours getting lighter, but because of increase in surface error, overall fitting decreases.
Bare sediment show a small increase at the beginning, which stays even below SS patchy; after resolution of 7 cells, the curve increases faster reaching the maximum steepness around resolution of 10 cells. Still, from this point on curve stays steeper than for the other landscape types.

Combining the increasing resolution results with the producer accuracy, we can assess at which spatial scale errors are made. The low producer accuracy of SS patchy (Table 23) and the little improve in R^2 by increasing resolution shows that mismatches are at large distance. We can compare mapped with prediction map (Figure 36 and 47); as we can see, we were able to predict right ecological range, shown by the fact that all the classified SS patches are at lower locations in the landscape and close to the sediment class, but it is not able to allocate this class as shown in the mapped landscape units. This indicates that for predicting these smaller landscape units, the geomorphic parameters calculated by CAESAR are too inaccurate to predict the exact location or that the samples used for the statistical analysis are not representative for the used independent variables. As stated before, increasing sample size and integrating grain size into the analysis might clarify the source of error.
For landscape type LS patchy, we can assess that even the low producer accuracy, its R^2 is the steepest one to increase. This shows that the errors are rather at short distance. Nevertheless, the total area predicted is only half of the observed one, so that the curve drops down from an aggregation of 30 cells on.
In summary, we can assess that the here proposed method suits for a scale of 210m (window size 21 cells) because being it the point where the R^2 curve of Figure 53 flattens. Anyway, adding more variable in the statistical model and improving the CAESAR vegetation growth model can enhance accuracy for higher resolution. Still, the simplified approach of CAESAR is a second limiting factor for the accuracy of especially smaller units.

Table 25: Multiple resolution validation; visual comparison of different window sizes. Blue colour indicate height errors while yellow low

	1 cell: overall fitting: 0.69	5 cell: overall fitting: 0.72	11 cells: overall fitting: 0.75	21 cells: overall fitting:0.80	50 cells: overall fitting: 0.83
Bare sed.	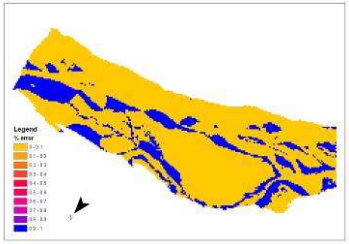	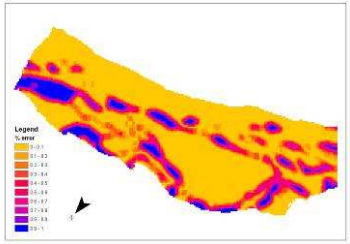	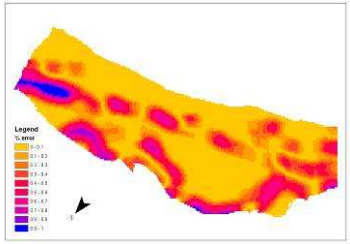	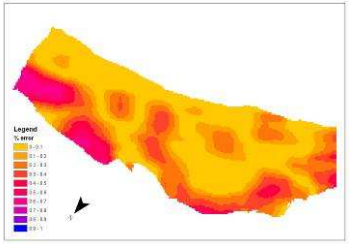	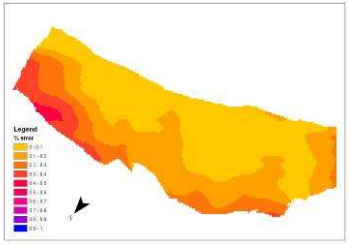
SS patchy.	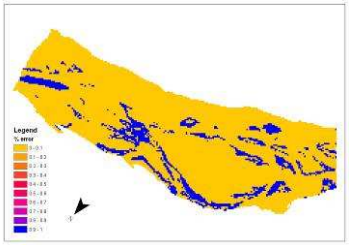	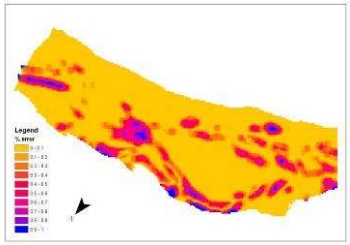	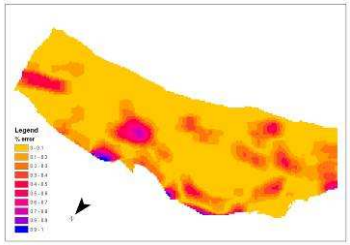	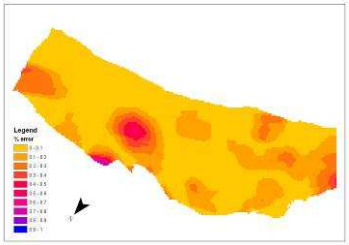	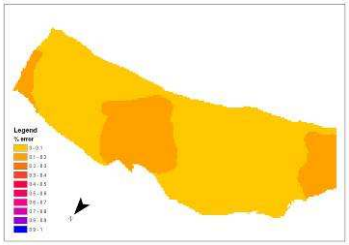
LS patchy	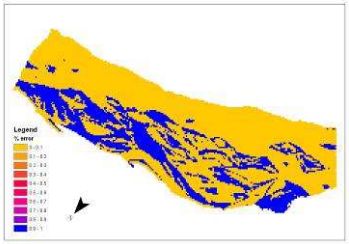	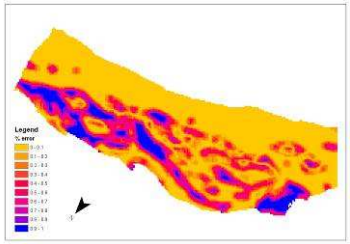	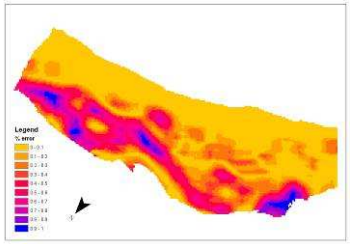	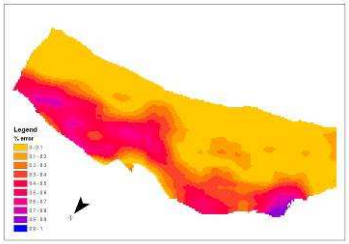	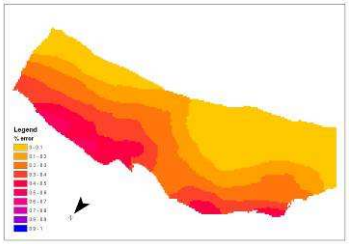
Wood	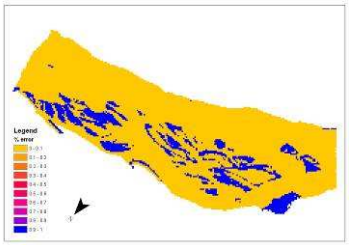	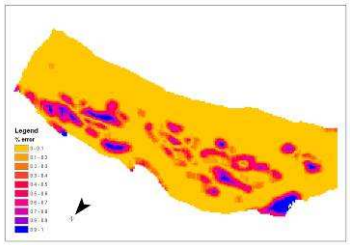	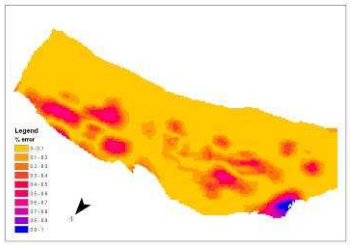	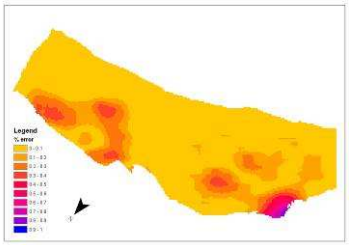	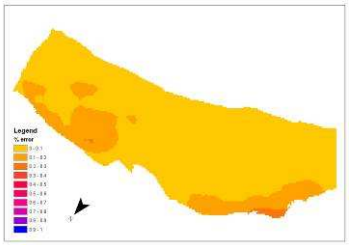

5 Conclusions

We proposed here a method to predict the spatial distribution of landscape units using the hydromorphic model CAESAR which includes interactions with vegetation. The probabilities for each landscape unit were calculated based on sampled geomorphic variables which CAESAR was able to predict.

Following we will give an answer on the research questions formulated at the beginning of this study.

1) Application of the reduced complexity model CAESAR to the Tagliamento River.

Is the application of CAESAR using general literature on braided rivers possible?

The informations about dynamic properties found in literature can be used to calibrate lateral erosion, bed erosion and sinuosity, by comparing modelling results with the process descriptions. Quantitative data which can be used for calibration are difficult to find, since, as ZANONI *et al.* (2008) states, dynamic properties of braided rivers are well known but a quantification of these is not possible by now. If looking at the differences in water stages in the period 2005-2009 at Venzone (Tagliamento), we see the maximum annual discharge varying between 280-1290 m^3/s over the years (see Figure 7 Chapter 2.2.1.1). The same variation appears within the same year. Because Q is the main actor in channel turnover, the difficulty in quantifying processes becomes clear. Nevertheless, the evaluation of aerial pictures to define study area specific turnover rates and sinuosity ranges is seen as a helpful tool to bridge the knowledge gap of process quantification.

Is the simple vegetation growth model integrated in CAESAR sufficient to assess eco-hydromorphic interactions of the Tagliamento River?

The demand of integrating eco-hydromorphic feedbacks into modelling (VAUGHAN *et al.* 2009) has been partially successfully applied. Especially the quantification of mechanism of interaction between vegetation and hydromorphic processes is integrated in CAESAR with a simple vegetation growth model. This allows vegetation to respond to hydromorphic processes such as burring and flooding. In the other way around, vegetation influences erosion and deposition by increasing roughness, influencing so hydromorphic processes.

Even if the CAESAR model does not integrate complex interactions as proposed in the conceptual model of GURNELL *et al.* (2001) it simulates the main effects of vegetation in riverine landscapes (MURRAY *et al.* 2008; VAUGHAN *et al.* 2009). The effects like changes in lateral erosion due to plant routes or different types of vegetation succession stages with different roughness functions are not integrated (COULTHARD *et al.* 2007; MURRAY *et al.* 2008).

Nevertheless, the valid use of this simple sub-model is shown by the high accuracy in classifying areas where no vegetation has the opportunity to grow. The validity of the index for grass growth hampered the use of this variable for classifying vegetated landscape units.
An extension of the simple linear model to a slightly more complex one integrating further succession steps (shrub and wood), would improve the considered feedbacks. Moreover, it would provide an additional tool which in combination with ecological conditions can increase classification accuracy of the predicted landscape types.

2) Identify properties which indicate habitat types.

Which landscape properties can be used to statistically differentiate habitat types?

The scale of landscape units, instead of habitats was chosen because of the low DEM resolution (10m). Also the time gap between field survey and CAESAR simulation end time, led for the choice of landscape types, which can be mapped through aerial pictures.
Nevertheless, field data show that the landscape types have the potential to integrate endangered FFH habitats. Especially, SS patchy vegetation indicates conditions for the development of a few endangered FFH habitats within the more dynamic areas of the floodplain. Also LS patchy vegetation includes one association of one FFH habitat. Landscape type wood is not clearly including some FFH habitat. The reason for this is that woody FFH habitats are largely defined through species composition and not through geomorphic attributes as the dynamic floodplain FFH habitats.
Anyway, the results showed that FFH habitats can be distributed over more landscape types because integrating vegetation associations with different habit. Further, due to the weak species characterization, we cannot exclude that associations of the FFH habitat are scattered over more landscape types.
The R^2 for the predicted landscape units of 0.69 is a satisfactory result. If higher scales are chosen R^2 even increases until 0.80. Still, the high accuracy is given through the better classified bare sediment landscape type by using the vegetation index of CAESAR. The statistical model for the classification of vegetated landscape types does not have a high predictive power.
If no mistakes were made in this study to calculate the grain-size distribution file of CAESAR, another variable could be add to the multinomial regression analysis and so improve the statistical model. This additional variable is rather ecological than hydromorphic, and could give some further hints for understanding ecological variability within the floodplain. Anyway, the here indicative analysis because of lucking sample number, shows an increase of classification accuracy from 58% to 84%.

3) **Investigation of the link between the CAESAR calculated geomorphic variables and indices pattern and the actual habitats assortment.**

Is CAESAR able to predict the spatial distribution of variables which explain distribution of habitats?

The calculated parameter and the vegetation index of CAESAR were able to predict the landscape types with an overall accuracy of almost 70%, for the sampled western sub reach. The potential of CAESARs predicting power is shown by the high accuracy in predicting non-vegetated areas which yield highest user and producer accuracy. The low accuracy for vegetated landscape types is thought to be more due to the statistical model than due to the CAESAR output. Anyway, integrating the grain-size into the statistical model as additional independent variable would improve accuracy.

The matching of landscape types as aggregated form of GURNELLS *et al.* (2001) conceptual model, shows that for future studies, even transformation probabilities or chain from one landscape type into another could be integrated in the prediction method. Further, it allows a better evaluation of future scenarios in terms of missing processes for the development of certain landforms.

4) **Assessing if the proposed method allows prediction of human impact on endangered NATURA 2000 habitats as a function of changes in morphological properties.**

Is the overall method suitable for human impact assessment on endangered habitats?

Through the development of scenarios, as climate change or the construction of a dam, inputs for CAESAR could be changed. For instance, if assuming climate change as scenario, the hydrograph could be changed by enhancing differences between low water and high water stages. The eco-hydromorphic processes will respond to these changes, and change the environmental setting of the explanatorily geomorphic variables used to calculate the probabilities for each landscape type.

VAUGHAN *et al.* (2009) asks for the integration of cross scale factors into the simulation. The integration of large scale factors, such as land use changes in the catchment, and its impact on the landscape distribution on the reach can be included as further scenario evaluation tool. CAESAR allows combining catchment simulation with reach simulations. The large scale provides the input data, such as discharge and sediment supply, for the connected reach simulation. The impact of changes in the catchment could then be analysed in terms of landscape type pattern changes in the reach, and so the connected endangered FFH habitats.

The limitation of the here proposed approach is the assumption that the vegetation composition and so related landscape types do not change over time. This limitation is difficult to counter since it is difficult to predict how the vegetation composition changes due to long term changes such as climate change and especially how this will lead to a new habitat assortment.

Overall, the integrated basic eco-hydromorphic feedbacks of CAESAR, the matching of landscape types with FFH habitats and the acceptable overall accuracy of prediction, which has the potential to improve, make this approach a good tool for the general assessment of human impact.

Acknowledgments

I thank Friederike Lang and Arnaud Temme for the constructive supervision of this master thesis. I thank also: Luca Ziliani, Walter Bertoldi, Angela Gurnell and Tom Coulthard for the help and for provided data; the students of the project “Bodenschutz vs. Hochwasserschutz” (TU Berlin – Bsc “Landscape Planning and Landscape Architecture”) and the IGB (Leibniz-Institute of Freshwater Ecology and Inland Fisheries) for the support in the field; NERC (Natural Environmental Research Council – UK) for providing basic data.

Bibliography

BERTOLDI, W., unpublished. "Digital Elevation Model (DEM) 2005 Braulis - Pinzano". Queen Mary University of London, Department of Geography (2009).

BERTOLDI, W., L. ZANONI and M. TUBINO, 2010. "Assessment of morphological changes induced by flow and flood pulses in a gravel bed braided river: The Tagliamento River (Italy)" In: *Geomorphology* (Vol. 114/ Issue 3/2010). pp. 348-360.

BERTOLDI, W., A. GURNELL, N. SURIAN, K. TOCKNER, L. ZANONI, L. ZILIANI, and G. ZOLEZZI, 2009. "Understanding reference processes: Linkages between river flows, sediment dynamics and vegetated landforms along the Tagliamento River, Italy" In: *River Research and Applications* (Vol. 25/ Issue 5/2009). pp. 501-516.

CATANI, G., 2007. "Studio Tessiturale dei Sedimenti in Alveo del Fiume Tagliamento tra Pioverno e Ronchis", Universita degli Studi di Trieste, Dipartimento di Scienze Geologiche, Ambientali e Marine. Trieste p. 23

CORONA, P., P. CALVANI, G.S. MUGNOZZA, and E. POMPEI, 2008. "Modelling natural forest expansion on a landscape level by multinomial logistic regression" In: *Plant Biosystems* (Vol. 142/ Issue 3/2008). pp. 509-517.

COULTHARD, T.J. (pbl.), n.d. "CAESAR landscape evolution model message board". Online available at: http://www.coulthard.org.uk/cgi-bin/discus/discus.cgi. Date: 2009-2010.

COULTHARD, T.J. and P. DE ROSA, 2009. "CAESAR-workshop". Perugia,

COULTHARD, T.J. and M.J. VAN DE WIEL, n.d. "The Cellular Automaton Evolutionary Slope And River model (CAESAR)" pp. 1-23. Online available at: http://www.coulthard.org.uk/downloads/visualcaesar.htm, Date: 14.10.09.

COULTHARD, T.J., D.M. HICKS and M.J. VAN DE WIEL, 2007. "Cellular modelling of river catchments and reaches: Advantages, limitations and prospects" In: *Geomorphology* (Vol. 90/ Issue 3-4/2007). pp. 192-207.

EC (*Europenan Councile*), 1985. Directive 85/337/EEC: "on the assessment of the effects of certain public and private projects on the environment ". Official Journal L 175 , 05/07/1985 P. 0040 - 0048

EC (*European Councile*), 1992. Directive 92/43/EEC: "on the conservation of natural habitats and of wild fauna and flora". Official Journal L 206, 22.7.1992, p. 7

EC (*European Councile*), 2000. Directive 2000/60/EC: "establishing a framework for Community action in the field of water policy ". Official Journal L 327 , 22/12/2000 P. 0001 - 0073

EC (*European Councile*), 2001. Directive 2001/42/EC: "on the assessment of the effects of certain plans and programmes on the environment ". Official Journal L 197 , 21/07/2001 P. 0030 - 0037

EC (*European Councile*), *D.G. Environment*, 2007. Interpretation Manual of European Union Habitats

EDWARDS, P.J., J. KOLLMANN, A.M. GURNELL, G.E. PETTS, K. TOCKNER, and J.V. WARD, 1999. "A conceptual model of vegetation dynamics of gravel bars of a large Alpine river" In: *Wetlands Ecology and Management* (Vol. 7/ Issue 3/1999). pp. 141-153.

FISHER, S.G., J.B. HEFFERNAN, R.A. SPONSELLER, and J.R. WELTER, 2007. "Functional ecomorphology: Feedbacks between form and function in fluvial landscape ecosystems" In: *Geomorphology* (Vol. 89/ Issue 1-2 SPEC. ISS./2007). pp. 84-96.

FRANCIS, R.A., D. CORENBLIT and P.J. EDWARDS, 2009. "Perspectives on biogeomorphology, ecosystem engineering and self-organisation in island-braided fluvial ecosystems" In: *Aquatic Sciences* 2009).

FRISSELL, C.A., W.J. LISS, C.E. WARREN, and M.D. HURLEY, 1986. "A hierarchical framework for stream habitat classification: Viewing streams in a watershed context" In: *Environmental Management* (Vol. 10/ Issue 2/1986). pp. 199-214.

GOOGLE MAPS (pbl.), 2009. Online available at: www.maps.google.de. Date: 16.10.2009.

GURNELL, A. and G. PETTS, 2006. "Trees as riparian engineers: The Tagliamento River, Italy" In: *Earth Surface Processes and Landforms* (Vol. 31/ Issue 12/2006). pp. 1558-1574.

GURNELL, A., N. SURIAN and L. ZANONI, 2009. "Multi-thread river channels: A perspective on changing European alpine river systems" In: *Aquatic Sciences* (Vol. 71/ Issue 3/2009). pp. 253-265.

GURNELL, A.M. and G.E. PETTS, 2002. "Island-dominated landscapes of large floodplain rivers, a European perspective" In: *Freshwater Biology* (Vol. 47/ Issue 4/2002). pp. 581-600.

GURNELL, A.M., G.E. PETTS, D.M. HANNAH, B.P.G. SMITH, P.J. EDWARDS, J. KOLLMANN, J.V. WARD, and K. TOCKNER, 2001. "Riparian vegetation and island formation along the gravel-bed Fiume Tagliamento, Italy" In: *Earth Surface Processes and Landforms* (Vol. 26/ Issue 1/2001). pp. 31-62.

HOSMER, D.W. and S. LEMESHOW, 2000. *Applied Logistic Regression*. Chapter 1-3, Hosmer, D.W. and S. Lemeshow [eds.], pp. 1-7, 47-56. Jonh Wiley &Sons, USA.

JUNK, W.J., P.B. BAYLEY and R.E. SPARKS, 1989. "The flood pulse concept in river–floodplain systems" In: *Canadian Special Publications for Fisheries and Aquatic Sciences.* (Vol. 106/1989). pp. 110-127.

KOLLMANN, J., M. VIELI, P.J. EDWARDS, K. TOCKNER, and J.V. WARD, 1999. "Interactions between vegetation development and island formation in the Alpine river Tagliamento" In: *Applied Vegetation Science* (Vol. 2/ Issue 1/1999). pp. 25-36.

MÜLLER, N., 2005. "Die herausragende Stellung des Tagliamento (Friaul, Italien) im Europäischen Schutzgebietssystem NATURA 2000" In: *Jahrbuch des Vereins zum Schutz der Bergwelt* Vol. 70. Linzmeyer, K. [ed.], pp. 19-35. Verein zum Schutz der Bergwelt e.V., Munich.

MURRAY, A.B., M.A.F. KNAAPEN, M. TAL, and M.L. KIRWAN, 2008. "Biomorphodynamics: Physical-biological feedbacks that shape landscapes" In: *Water Resources Research* (Vol. 44/ Issue 11/2008).

PERONA, P., P. MOLNAR, M. SAVINA, and P. BURLANDO, 2009a. "An observation-based stochastic model for sediment and vegetation dynamics in the floodplain of an Alpine braided river" In: *Water Resources Research* (Vol. 45/ Issue 9/2009a).

PERONA, P., C. CAMPOREALE, E. PERUCCA, M. SAVINA, P. MOLNAR, P. BURLANDO, and L. RIDOLFI, 2009b. "Modelling river and riparian vegetation interactions and related importance for sustainable ecosystem management" In: *Aquatic Sciences* (Vol. 71/ Issue 3/2009b). pp. 266-278.

PONTIUS JR, R.G., W. BOERSMA, J.C. CASTELLA, K. CLARKE, T. NIJS, C. DIETZEL, Z. DUAN, E. FOTSING, N. GOLDSTEIN, K. KOK, E. KOOMEN, C.D. LIPPITT, W. MCCONNELL, A. MOHD SOOD, B. PIJANOWSKI, S. PITHADIA, S. SWEENEY, T.N. TRUNG, A.T. VELDKAMP, and P.H. VERBURG, 2008. (Vol. - 42/ Issue - 1/2008). pp. - 37.

RUTHERFORD, G.N., A. GUISAN and N.E. ZIMMERMANN, 2007. "Evaluating sampling strategies and logistic regression methods for modelling complex land cover changes" In: *Journal of Applied Ecology* (Vol. 44/ Issue 2/2007). pp. 414-424.

SCHWAB, J.A. (pbl.) (*Course material SW388R387 "Data Analysis & Computers II"*). "Multinomial Logistic Regression Basic Relationships". Online available at: http://www.utexas.edu/courses/schwab/sw388r7/SolvingProblems/MultinomialLogisticRegression_BasicRelationships.ppt. Date: 05.2010.

TEMME, A., 2010. Personal talk about: Probability calcualtion using multinominal logistic regression analysis. Wageningen (NL).

TOCKNER, K., A. PAETZOLD, U. KARAUS, C. C., and J. ZETTEL, 2006. "Ecology of Braided Rivers" In: *Braided Rivers: Process, Deposits, Ecology and Management* Vol. (Special Publication 36 of the IAS). G. H. Sambrook Smith, et al. [eds.], pp. 339-359. Wiley-Blackwell.

TOCKNER, K., J.V. WARD, D.B. ARSCOTT, P.J. EDWARDS, J. KOLLMANN, A.M. GURNELL, G.E. PETTS, and B. MAIOLINI, 2003. "The Tagliamento River: A model ecosystem of European importance" In: *Aquatic Sciences* (Vol. 65/ Issue 3/2003). pp. 239-253.

VAN DE WIEL, M.J., T.J. COULTHARD, M.G. MACKLIN, and J. LEWIN, 2007. "Embedding reach-scale fluvial dynamics within the CAESAR cellular automaton landscape evolution model" In: *Geomorphology* (Vol. 90/ Issue 3-4/2007). pp. 283-301.

VAN DER NAT, D., A.P. SCHMIDT, K. TOCKNER, P.J. EDWARDS, and J.V. WARD, 2002. "Inundation dynamics in braided floodplains: Tagliamento River, northeast Italy" In: *Ecosystems* (Vol. 5/ Issue 7/2002). pp. 636-647.

VAUGHAN, I.P., M. DIAMOND, A.M. GURNELL, K.A. HALL, A. JENKINS, N.J. MILNER, L.A. NAYLOR, D.A. SEAR, G. WOODWARD, and S.J. ORMEROD, 2009. "Integrating ecology with hydromorphology: A priority for river science and management" In: *Aquatic Conservation: Marine and Freshwater Ecosystems* (Vol. 19/ Issue 1/2009). pp. 113-125.

WARD, J.V., K. TOCKNER, D.B. ARSCOTT, and C. CLARET, 2002. "Riverine landscape diversity" In: *Freshwater Biology* (Vol. 47/ Issue 4/2002). pp. 517-539.

WELBER, M., S. PICCOLROAZ, W. BERTOLDI, and M. TUBINO(COORDINATOR), unpublished. "Formula for discharge calcualtion out of the water stages at Venzone and Villuza at the Tagliamento river". Department of Civil and Environmental Engineering, University of Trento (I) (2009).

ZANONI, L., A. GURNELL, N. DRAKE, and N. SURIAN, 2008. "Island dynamics in a braided river from analysis of historical maps and air photographs" In: *River Research and Applications* (Vol. 24/ Issue 8/2008). pp. 1141-1159.

ZILIANI, L., 2009. Personal talk about: Discharge data for the Tagliamento. 25.11.2009.E-mail.

Appendix 1: Laser analysis

campione	**180_62**	**180_7**	**180_97**	mean	classification	% out of the 22.98% overlap
micron	%	%	%	%		
0.5						
0.7	0.57	1.48	0.00	0.68	colloid	0.157
1.0						
1.4						
2.0						
2.8	1.93	3.38	0.33	1.88	clay	0.432
3.9						
5.5						
7.8						
11.0						
15.6						
22.1						
31.3						
44.2	9.37	43.94	7.26	20.19	silt	4.640
62.5						
88.4	3.87	25.27	9.69	12.94	very fine sand	2.975
125.0						
176.8	14.85	17.09	32.08	21.34	fine sand	4.904
250.0					medium sand	
353.6	37.23	6.52	40.70	28.15		6.470
500.0						
707.1	24.36	1.80	9.94	12.03	coarse sand	2.765
1000.0						
1414.2	7.81	0.52	0.00	2.78	very coarse sand	0.637

(CATANI 2007)

Appendix 2: Sieve analysis

sample	**180_-20**	**180_-40**	**180_-60**		
Grain size cm	%	%	%	mean	Classification
0.10				22.98	coarse sand and below + very coarse sand
0.20	21.67	25.32	21.96		
0.40	12.87	12.91	5.71	10.50	very fine gravel
0.80	20.78	15.55	15.36	17.23	fine gravel
1.60	25.16	14.79	23.88	21.28	medium gravel
3.15	19.53	7.90	33.09	20.17	coarse gravel
6.00	0.00	23.52	0.00	7.84	very coarse gravel
12.50	0.00	0.00	0.00	0.00	cobble

(CATANI 2007)

Appendix 3: Example of hydrograph processing

Date	Q09	Q08	Q07	Q06	Q05	mean over the years	Std	hydrograph producer	hydro smother
01.01.	56.77	0.93	7.92	34.32	36.60	27.31	22.778	15.32	26.67
02.01.	55.20	0.87	7.18	34.50	35.90	26.73	22.394	38.01	32.84
03.01.	53.25	0.79	6.16	34.14	34.48	25.76	21.849	45.19	47.41
04.01.	51.59	1.54	5.89	33.82	33.83	25.33	21.083	59.02	59.02
05.01.	50.97	2.64	5.17	34.12	33.56	25.29	20.759	16.19	42.16
06.01.	49.77	5.06	4.77	34.07	33.69	25.47	19.853	51.27	51.27
...	...	...	...	....	....	...	...	...	...
31.10.		684.44	25.18	24.24	42.36	194.05	327.027	356.13	538.25
01.11.		745.45	22.90	23.26	41.57	208.29	358.209	215.01	221.21
02.11.		286.42	22.16	20.53	40.86	92.49	129.616	92.49	135.53
03.11.		170.81	21.08	19.82	40.68	63.10	72.441	99.08	79.24
04.11.		180.13	20.31	18.62	40.33	64.85	77.486	46.15	86.31
median	39.35	41.68	29.11	44.38	36.28	49.65	36.144		
mean	54.60	70.75	31.45	49.21	39.87	346.50	629.325		
std	55.17	109.84	40.52	48.137	25.61	31.40	--		
min	11.96	0.79	0.40	8.55	17.94	22.65	4.89		
max	455.44	1290.43	577.41	727.32	280.24	346.50	629.32		

Appendix 4: Sensitivity analysis for CAESAR parameter influencing calculation time.

Particularly we investigated sensitivity of calculation time for:

“Max erod limit”, which is main parameter influencing simulated time per iteration step (time step; chapter 1.3). As soon as entrainment passes this limit, time step is divided by two and erosion calculated again, allowing detailed simulation during high hydromorphic activity (COULTHARD n.d.).

“Slope used to calculate Tau” has three options to calculate shear stress (TAU):

- Bedslope: erodes in every direction in which bed slope is positive (COULTHARD n.d.).
- Bedslope2: shear stress is calculated using max bed slope. Erosion is calculated using this max shear stress and eroded material is redistributed according to bedslope (COULTHARD n.d.).
- TAUvel: this method derives shear stress from flow velocity (from Q). Max velocity can be set due to the fact that CAESAR does not model superficial flow, leading in some spots to an over high velocity (high erosion). Velocities higher than set value are cut-off to max velocity value. Reducing this parameter can speed up simulation (at the expenses of realism). Further this method allows development of pool-riffle (COULTHARD n.d.).

“Min Q for depth calc” sets the threshold Q above which erosion and deposition is calculated (COULTHARD n.d.).

“Flow distribution” defines through how many cells water is pushed from one cell to set front ones (COULTHARD n.d.).

It was found that “erod limit” and “Slope used to calculate Tau” are parameter influencing most computational time and performance.

For the before chosen 10m DEM, “max erod limit” = 0.05 was found to be best, having a maximum allowed slope change of 0.01m per calculation step and lowest calculation time.

In performance (visual comparison of the results) no clear difference was visible, so only maximum slope change and calculation time was taken in consideration to define proper settings.

For “Slope used to calculate Tau”, “Bedslope” was found to be slowest method. No clear difference in erosion/deposition and flow pattern with “Beslope 2” method was visible, only erosion rates were higher for the second method.

Comparing two different limits of velocity for the “Tau based on velocity” method we found that reducing this limit reduces calculation time considerably. Looking more at erosion and flow pattern, we evaluated that the lower the set limit the lower the channel incises, due to lower difference in velocity between middle channel and .

Finally, we compared “Bedslope 2” method and “Tau based on velocity” (TAUvel=1) with velocity limit set at 1. “Bedslope 2” method was found to be slower from the calculation point of view. Assessing after erosion pattern, we assert that “Bedslope 2” eroded 12.5 times more than TAUvel=1. This was found to be due to a higher erosion power with increasing discharge for “Bedslope 2” method.

Also erosion and deposition pattern was different for the two methods. TAUvel=1 erosion/deposition follows channel pattern, where velocity is higher. Due to higher sensitivity of “Bedslope 2” to increasing Q, erosion/deposition pattern follows bed slope pattern at high water level, not taking into account feature such as meanders.

We selected “Tau based on velocity” limiting velocity to values below 1. Even limit below two might have consequence in a unrealistic output (COULTHARD n.d.), we consider output of TAUvel=1 much better than TAUvel=2. This is considered to be best option for the spin-up, in which no lateral erosion is integrated. Later we will reconsider this option.

Other parameter were found to have only a slight impact on calculation time so setting was calibrated to get highest amount of sediment redistribution.

Appendix 5: Landscape prediction accuracy with decreasing resolution

Scale 1 cell wood

Modelled: black=100% white=0%

Mapped: black=100% white=0%

Difference: red=100% green=0% difference

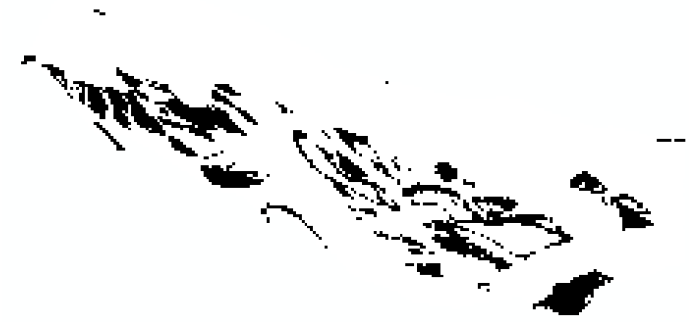

Mean error= 0.13; STD= 0.34

Scale 21 cell wood

Modelled: black=100% white=0%

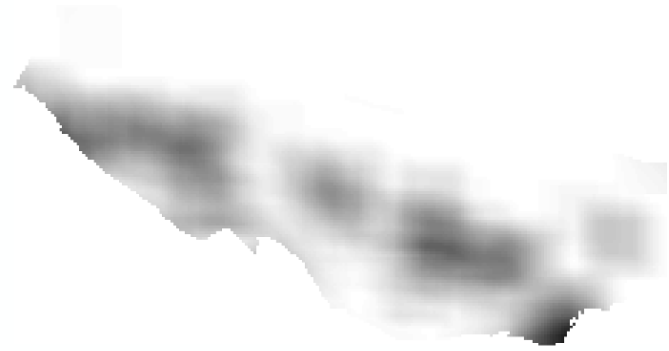

Mapped: black=100% white=0%

Difference: Black=100% white=0% difference

Mean error= 0.08; STD= 0.10

Scale 1 cell sediments

Modelled: black=100% wood white=0%

Mapped: black=100% white=0%

Difference: Black=100% white=0% difference

Mean error= 0.21; STD= 0.40

Scale 21 cell sediments

Modelled: black=100% white=0%

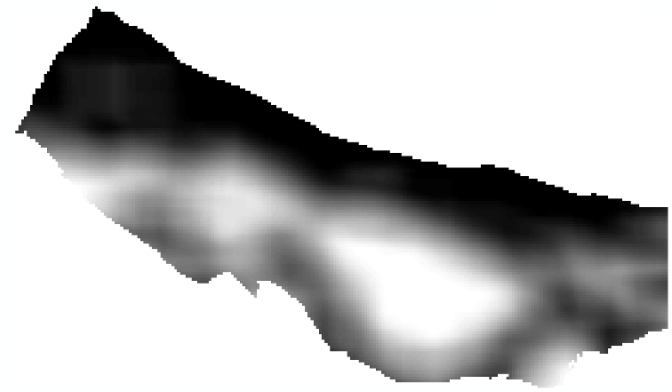

Mapped: black=100% white=0%

Difference: Black=100% white=0% difference

Mean error= 0.17; STD= 0.16

Scale 1 cell LS patchy

Modelled: black=100% wood white=0%

Mapped: black=100% white=0%

Difference: Black=100% white=0% difference

Mean error= 0.27; STD= 0.44

Scale 21 cell LS patchy

Modelled: black=100% white=0%

Mapped: black=100% white=0%

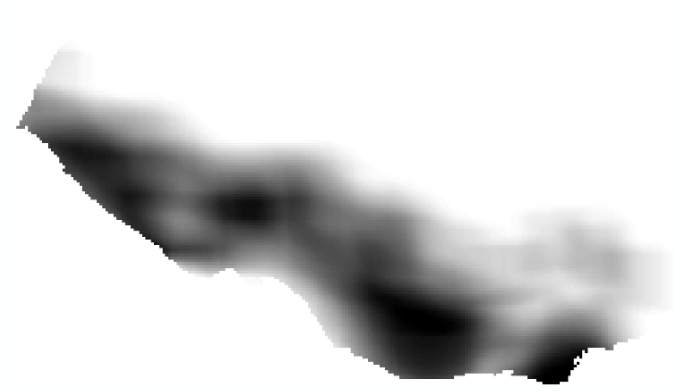

Difference: Black=100% white=0% difference

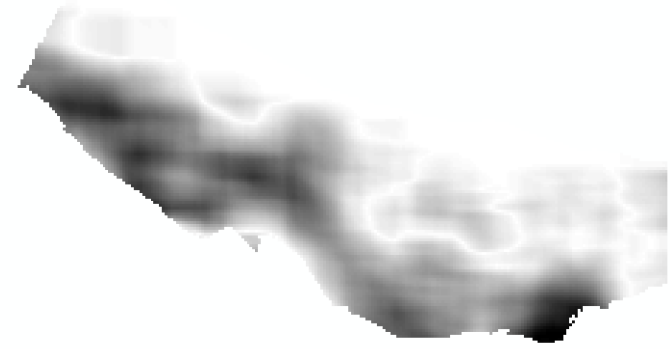

Mean error= 0.21; STD= 0.21

Scale 1 cell SS patchy

Modelled: black=100% wood white=0%

Mapped: black=100% white=0%

Difference: Black=100% white=0% difference

Mean error= 0.12; STD= 0.33

Scale 21 cell SS patchy

Modelled: black=100% white=0%

Mapped: black=100% white=0%

Difference: Black=100% white=0% difference

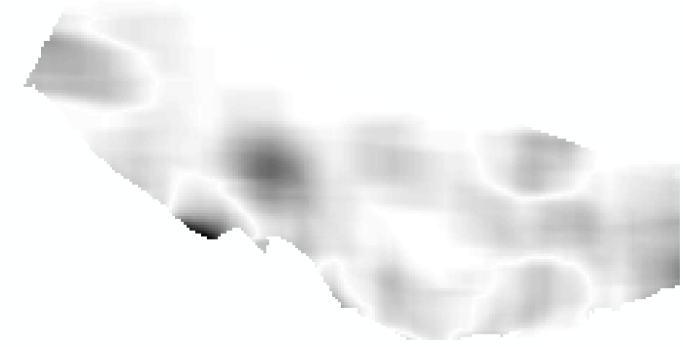

Mean error= 0.09; STD= 0.09